

https://dspace.org/

Engineering HIV viral variants as immunogens to stimulate Broadly Neutralizing Antibodies

Madzorera, Vimbai Sharon

2018

https://hdl.handle.net/10539/25326

Downloaded from a DSpace repository. https://dspace.org/

ENGINEERING HIV VIRAL VARIANTS AS IMMUNOGENS TO STIMULATE BROADLY NEUTRALIZING ANTIBODIES



Vimbai Sharon Madzorera

A dissertation submitted to the Faculty of Health Sciences, University of the Witwatersrand, Johannesburg, in fulfilment of the requirements for the degree

of

Master of Science in Medicine

Johannesburg, 2018

Declaration

I, Vimbai Sharon Madzorera, declare that this dissertation is my own work. It is being submitted for the degree of Master of Science in Medicine in the University of the Witwatersrand, Johannesburg. It has not been submitted before for any degree or examination at this or any other University.

Signed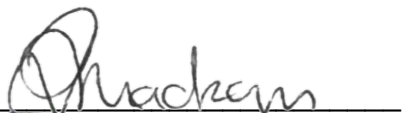

Date 7 June 2018

For Nash, Mbali and Maya

Abstract

Southern Africa is currently the most affected region of the world in terms of the HIV/AIDS pandemic and despite decades of research into this virus, a vaccine that is adequately effective is yet to be developed. However, it is widely believed that broadly neutralizing antibodies (bNAbs) are likely to be required for protection. Eliciting bNAbs by vaccination has been challenging for several reasons, one of which is the failure of most viral proteins to bind the germline versions of bNAbs (bNAb precursors). For vaccine design, it will be necessary to either select or engineer suitable immunogens that bind the inferred bNAb precursors *in vitro*, which is the first step in driving such responses towards breadth. This study focused on an unusual set of six previously identified viral escape mutations (collectively referred to as CS-Mut) that enhance neutralization by bNAbs to the membrane proximal external region (MPER). These mutations were used to engineer and test a variety of viral constructs for their potential as vaccine candidates.

We first tested the effect of each individual cleavage site mutation on viral entry and MPER exposure. We showed that individual mutations resulted in reduced viral entry potential, but not to the same extent as all six mutations combined in the CS-Mut. We next tested the effect of the individual mutations on neutralization by MPER bNAbs. We showed that most of the single mutations enhanced viral sensitivity to MPER bNAbs, with three of the six mutations most promising in terms of MPER exposure. However, the MPER enhancement was less marked than the combined set of six mutations, suggesting further improvement was needed.

We therefore next combined the three most promising mutations into a single construct and showed that enhancement of MPER sensitivity was improved for this triple mutant compared to the individual mutants. Indeed, for some MPER bNAbs, the triple mutant was more sensitive to MPER bNAbs than the matched virus containing all six mutations. Moreover, the entry capacity of the triple mutant was significantly improved over the six mutant construct, making it more amenable to incorporation into virus-like particles for vaccine design.

Lastly, we engineered dual germline targeting immunogens by simultaneously adding the MPER enhancing mutations to five viruses that were previously shown to have a

high probability of binding V2 bNAb precursors (V2 “special strains”). The “special strain” CS-Mut viruses exhibited varying degrees of reduction in viral entry potential, with infectivity abrogated for two. For the remaining three “special strain” CS-Mut viruses, enhancement in MPER sensitivity was observed. Increased sensitivity was largely specific for bNAbs targeting the MPER epitope or interface, as bNAbs and plasma to other viral epitopes showed no enhanced neutralization. However, despite enhanced sensitivity to mature MPER bNAbs, no neutralization was observed using germline reverted MPER bNAbs, the best available approximate of MPER precursors.

In conclusion, the cleavage site mutations resulted in favorable exposure of the MPER epitope, a trait that is promising for immunogen design. However, the fitness cost that results from the addition of the cleavage site mutations is problematic for use of these constructs in vaccines using virus-like particles. In future studies, a balance between viral entry potential and enhancement of MPER neutralization needs to be determined to optimize immunogen candidates. The CAP256 SU CS-Mut construct showed promise as a dual germline targeting immunogen, exhibiting limited reduction in entry potential while favorably exposing the MPER epitope, with minimal disruption to the native envelope trimer structure.

Acknowledgements

My sincere gratitude goes out to my supervisor Prof Penny Moore, who against all odds, believed in me and my capabilities, and on whose proverbial “giant shoulders” I stood throughout my research. She represents the scientist I aspire to become and I greatly value her mentorship.

To my H.O.D, Prof Lynn Morris, many thanks for the critical appraisal and brilliant suggestions that formed a big part of this work. I could always rely on her honesty and expertise to guide me in the right direction.

To my mother, thank you for the selfless sacrifices, for babysitting, for asking the right questions, for pushing me to be more.

To my husband, thank you for standing in the huge gap that I left in the family to pursue my studies, for pre-school runs, for babysitting, for listening and saying all the right things

A big thank you also goes to my colleagues and fellow students at the NICD HIV Virology research lab. Thank you for guidance, input, and daily laughs. It is such a pleasure working among and learning from them.

This work was made possible by funding from the NRF, Poliomyelitis Research Fund and Wits University. Many thanks for the financial support that carried the study.

Lastly, I would like to express my gratitude to CAPRISA and the women of the CAPRISA 002 and 004 cohorts, namely donor CAP248, for making it possible to produce this data.

Table of contents

Declaration ..... **i**

Dedication ..... **ii**

Abstract ..... **iii**

Acknowledgements ..... **v**

Table of contents ..... **vi**

List of Figures ..... **x**

List of Tables ..... **xii**

Amino Acid Abbreviations ..... **xiv**

List of Abbreviations ..... **xv**

CHAPTER 1: INTRODUCTION **1**

1.1 The HIV/AIDS Pandemic and the need for a vaccine 2

1.2 Transmission of the virus 3

1.3 The structure and replication of the virus 5

1.3.1 The structure of the envelope glycoprotein (Env) 8

1.3.2 Gp120 structure and function 9

1.3.3 Gp41 structure and function 11

1.4 The human humoral immune response and HIV 12

1.4.1 Broadly neutralizing antibodies 13

1.4.2 Targets of broadly neutralizing antibodies 14

1.4.3 The Membrane Proximal External Region (MPER) bNAb epitope 15

1.4.4 The gp120-gp41 Interface bNAb epitope 16

1.5 The passive use of bNAbs for therapy and vaccination 17

1.6 The developmental pathway for bNAbs: Implications for vaccine design 18

1.7 Aims and objectives 20

1.7.1 Assessing the effect of cleavage site mutations on neutralization by MPER and interface-directed bNAbs 20
1.7.2 To design dual germline targeting envelopes for MPER and V2 bNAbs ... 21
CHAPTER 2: MATERIALS AND METHODS 22
2.1 Participants 23
2.2 HIV Envelope plasmids 23
2.3 Overlapping PCR for the simultaneous introduction of multiple mutations 23
2.4 Gel electrophoresis and purification of DNA from gel 25
2.5 Cloning of Env genes into mammalian expression vector 25
2.6 Transformation 26
2.7 Colony Polymerase Chain Reaction 27
2.8 Small-scale production of plasmids from cloned envelope DNA 28
2.9 Sanger Sequencing 29
2.10 Sequence analysis 31
2.11 Large-scale production of plasmids from cloned envelope DNA 31
2.12 Site Directed Mutagenesis 32
2.14 Antibody Expression 36
2.15 Antibody purification 37
2.16 SDS-Polyacrylamide gel electrophoresis analysis of purified mAbs 38
2.17 Production of Env-pseudoviruses 40
2.19 The TZM-bl Neutralization assay 42
2.20 Statistical analysis 44
CHAPTER 3: RESULTS 45
3.1 Assessing the effect of individual cleavage site mutations on viral fitness 47
3.1.1 Generation of single mutations within the gp120-gp41 cleavage site 47
3.1.2 Confirmation of the functionality of mutant viruses 48
3.1.3 Assessing the effect of individual gp120-gp41 cleavage site mutations on viral fitness 48

3.2 Assessing the effect of single cleavage site mutations on MPER exposure ... 52
3.2.1 Neutralization sensitivity of CAP45.G3 cleavage site mutants to MPER antibodies ... 52
3.2.2 Neutralization sensitivity of CAP45.G3 cleavage site mutants to gp120-gp41 Interface antibodies ... 60
3.2.3 Neutralization sensitivity of CAP45.G3 cleavage site mutants to bNAbs targeting other epitopes ... 62
3.3 Design and testing of a CAP45.G3 triple mutant for viral fitness and MPER exposure ... 63
3.3.1 Generation of a CAP45.G3 triple mutant plasmid and pseudovirus production ... 63
3.3.2 Neutralization of the CAP45.G3 triple mutant by MPER bNAbs ... 64
3.3.3 Neutralization of the CAP45.G3 triple mutant by gp120-gp41 Interface bNAbs ... 65
3.3.4 Neutralization of the CAP45 triple mutant by bNAbs targeting the V2, V3 and CD4bs epitopes ... 66
3.4 Designing dual germline targeting envelopes as HIV-1 vaccine immunogens 67
3.4.1 Site directed Mutagenesis of viral plasmids ... 69
3.4.2 Production of pseudoviruses and determining the effect of CS-Mut on viral fitness ... 70
3.4.3 Neutralization sensitivity of V2 “special strains” and their CS-Mut mutants to mature MPER bNAbs ... 72
3.4.4 Neutralization of cleavage site mutants by germline reverted MPER bNAbs ... 77
3.4.5 Neutralization sensitivity of V2 special strains and their CS-Mut to bNAbs targeting other epitopes ... 78
3.5 Assessing the effects of the cleavage site mutations on Envelope structure using polyclonal plasma ... 80
CHAPTER 4: DISCUSSION AND CONCLUSIONS ... 82

CHAPTER 5: REFERENCES 88

CHAPTER 6: APPENDICES 104

APPENDIX A: SEQUENCE ACCESSION NUMBERS (GENBANK)..... 105

APPENDIX B: ETHICS CLEARANCE CERTIFICATE 106

APPENDIX C: PLIAGIARISM DECLARATION 107

List of Figures

Chapter 1

Figure 1.1: Flow chart of HIV-1 transmission 4

Figure 1.2: The structure of the Human Immuno-Deficiency Virus (HIV) 5

Figure 1.3: The replication cycle of HIV-1 7

Figure 1.4: The structure of the HIV-1 envelope glycoprotein (Env) 8

Figure 1.5: Structure showing the conformation of the five gp120 variable loops 10

Figure 1.6: The different regions of gp41 11

Figure 1.7: Envelope trimer structure showing the five known epitopes of HIV-1 bNAbs 15

Chapter 2

Figure 2.1: An outline of overlapping PCR 24

Figure 2.2: Properties of the pcDNA3.1/v5His-TOPO vector s system 26

Figure 2.3: Sanger sequencing reaction set-up 30

Figure 2.4: Overview of the Quick-change Lightning site directed mutagenesis 35

Figure 2.5: The layout of a 96 well neutralization assay plate 43

Chapter 3

Figure 3.1: Sanger sequencing chromatograms of the CAP45-G3 cleavage site mutants 47

Figure 3.2: Comparison of viral fitness between CAP45.G3 wild type, CS-Mut and individual mutants 49

Figure 3.3: Logogram showing cleavage site residues in global viruses 50

Figure 3.4: SDS Page gel of MPER bNAbs 54

Figure 3.5: Neutralization of CAP45.G3 single mutants by 4E10 57

Figure 3.6: Neutralization of CAP45.G3 single mutants by 10E8 58

Figure 3.7: Neutralization of CAP45.G3 single mutants by DH511 58

Figure 3.8: Neutralization of CAP45.G3 triple mutant by MPER bNAbs 64

Figure 3.9: Neutralization of CAP45.G3 WT, CS-Mut and triple mutant by interface bNAbs 66

Figure 3.10: Alignment of V2 Special strains in which mutations were made 69

Figure 3.11: Differences in infectivity between wild type and CS-Mut V2 special strains 71

Figure 3.12: Neutralization of T250-4 CS-Mut and wild type by MPER bNAbs 73

Figure 3.13: Neutralization of CAP256 SU CS-Mut and wild type by MPER targeting bNAbs 74

Figure 3.14: Neutralization of WITO.33 CS-Mut and wild type by MPER bNAbs 76

Figure 3.15: Neutralization of wild type and CS-Mut V2 special strains by V3 bNAb PGT130 78

List of Tables

CHAPTER 2

Table 2.1: Cycling conditions for overlapping PCR 24

Table 2.2: Cycling conditions of colony PCR reactions 28

Table 2.3: Cycling conditions of the Sanger sequencing reactions 31

Table 2.4: Sequences of primers used in the study 32

Table 2.5: Cycling Conditions of Site Directed Mutagenesis reactions 35

Table 2.6: Reagents used for 12% SDS PAGE resolving gel 38

Table 2.7: Reagents used for SDS PAGE stacking gel 39

Table 2.8: Reagents used for 10x running buffer for SDS PAGE 40

CHAPTER 3

Table 3.1: Confirmation of functionality of CAP45.G3 single mutants 48

Table 3.2: Reported neutralization breadth and potency of MPER bNAbs 53

Table 3.3: Yields of expressed MPER bNAbs 54

Table 3.4: Neutralization profile of expressed MPER bNAbs 55

Table 3.5: Neutralization of CAP45.G3 wild type and CS-Mut viruses by mature MPER bNAbs 56

Table 3.6: Neutralization of CAP45.G3 wild type and single mutants by mature MPER bNAbs 59

Table 3.7: Neutralization of CAP45.G3 single mutants by CAP248-2B 60

Table 3.8: Neutralization of CAP45.G3 wild type and single mutants by gp120-gp41 interface bNAbs 61

Table 3.9: Neutralization of CAP45.G3 single mutants by bNAbs targeting other epitopes 62

Table 3.10: Neutralization of CAP45.G3 triple mutant by bNAbs targeting all epitopes 67

Table 3.11: Virus infectivity of wild type and CS-Mut V2 special strains 71

Table 3.12: Neutralization of T250-4 wild type and T250-4 CS-Mut viruses by mature MPER bNAbs 74

Table 3.13: Neutralization of CAP256 SU wild type and CAP256 SU CS-Mut viruses by mature bNAbs 75

Table 3.14: Neutralization of WITO.33 wild type and WITO.33 CS-Mut viruses by mature MPER bNAbs 77

Table 3.15: Neutralization of wild type and CS-Mut V2 special strain viruses by germline reverted MPER bNAbs 77

Table 3.16: Neutralization of wild type and CS-Mut V2 special strain viruses by bNAbs targeting other epitopes 79

Table 3.17: Neutralization of V2 “special strain” wild type and CS-Mut by non-broad plasma 81

Amino Acid Abbreviations

Amino Acid	Three-Letter code	One-Letter code
Alanine	Ala	A
Arginine	Arg	R
Asparagine	Asn	N
Aspartic acid	Asp	D
Cysteine	Cys	C
Glutamic acid	Glu	E
Glutamine	Gln	Q
Glycine	Gly	G
Histidine	His	H
Isoleucine	Ile	I
Leucine	Leu	L
Lysine	Lys	K
Methionine	Met	M
Phenylalanine	Phe	F
Proline	Pro	P
Serine	Ser	S
Threonine	Thr	T
Tryptophan	Trp	W
Tyrosine	Tyr	Y
Valine	Val	V

List of Abbreviations

AIDS	Acquired Immuno Deficiency Syndrome
ART	Anti-Retroviral Therapy
ATP	Adenosine Triphosphate
bNAbs	Broadly Neutralizing Antibodies
C1-C5	Constant regions 1-5 of gp120
CAP	CAPRISA
CAPRISA	Centre for the AIDS Program of Research in South Africa
CBB	Coomasie brilliant blue
CCR5	C-C chemokine receptor type 5
CD4	Cluster of differentiation 4
CD4bs	CD4 binding site
cDNA	Complementary DNA
CDRH3	Complementarity Determining Region 3 (Heavy Chain)
CDRL3	Complementarity Determining Region 3 (Light Chain)
CHR	C-terminal heptad repeat
CS	Cleavage Site
CS-Mut	Cleavage site mutant (six mutations)
CXCR4	C-X-C chemokine receptor type 4
DEAE dextran	Diethylaminoethyl dextran
DMEM	Dulbecco's Modified Eagle Medium
DNA	Deoxyribonucleic Acid
Env	Envelope glycoprotein
dNTPs	Deoxynucleoside triphosphates
dsDNA	Double stranded DNA
E. coli	*Escherichia coli*
FP	Fusion peptide

Gag	Group specific antigen
Gp41	Glycoprotein 41kDa
Gp120	Glycoprotein 120kDa
HEK	Human embryonic kidney
HIV-1	Human immunodeficiency virus type 1
ID	Immunodominant
IgG	Immunoglobulin G
Indels	Insertions and deletions
LB	Lysogeny broth
mAb	Monoclonal antibody
MPER	Membrane Proximal External Region
nAbs	Neutralizing antibodies
Nef	Negative regulatory factor
NHR	N-terminal heptad repeat
NIH	National Institutes of Health
PBS	Phosphate buffered saline
PCR	Polymerase chain reaction
PEI	Polyethyleneimine
PR	Polar region
RLUs	Relative light units
RNA	Ribonucleic acid
RSC3	Resurfaced stabilised core 3
SDS PAGE	Sodium dodecyl sulfate poly-acrylamide gel electrophoresis
SHM	Somatic hyper mutation
SOC	Super optimized broth with catabolite repression
ssRNA	Single stranded RNA
SU	Superinfecting
TEMED	Tetramethylethylenediamine
T/F	Transmitted/Founder

UNAIDS	United Nations program on HIV/AIDS
V1-V5	Variable regions of gp120
Vif	Viral infectivity factor
Vpr	Viral protein r

CHAPTER 1: INTRODUCTION

1.1 The HIV/AIDS Pandemic and the need for a vaccine

The HIV/AIDS pandemic is of great concern globally, and is a major focus of vaccine research. In 2015, global estimates showed that about 36.9 million people were living with HIV (1). Since the initial identification of the disease, about 78 million people have become infected, and 39 million people have died from AIDS related conditions (1). A vaccine is therefore a top priority, particularly in southern Africa where millions are affected directly or indirectly by the disease, and thousands more are infected every day. In South Africa alone, an estimated 6.8 million people are currently living with HIV (1).

HIV vaccine researchers worldwide have tested many different approaches but a vaccine that offers significant protection is yet to become a reality (2-5). To date, five phase 3 HIV-1 vaccine trials have been conducted, of which four showed no evidence of protection (2). In 2009, the RV144 trial conducted in Thailand was the first to show some level of efficacy (preventing 31.2% of infections) (6). Although the moderate level of efficacy was not enough for the deployment of the vaccine, the success of the RV144 trial suggested that a preventative vaccine could be made. The mechanism of protection in this trial, however, is unclear. Although antibodies targeting the V1V2 region of the HIV-1 envelope glycoprotein have been shown to be a correlate of protection, there was no evidence of neutralizing antibodies, which block viral infection and are the basis of many other successful vaccines (7, 8).

A trial similar to the RV144 trial is currently being repeated in South Africa, mainly to determine if differences in geographical location, prevalence and viral subtype may lead to a difference in efficacy compared to the Thailand trial. In addition, the P5 partnership is conducting a wide range of small-scale research trials based on the findings of RV144, to attempt to improve the potency and durability of responses, especially as protection was highest early after vaccination (6). However, it is widely believed that a more efficacious vaccine may require broadly neutralizing antibodies (bNAbs), described below, which were not elicited by this regimen.

Different subtypes of the virus are predominant in different geographical areas. Subtype B viruses for example are is the predominant subtype in the United States of America and Europe (9). Subtype C is prevalent in India and Southern Africa, and new

infections in this region are highly likely to be of that subtype. In order to better design a vaccine that is specifically aimed at subtype C infections, studies have to be focused on viruses of this subtype along with studies of bNAbs that show broader and more potent neutralization of subtype C viruses (10-12).

1.2 Transmission of the virus

HIV is primarily transmitted through exposure at mucosal surfaces as well as through percutaneous inoculation (10). In order to assess the transmission of HIV, factors including viral and host genetics, epidemiology, animal studies and risk factors are well studied, and have contributed to much of the current knowledge on the subject (13).

Several risk factors determine if HIV is transmitted, for example, high viral loads in the infecting partner are associated with increased risk of transmission (10). Sexual partners that are on Anti-Retroviral Therapy (ART) generally have a suppressed viral load and thus have a lower chance of transmitting the virus compared to those who are not (10, 14-16). Genital inflammation has also recently been shown to increase the risk of infection in women (17).

Initially following transmission, the virus is not detectable in the plasma. This is called the eclipse phase of infection (10, 13). During this phase, the virus is replicating in the CD4+ T-cells of the mucosa, submucosa and draining lymphatic system (18, 19). After approximately 7-21 days, the virus becomes detectable in the plasma, and thereafter replication is exponential (10, 20). Detecting the virus as soon as possible after infection is of the utmost importance for several reasons, which include blood transfusions, early treatment for the infected person and organ donations. Nucleic acid methods are available for this as they detect viral sequences in concentrations as low as 1-5 RNA copies per milliliter (10, 21).

Several studies have been conducted into the nature of the actual transmission event as well as that of the infecting viral variant(s). A viral variant “bottleneck” model was confirmed in most of the studies conducted (10, 22). This model suggests that although the infected partner is exposed to diverse circulating viral quasi-species, only

a single or very few viruses establish infection in the exposed partner (22). In 80% of heterosexual transmissions, only one viral variant initiates a productive infection, and the newly infected individual has limited viral diversity at this initial stage of infection (**Figure 1.1**) (10, 23, 24). This raised the question of whether the transmitted/founder (T/F) virus exhibits enhanced viral fitness or other features that accounts for its preferential transmission, or whether this is simply a stochastic event that is the result of stringent mucosal defenses (25).

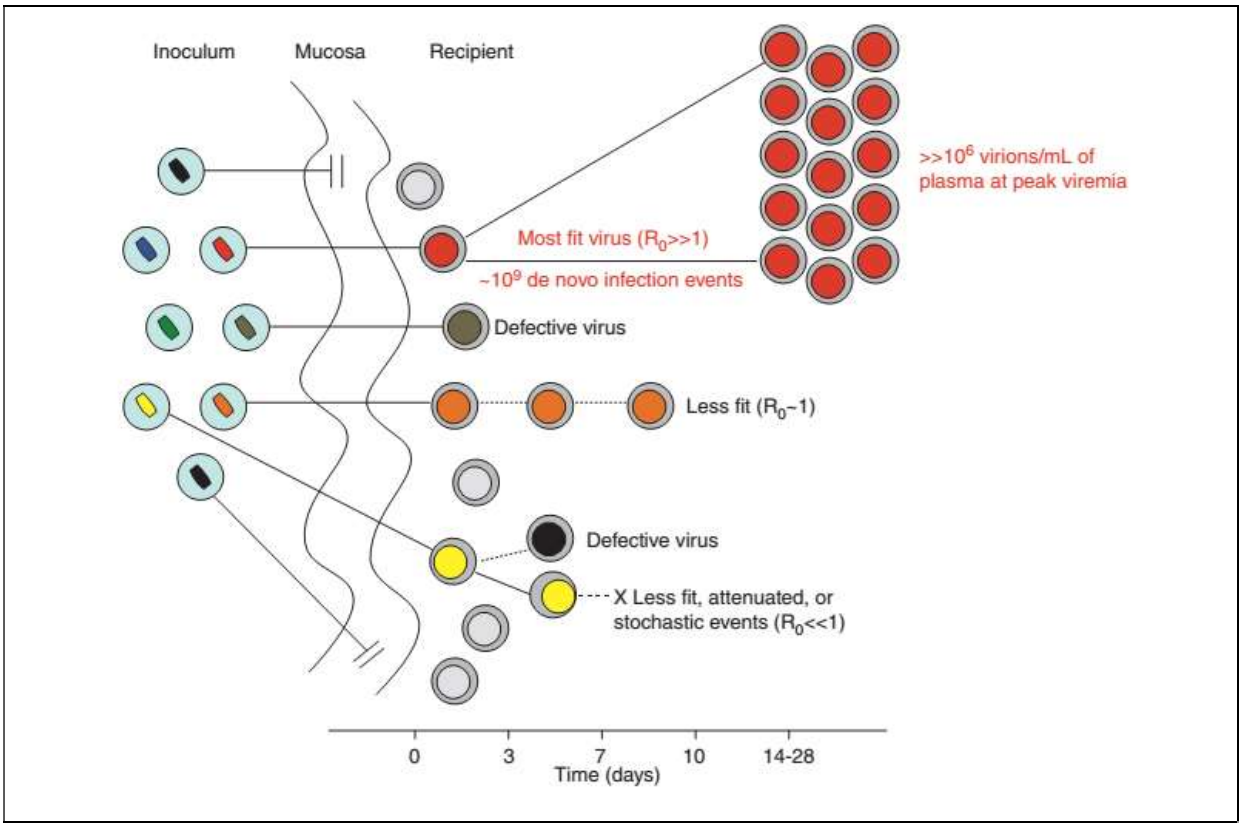

Figure 1.1: A flow chart showing the process by which a viral variant is selected to propagate in a newly infected individual. Blue circle with colored rectangular blocks indicate the initial inoculum from the infecting partner. Once these viruses cross the mucosa, defective and fit viruses are shown with colored circles. R_0 is the reproductive ratio. $R_0 > 1$ leads to productive clinical infection, whereas $R_0 < 1$ results in an extinguished infection. The red circle represents the fittest virus, which then becomes the T/F and propagates (9).

In most cases that have been studied, the T/F virus exhibited a tier 2 or tier 3 phenotype, meaning these viruses are not easily neutralized by host antibodies (10, 25, 26). Of the two cellular receptors that HIV uses to enter the host cells, (C-C

chemokine receptor type 5 (CCR5) and C-X-C chemokine receptor type 4 (CXCR4)), the T/F virus usually has CCR5 tropism (10, 27).

Several genotypic studies have assessed differences between the T/F viruses in a number of individuals and other (non-transmitted) variants from the infecting individual (23, 28). These studies have shown that T/F viruses show increased resistance to interferon mediated antiviral activity within the mucosal surface, potentially providing a transmission advantage (23). Apart from these findings, there have been no obvious traits that clearly differentiate T/F viruses from others, and there is thus no obvious viral "signal" that can be used to prevent infection (23, 29).

1.3 The structure and replication of the virus

HIV belongs to the family *Retroviridae,* and the *Lentivirus* genus. Viruses belonging to this family share the same replication process, described below, and the fact that disease progression is slow once a patient is infected (30, 31). The virion is spherical in shape (approximately 100-130 nm in diameter) and is surrounded by an outer envelope, which is made up of phospholipids and is derived from the host's cell membrane (32-34) (**Figure 1.2**).

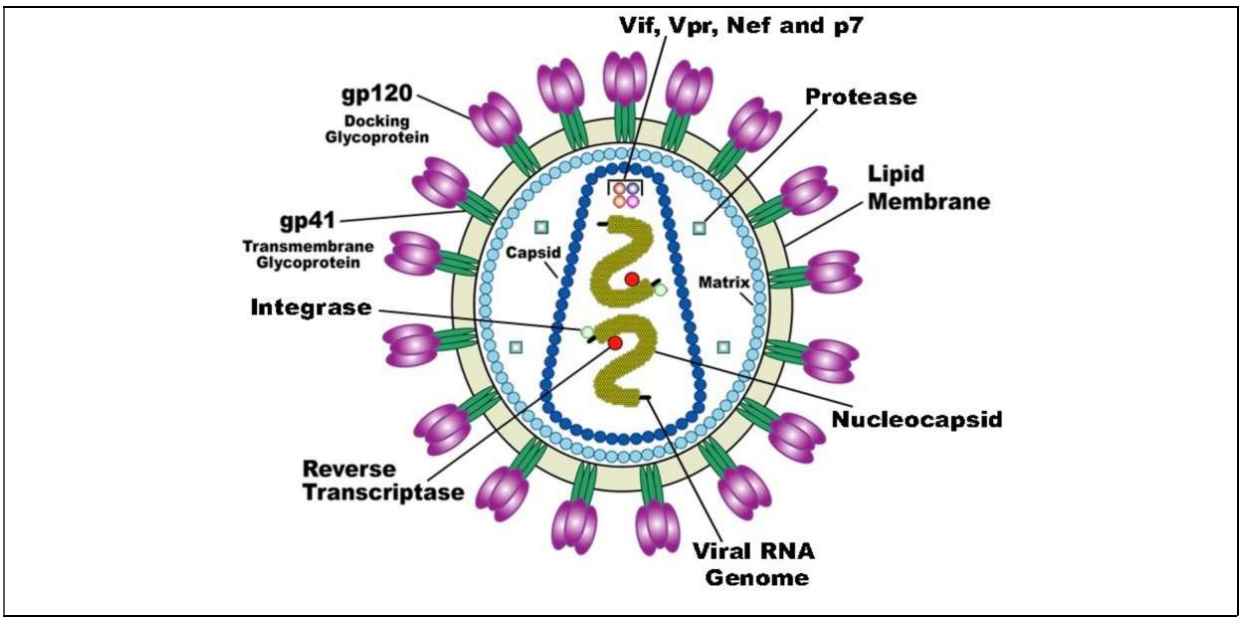

Figure 1.2: The structure of the Human Immunodeficiency Virus (HIV). Vif, Vpr, Nef and p7 are accessory proteins that are coded for by the viral RNA (35).

Embedded in the viral envelope are a number of envelope (Env) glycoproteins, composed of gp120 and gp41 (35, 36). Inside the virus envelope is the capsid, which encloses the viral RNA as well as proteins that are crucial for the replication and survival of the virus in the host (32). Each viral particle has two strands of RNA, and possesses three important enzymes; reverse transcriptase, protease and integrase (30, 35). Various accessory proteins, namely Vif (viral infectivity factor), Vpr (viral protein r) and Nef (negative regulatory factor), are key components of the nucleocapsid.

In order to replicate, the gp120 component of the envelope binds to the primary viral receptor, CD4. This alters the conformation of the envelope trimer to allow subsequent binding to a co-receptor (either CCR5 or CXCR4) (35, 36). Co-receptor binding induces additional conformational changes to the envelope trimer that exposes the trans-membrane protein of gp41 which was originally hidden by gp120 (30, 35). The hydrophobic fusion protein on the trans-membrane domain of gp41 makes first contact with the host cell membrane when it is inserted into the cell (35). A helical structure formed by rearrangement of the gp41 trimeric protein merges the cellular and viral membranes, resulting in the emptying of the viral contents into the cell (34, 37) (**Figure 1.3**).

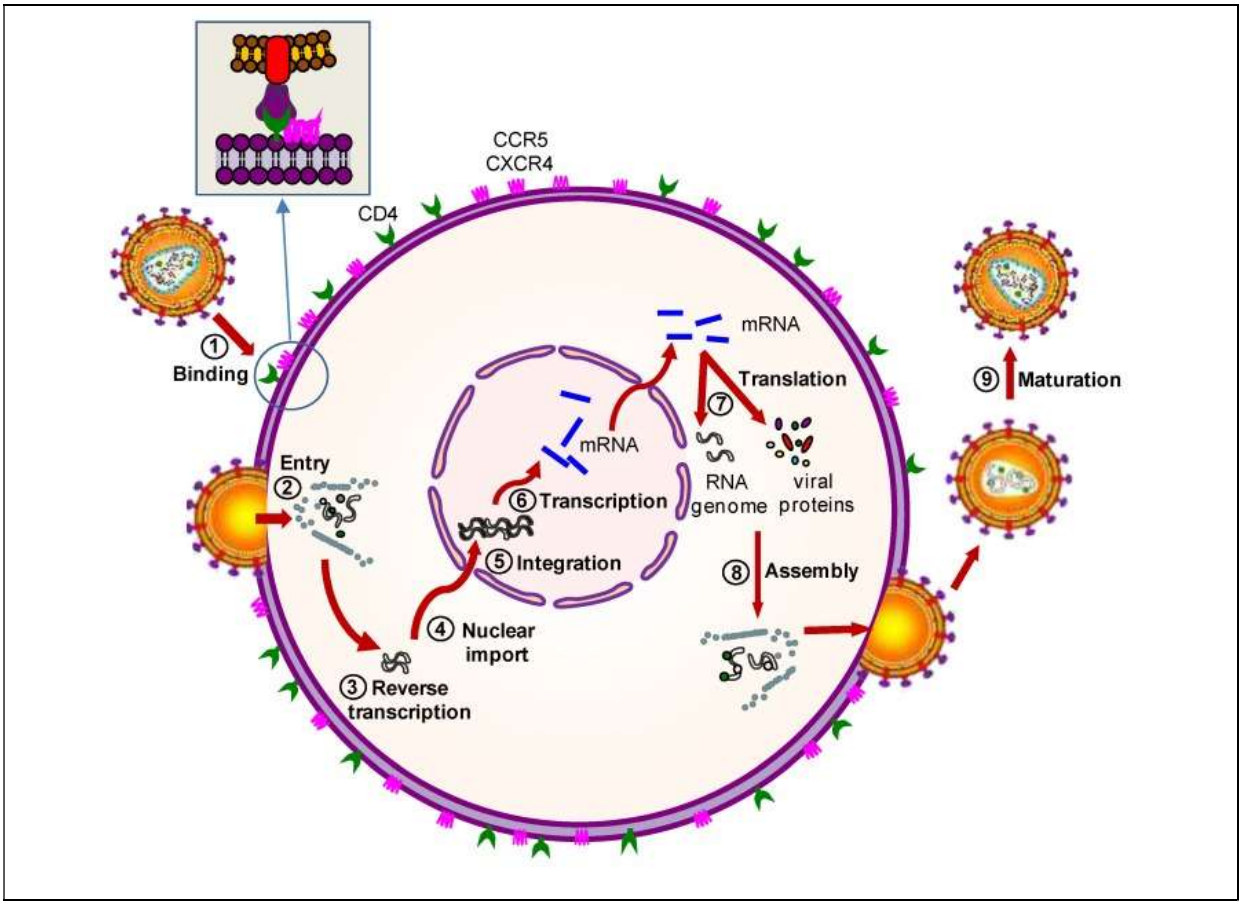

Figure 1.3: The replication cycle of HIV-1. Numbers indicate each stage of the life cycle as follows: 1) Binding of gp120 to the receptor and co-receptor, 2) Entry of viral contents into host cell, 3) Reverse transcription of viral RNA into dsDNA, 4) Importation of viral DNA into host nucleus, 5) Integration of viral dsDNA into the host genome 6) Transcription of proviral DNA into RNA 7) Translation of viral RNA into necessary viral proteins 8) Assembly and budding of the new, immature virion 9) Maturation into an infectious virion (38).

Following its entry into the host cell, the viral capsid dissociates and the single stranded viral RNA is firstly reverse transcribed into ssDNA, then transcribed into dsDNA. Integrase subsequently merges the viral genome with the host DNA (30, 39). This process of integration is how the virus forms what is referred to as the “reservoir” (latent phase), which is not detectable in the blood. The presence of this reservoir explains why it is so difficult to eliminate HIV from infected individuals, and is the basis of ongoing research aimed at curing HIV infected people (30, 40, 41). For the purpose of continued viral replication, proviral DNA (viral DNA that has been integrated into the host genome) is transcribed into the HIV ssRNA genome by the host DNA polymerase II. The transcribed RNA is subsequently translated into viral proteins that include Tat (trans-activator of transmission), Rev and Nef, which, together with the viral RNA are assembled at the cell membrane and bud off as a non-infectious, immature form of

new virions (30, 35). Immediately following budding, the protease is activated to cleave gag (group specific antigen) and gag-pol precursors into mature components. Protein configuration is reorganized and a mature, infectious virion results (35, 41).

1.3.1 The structure of the envelope glycoprotein (Env)

On the surface of the viral envelope are several Env glycoprotein spikes (30) (**Figure 1.4**). These are responsible for the entry of the virus into cells and are the sole target of the host antibodies that are the subject of this thesis (36, 42). Env is a hetero-trimer composed of three gp120 molecules that are non-covalently bound to three gp41 molecules (43, 44). These gp120 and gp41 proteins are cleaved by the proteolytic host enzyme furin from a precursor gp160 molecule (43, 44). Cysteine residues along both gp41 and gp120 form disulphide bridges that are necessary for the formation and stability of the trimer structure (42, 45, 46).

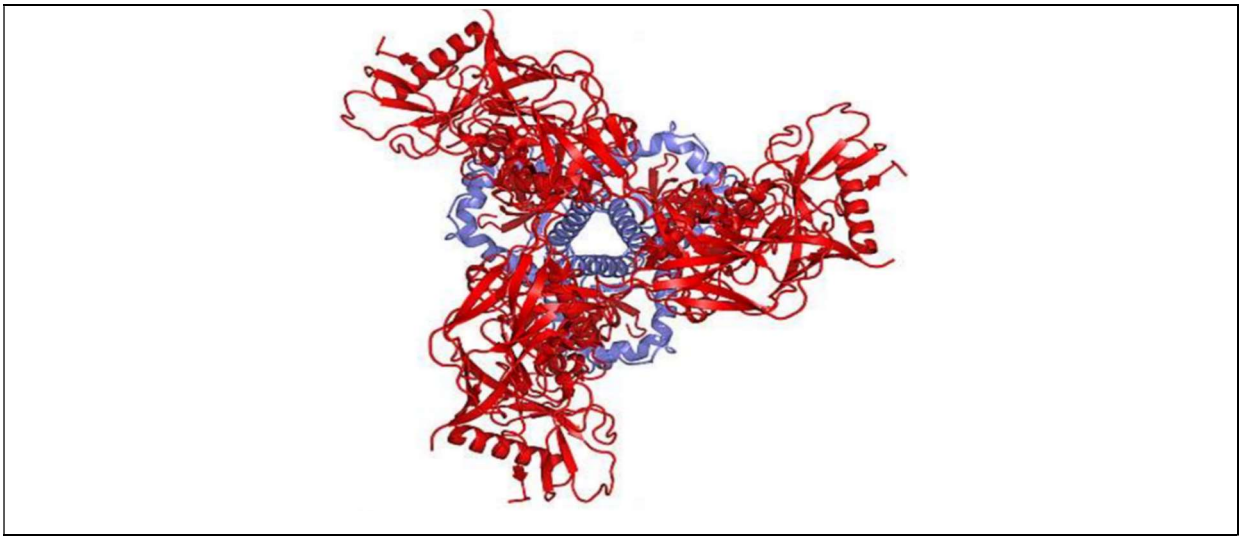

Figure 1.4: This structure portrays the arrangement of the Env glycoprotein in a closed pre-fusion state. Red shows the three gp120 molecules and blue shows the three gp41 molecules (47).

The Env glycoproteins mediate viral entry in two stages. The initial virus-cell engagement occurs by binding of gp120 to CD4 (the major viral receptor), and a co-receptor that is usually CCR5 (**Figure 1.3**). In some cases, alternate co-receptors can be used, and viruses able to use different co-receptors (such as CXCR4) often emerge

late in infection (37). After viral binding to receptors and several conformational changes, the gp41 enables fusion of the host and viral membranes.

The structure of Env has been a challenge to study in its native form due to the fact that the gp120 and gp41 components readily dissociate into their monomeric forms (42, 43). This area of research has been enormously active in recent years, and has resulted in the generation of engineered soluble trimers that are often derived from unusually stable viral isolates, and further engineered to be stable through the introduction of several cysteine residues (at positions 501C-605C, referred to as SOS) along with a mutation in the first heptad repeat of gp41 (I559P) (36, 48, 49). These next generation "SOSIP" trimers have reignited the HIV vaccine field, providing the basis of immunogen design.

1.3.2 Gp120 structure and function

Gp120, sometimes referred to as the docking protein, is responsible for the receptor binding that "docks" the virus onto the host cell in preparation for fusion (50, 51). Gp120 binds to CD4, which leads to a conformational change that triggers binding to a co-receptor (either CCR5 or CXCR4) (42, 43). Co-receptor binding further triggers another conformational change which facilitates membrane fusion (42). Gp120 consists of an "inner domain" and an "outer domain" joined by a bridging sheet (43). Gp120 is a highly variable protein in terms of amino acid sequence, varying by as much as 30% between individuals. This variation in sequence is due to the error prone nature of the reverse transcriptase. Gp120 consists of hyper-variable loops, termed V1 to V5, each of which is bracketed by cysteine residues that form stabilizing disulphide bridges (50, 52) (**Figure 1.5**) Variable regions are interspersed by a number of relatively conserved regions termed C1 to C5 (43, 50).

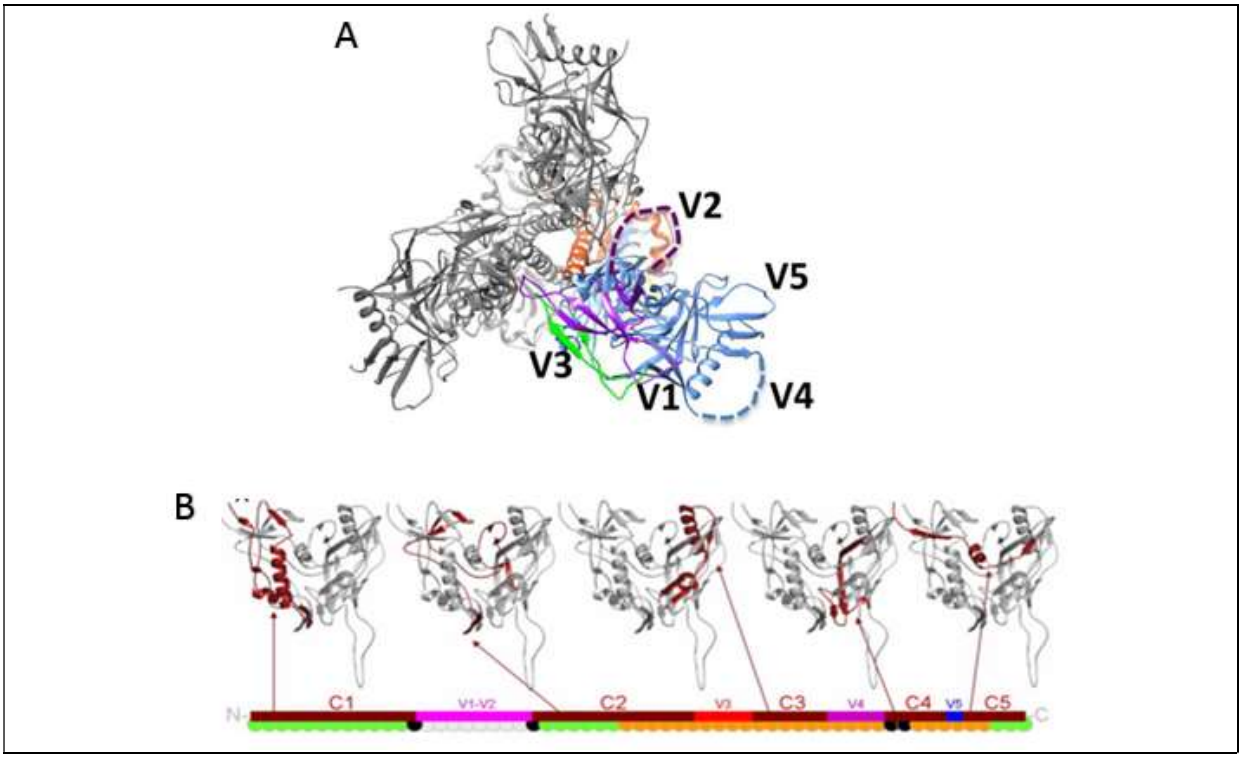

Figure 1.5: Conformation of the five gp120 hypervariable loops: A) Within the trimer structure and B) In a linear schematic showing the order of the variable and constant regions of gp120 (Adapted from Wibmer, 2011 and Ward *et a*l, 2015).

In the trimeric conformation, the hyper-variable loops are easily accessible to neutralizing antibodies (described below) and they shield the less accessible conserved regions (43). The V1 to V3 variable loops are positioned on the trimer apex in the trimer's pre-fusion state (43). The V1 and V2 domains tolerate variation in both sequence and length (including deletions and insertions), without compromising the structure of the trimer as a whole (43). This is due to the fact that each of these variable regions extends out of the envelope spike at the apex (43). The three variable loops interact with each other to stabilize each protomer, while V4 and V5 protrude out of the structure and do not make contact with the rest of the variable loops (43).

The outer domain of gp120 is heavily glycosylated, such that half of the mass of the protein in fact comes from glycan residues (53). This dense glycan shield (a median of 93 *N*-linked glycans on the trimer spike) was once thought to protect it from the host immune response, and indeed the high levels of glycans do limit antigenicity (43, 54). However, subsequent work has showed that many human bNAbs (described below) utilize these glycans in their neutralization of the virus (43, 55). The glycans in this region are made up of both high mannose glycans as well as other complex glycans,

and there is substantial heterogeneity in glycan processing between and within viral envelopes that add to the complexity of this protein (56). The virus escapes the humoral immune system by deleting, adding or moving glycans from antibody epitopes, especially in regions with high variability where the glycans are relatively less conserved. Several glycosylated sites that are highly conserved have been shown to be associated with bNAb epitopes (56, 57). Examples of these are the highly conserved glycans at N611 and N637 that are key elements of the PGT151 antibody epitope along with the glycan at position N88, that forms part of the 35O22 antibody epitope (58, 59).

1.3.3 Gp41 structure and function

The gp41 protein anchors the Env trimer onto the viral envelope and plays a crucial role in fusion of the virus and the host cell (46, 60). It can be divided into three distinct regions, that is, the ectodomain, the transmembrane domain and the cytoplasmic tail (**Figure 1.6**) (61-63). It is relatively conserved and less glycosylated compared to gp120, due to its greater functional constraints (61, 64).

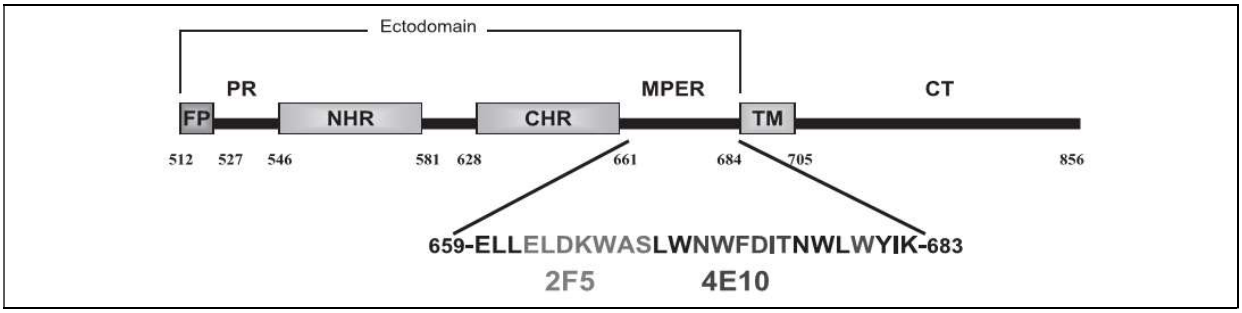

Figure 1.6: Schematic showing the different regions of gp41. Amino acid numbering is based on the HIV-1 strain HXB2. The different regions are depicted as follows: FP: Fusion protein; PR: Polar region; NHR: N-terminal heptad repeat; CHR: C-terminal heptad repeat; MPER: Membrane proximal external region; TM: Trans-membrane domain; CT: Cytoplasmic tail (61).

The ectodomain of gp41 can be divided into further distinct regions that are specialized for different functions during infection. These include the hydrophobic N-terminus fusion peptide (FP), the polar region (PR), the two alpha helix sheets termed the N

and C terminus heptad repeats (NHR and CHR respectively), and the tryptophan rich membrane proximal external region (MPER) (**Figure 1.6**) (46, 61).

In the pre-fusion state of the Env trimer, the fusion peptide, recently found to be a target of the bNAb VRC34.01, is well hidden within the gp120/gp41 quaternary structure, and is only exposed after CD4 binding by gp120 (42, 61, 65). The MPER is made up of the last 24 amino acids of gp41's ectodomain, and is a well conserved epitope of some well-known neutralizing antibodies such as 2F5 and 4E10 (**Figure 1.6**) (42). Studies have shown that both the fusion peptide and the MPER are necessary for membrane fusion, and that the MPER is necessary for viral entry. It is, however, currently unclear how the MPER is involved in the process of fusion (42, 61, 63). The transmembrane region of gp41 spans the viral envelope and is necessary for the fusion process, and the cytoplasmic tail is found inside the viral particle (42).

1.4 The human humoral immune response and HIV

Within a few months of infection, all infected individuals develop autologous neutralizing antibodies (AnAbs) that generally target the sequence variable loops of gp120 and for this reason are largely strain-specific. Mapping studies have shown these antibodies largely target the V1V2 and (in subtype C viruses) the C3V4 regions of the viral envelope (66-68). Subtype C envelopes are different from their counterparts in that the V3 region is more conserved than most other subtypes, while the C3 region is highly variable (69, 70).

The virus, however, rapidly escapes the immune response, by acquiring mutations, insertions and deletions within the antibody epitopes (71). This high level of mutation is achieved through an error prone reverse transcriptase which is responsible for the highly variable nature of the envelope glycoprotein Env (72). For this reason, despite potent autologous neutralizing responses, at any given time point, the circulating virus will be resistant to the contemporaneous neutralizing antibodies (69). These strain-specific antibodies are limited interest for vaccine design.

1.4.1 Broadly neutralizing antibodies

Although most people develop only strain-specific neutralizing antibodies (AnAbs), approximately 5-20% of infected people have been shown to develop bNAbs (3, 71, 73, 74). BNAbs are able to neutralize a wide range of globally circulating viral strains, and as such these antibodies are a major focus for HIV vaccine design (75).

BNAbs that have been isolated to date exhibit a wide range of breadth and potency when tested against global viral isolates. Some of the broadest and most potent bNAbs to date include 10E8, which targets the MPER epitope and neutralizes over 90% of global viral isolates, VRC01, which targets the CD4bs and neutralizes over 70% of global viruses and CAP256-VRC26.25 which neutralizes over 70% of global viruses and is extremely potent (76, 77). These and other bNAbs have, over the years, shaped much of the knowledge we have on HIV-1 neutralization breadth.

It is not entirely clear how the individuals who develop breath do so, but several factors that are associated with development of breadth have been identified. One such factor is high viral load, which likely presents high antigenic stimulation, leading to the development of breadth (73, 78). Viral load in early infection (up to six months post infection) seems to influence the development of breadth along with a low count of CD4+ T-cells (73, 79). It can therefore be said that early infection events determine the ability to develop breadth in chronic infection (80). Factors like antigen load, the duration of exposure to the virus as well as viral diversity link the development of breadth to the antigen (76, 81-83). Moreover, subtype specific envelope features have been shown to influence the nature of bNAbs. Specifically CD4 binding site directed bNAbs were associated with subtype B infection, whereas V2 glycan specific bNAbs developed in individuals with non-subtype B infection (83). In addition to subtype, a specific HLA type was associated with development of breadth (83, 84).

In recent years, technological advancement has allowed for isolation and characterization of a wide range of bNAbs which has improved our understanding of their development, epitopes and neutralization profiles (85, 86). Techniques such as identification and culturing of specific memory B cells have opened up new avenues for the isolation of bNAbs from infected donors (86). A combination of binding and neutralization assays was used in studies by Walker and colleagues to assess the

properties of memory B cell clones and subsequently isolate a number of bNAbs (82, 87). Moreover, an artificial antigen that mimics the CD4bs (termed the resurfaced stabilized core 3) was designed and used to isolate B cells from donors that exhibited CD4bs-directed bNAbs (88). Methods of isolating and characterizing bNAbs are still a subject of intense research and improvements are constantly being made (85). Since the gp120 and gp41 protomers have been known to dissociate in solution, the engineering of stable forms of soluble envelope trimer represents one of the biggest leaps that vaccine research has taken forward in recent years (89). The BG505 $SOSIP_{664}$ was engineered specifically to mimic the pre-fusion HIV-1 native trimer in solution (36). The native-like nature of the trimer enabled the binding of neutralizing antibodies well, while generally excluding the non-neutralizing antibodies that target the immunodominant, V3 region of the envelope (89-91). Further engineering of this and other such trimers is being looked into for the isolation of bNAbs (89, 92) as well as for the design of immunogens to use in the quest for an HIV-1 vaccine (89).

The development of breadth, however, does not prevent disease progression as the virus is able to escape the broadest of responses over time (80, 81, 93). This has been documented in many cohorts including the Centre for the Program for AIDS research in South Africa (CAPRISA) where escape from several bNAbs have been defined. For example, the study of donor CAP248 from CAPRISA that was previously conducted in our lab is one example that looked at the nature of viral escape from bNAbs that mapped to an epitope at the cleavage site of the viral envelope (94).

1.4.2 Targets of broadly neutralizing antibodies

Understanding the epitopes of bNAbs defines viral vulnerabilities that may be useful for vaccine design. To date, five bNAb epitopes have been identified: the CD4 binding site (CD4bs), the membrane proximal external region (MPER), the V2 site, the V3-glycan supersite and the gp120-gp41 interface (**Figure 1.7**) (85, 95, 96). This study has focused on the MPER and gp120-gp41 interface, which are described in more detail below.

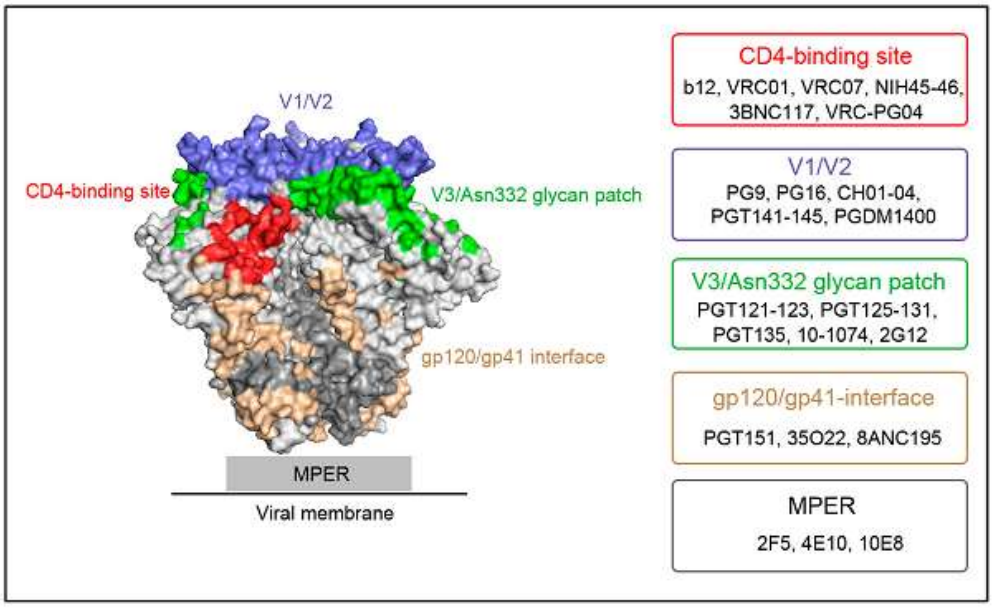

Figure 1.7: Envelope trimer structure portraying the five known epitopes of HIV-1 bNAbs. Epitopes are color coded as follows: Red for CD4binding site, blue for V1V2, green for V3, brown for gp120/gp41 interface and the grey box for MPER (85)

1.4.3 The Membrane Proximal External Region (MPER) bNAb epitope

The MPER is the most conserved of the known HIV-1 bNAb epitopes (97, 98). It is a linear, alpha helical epitope composed of the last twenty-four amino acids of the C-terminal region of the gp41 ectodomain. The hydrophobicity of the MPER is owed to its high aromatic tryptophan content (99), an attribute that is necessary given that the MPER is associated with fusion of the virus with the host membrane (61). Substitution of the tryptophan residues has been associated with poor incorporation of gp41 into virions (61). It is believed that this hydrophobicity is part of the reason why most of the known MPER bNAbs have shown considerable levels of auto-reactivity (100).

Monoclonal antibody 10E8 is the only MPER bNAb that does not exhibit any autoreactivity (101). The MPER was initially considered not strongly immunogenic, but several studies have shown that it is immunogenic in infection, and a number of infected people show some MPER specificity (84, 102, 103). It is believed that due to its conserved nature, it is an ideal target for an HIV vaccine (101, 104).

A number of MPER targeting bNAbs, including 10E8, 4E10, M66.6, 2F5, Z13e1 and DH511 have been isolated and studied in recent years. 10E8 and 4E10 target an

overlapping epitope on gp41, with dependence on different residues (both include N671 and T676) along their epitopes (105). M66.6 and 2F5 have a similar epitope, with dependence on the D664, K665 and W666 residues along gp41 (101, 105). The more recently isolated antibody, DH511 has been termed “10E8-like” in its neutralization profile and in the fact that it targets the same epitope as 10E8. Z13e1 requires residues N671 and D674 for binding. The six bNAbs target subtly different specific epitopes within the MPER.

The neutralization breadth and potency of the MPER bNAbs is highly varied as shown in several studies that were conducted against globally circulating virus strains (106). Most of the MPER bNAbs showed breadth of over 90%, with the exception of M66.6, which was only 57% broad. The two most potent MPER antibodies are 10E8 and DH511, with geometric mean IC_{50} values below 0.5 µg/ml (101, 107). Although 4E10 has a breadth of over 90%, it is the least potent of all the MPER bNAbs, with a geometric mean IC_{50} of 8.46 µg/ml. Neutralization data is limited for Z13e1 and thus no significant panel has described in detail how broad or potent it is (101, 107).

Despite its appeal as a target, no vaccine has been able to elicit MPER directed responses, and research into this epitope is necessary from many angles. This is the basis of the research conducted in this dissertation.

1.4.4 The gp120-gp41 Interface bNAb epitope

The gp120-gp41 interface has only recently been shown to be an epitope for bNAbs. Several bNAbs that were recently isolated were found to bind residues on both gp120 and gp41 of the HIV-1 envelope trimer spike in their neutralization of the HIV-1 virus (59, 65, 94, 108). Different bNAbs target different residues within this region, and bind varying numbers of protomers on the envelope trimer. The PGT151 family of bNAbs, for example, binds residues from both inter-protomer and intra-protomer gp120 and gp41 subunits on the native, cleaved, trimer structure. The epitope of the bNAbs belonging to this family is thus neither present on isolated gp120 and gp41 subunits or on uncleaved gp160 proteins (59, 108).

One of the most recently identified gp120-gp41 interface targeting bNAbs is VRC34.01, which binds residues 512 through to 519 on the fusion peptide of gp41

along with the glycan linked residue N88 on gp120 (65). The mode of neutralization employed by VRC34.01 is targeted at the pre-fusion trimer, and this monoclonal antibody (mAb) was shown to stabilize the trimer in an intermediate conformation that impedes CD4 binding (65). The gp120-gp41 interface is a subject of intense research currently as a site of key vulnerability in the virus, and especially the fairly new fusion peptide epitope holds a high level of potential for vaccine design (65).

A recent study in our lab described the isolation of a broad gp120-gp41 interface bNAb that targets a novel epitope within this region (94). As is characteristic of bNAbs targeting the interface, the epitope of this bNAb is only present on the native trimer, and not on monomeric gp120 (94). The antibody, termed CAP248-2B, was isolated from CAPRISA donor CAP248 and targets an epitope within the furin cleavage site between gp120 and gp41, a highly conserved region of the envelope (94). To escape this response, the autologous CAP248 viruses inserted a series of six mutations in the furin cleavage site that are rarely seen in globally circulating viruses (94). The unique mutations form an integral part of this study due to their enhancement of viral MPER sensitivity (94).

1.5 The passive use of bNAbs for therapy and vaccination

Several animal studies along with clinical trials have shown that bNAbs are effective when used in therapy, although this protection is short lived (109-111). One study that used the CD4bs bNAb 3BNC117 showed that not only did the antibody reduce viremia when administered to infected people, it also improved the antibody response in some of its recipients (109). Moreover, animal and *in vitro* studies have shown that the use of bNAbs that target different epitopes in combination results in improved reduction of viremia compared to just one (112). Mathematical modelling has further shown that combinations of three or four bNAbs are better in therapy compared to just a double approach, an option that is most likely to be better for vaccination as well (113). Several bNAbs are being looked into for use in passive immunization, although short half-lives are a major roadblock in this regard. The CD4bs bNAb VRC01, for example, is currently being used in a phase two trial in Southern Africa in order to assess the extent of protection in passive immunization (114). Alternative approaches include engineering bNAbs to be more stable and to offer more protection *in vivo* for therapy

and potentially passive vaccination (115). An example of such engineering is the mutation of the CD4bs bNAb VRC01 to improve its half-life *in vivo* (116). The mutant version of VRC01, termed VRC01-LS, exhibited higher affinity for FcRn and a half-life that was threefold that of VRC01 (85, 117). This mutation is being incorporated into many other bNAbs for potential use in passive immunization.

1.6 The developmental pathway for bNAbs: Implications for vaccine design

Although bNAbs have yet to be elicited by vaccination, studies of their development in infected donors have provided clues for vaccination (2, 3, 81). A challenge in eliciting bNAbs is that they tend to have unique properties that other neutralizing antibodies do not generally have. These include insertions or deletions (indels) and a high level of somatic hypermutation (SHM) (118). Inducing these crucial properties by vaccination would provide a necessary leap forward in vaccine design. Unfortunately, this is a puzzle that is yet to be solved.

As bNAbs arise through a complex and prolonged co-evolution with emerging viral variants (76, 81) it has been suggested that perhaps immunogens designed to mimic these viral evolutionary processes may favor the formation of bNAbs (119). The race between virus and antigen begins in the germinal center where the process known as affinity maturation starts (89). During affinity maturation, the earliest, immature forms of antibodies (termed germline or unmutated common ancestors (UCAs)) undergo SHM that culminates in improved antigen binding and anti-pathogen properties (120). The process continues for several cycles in chronic infection, leading to mature antibodies that are highly mutated compared to their earliest precursors (120, 121). It has been argued that perhaps affinity maturation can be guided towards breadth by a suitable vaccine immunogen. In various clinical trials, several different immunogens are given over time in an attempt to stimulate a broad response in a process termed sequential immunization. However, evidence suggests that high SHM does not necessarily mean an antibody will develop breadth (81, 89).

Although sequential immunization approaches show promise in animal studies (122), these studies are highly artificial in that these experiments are generally performed in mice engineered to express high levels of bNAb precursors. In humans, in contrast, a

major roadblock to the elicitation of bNAbs is that their germline precursors are rare, and sometimes have unusual properties. These include relatively long third complementarity determining regions in their heavy chains (CDRH3s) for V2-directed antibodies and relatively short third complementarity determining regions in the light chains (CDRL3s) of VRC01 class CD4bs antibodies (76, 88). In order to carry out experiments with precursors of bNAbs *in vitro*, it is necessary to have an idea of what the germline precursors or UCAs of the bNAbs are. Few studies know the true UCA of any antibody as it is not possible to pinpoint an exact UCA in a patient, or backtrack every characteristic of a bNAb to the starting point. In an attempt to fill this gap, researchers infer germline gene sequences, although the inferred germline revertant antibodies have mature features, such as the CDRH3 which cannot be inferred using bioinformatics (123). Unfortunately, several studies have shown that most HIV-1 isolates are unable to bind to inferred germline forms of bNAbs (124, 125). This indicates that the virus strains that elicited bNAb precursors (which we have termed bNAb-initiating Envs) may have unusual properties (81). Thus bNAb-eliciting immunogens would have to be identified or designed to specifically engage germline forms of the antibodies, which was the overall aim of this project.

One approach to identify such Envs is to study patients who have developed a bNAb response over time so as to identify natural bNAb-initiating envelopes (81). An example is the study from our laboratory of CAPRISA donor CAP256 (81). Longitudinal plasma samples were available from acute infection into chronic infection, and therefore the development of breadth in this patient could be closely followed (81). This allowed the precise identification of the envelope that mostly likely initiated the bNAb antibody lineage in this patient (81). This approach is challenging, requiring detailed sampling and deep sequencing of antibody and virus from acute into chronic infection.

An alternative approach is to identify viruses that are naturally more reactive with bNAb precursors. This entails screening large virus panels, and identifying strains that bind to germline antibodies. This approach was informative in two studies of bNAbs that target the V2 apex region of the Env trimer (126, 127). In a study by Gorman *et* al, a panel of 200 globally circulating virus strains were tested for binding to inferred and actual bNAb precursors (UCAs), as compared to binding to the mature antibodies (126). Of these 200 viruses, ten were shown to bind to the germline precursors of V2-

directed bNAbs, with some of the same strains also identified in a similar parallel study (127).

A third approach is to identify viruses which have unusual exposure of bNAb epitopes, which might be harnessed for HIV vaccine design. This dissertation made use of one such study, based on six viral mutations identified in CAPRISA donor CAP248 at three years post infection (94). The viral escape mutations at the furin cleavage site of the envelope resulted in escape from the CAP248 bNAbs, but also resulted in increased viral sensitivity to bNAbs targeting the MPER epitope (94). Here, we have investigated the possibility of using these naturally identified mutations that result in enhancement of neutralization by MPER targeting bNAbs, to further define the minimal requirements for MPER exposure. We also aimed to harness these mutations, in the context of viruses previously shown to recognize V2 bNAb precursors, to develop immunogens able to trigger two distinct bNAb epitopes.

1.7 Aims and objectives

This study aims to engineer natural HIV viral variants as candidate immunogens to stimulate two classes of bNAbs, through the following specific aims:

1.7.1 Assessing the effect of cleavage site mutations on neutralization by MPER and interface-directed bNAbs

A combination of six simultaneous cleavage site mutations has been shown in our laboratory to enhance neutralization by MPER bNAbs. These mutations are E500K, R502Q, V505M, E507G, R508K and E509G. However, their individual contribution to MPER exposure is not known. We first aimed to assess the effect of these mutations on viral infectivity since they appear at a highly conserved area of the envelope. Secondly, we aimed to test whether all mutations were required simultaneously for MPER exposure. We extended this analysis to additional MPER and gp120-gp41 interface targeting bNAbs to assess the extent of exposure of the MPER and further verify that exposure was epitope-specific by assaying Env mutants against bNAbs to

other epitopes. Moreover, we aimed to look for gross conformational changes using non-neutralizing antibodies.

1.7.2 To design dual germline targeting envelopes for MPER and V2 bNAbs

Using a subset of the envelopes that have previously been shown able to bind V2-directed germline bNAbs, namely ZM233.6, WITO.33, T250-4, A244 and CAP256 SU (126), we aimed to engineer dual germline targeting immunogens to elicit both V2 and MPER antibodies. This was achieved by adding MPER enhancing cleavage site mutations, described above, to V2-reactive envelopes through site-directed mutagenesis. The effect of the mutations on epitope exposure was assessed for both mature and germline reverted MPER antibodies. We also tested the gp120-gp41 interface bNAbs to assess the effects of these mutations at this site, along with the V2, V3 and CD4bs epitopes.

CHAPTER 2: MATERIALS AND METHODS

2.1 Participants

The CAPRISA 002 cohort was established in Durban in 2004 and was recruited from 245 HIV negative women that were considered at high risk of infection (128). The women were followed up regularly, and detection of HIV infection lead to enrollment into the study (128). The study entailed regular clinical follow ups and sample collection from enrolment until the donors commenced antiretroviral therapy. Viral load and CD4 T cell count data were collected at each visit, along with plasma and serum samples. The samples were stored at -80°C. Plasma samples from a total of forty participants were previously tested against a panel of globally circulating HIV-1 strains (73). A donor was defined as having bNAbs when her serum was able to neutralize more than 40% of the viruses in the panel at three years post-infection. Donor CAP248 exhibited 59% breadth when tested at three years, and was therefore defined as a broad neutralizer (129). Subsequent studies of the specificities of her bNAbs and of viral escape pathways were described in a previous study (Wibmer et al, 2017).

2.2 HIV Envelope plasmids

Cloned envelope plasmids used in these studies were available in the laboratory. The CAP45.G3 plasmid contains the transmitted envelope from CAPRISA donor CAP45, cloned into the vector pcDNA 3.1 (Gray et al, 2007). The CAP45.G3 CS-Mut envelope was described in a previous study by Wibmer et al (2017). The CAP256 SU strain was also derived in a previous study from our laboratory, and represents the transmitted superinfecting strain from CAPRISA donor CAP256 (Moore et al, 2013). Strains WITO.33, T250-4, ZM233 and CM244 were kindly provided by the NIH AIDS reagent program (Accession numbers shown in Appendix A).

2.3 Overlapping PCR for the simultaneous introduction of multiple mutations

In instances where the simultaneous introduction of multiple mutations was desired, we used overlapping PCR. The Phusion® polymerase enzyme (Thermo-Scientific, Wilmington, USA) was used with specified PCR protocols from the manufacturer (**Table 2.1**).

Table 2.1: The Phusion® kit thermal cycling conditions used for the overlapping PCR used to mutate HIV-1 envelope plasmids

SEGMENT	CYCLES	TEMPERATURE	TIME
Initial denaturation	1	98°C	30 seconds
Denaturation	25-35	98°C	5-10 seconds
Annealing		68°C	10-30 seconds
Extension		72°C	15-30 seconds/kb
Final extension	1	72°C	5-10 minutes

The Phusion® buffer used in this PCR contains excess magnesium for stabilization of DNA double strands and prevention of random annealing of primers at incorrect template sites. Site-specific synthetic primers were designed to introduce the mutations in two steps. Firstly, the newly designed primers that contained the mutations (forward and reverse primers) were used to generate two different amplicons of Env, namely the front portion before the cleavage site and the end portion after the cleavage site (**Figure 2.1**). These two PCR products were joined in second PCR using specific synthetic primers that amplify the entire Env gene, namely Env M and Env A stop (**Table 2.4**).

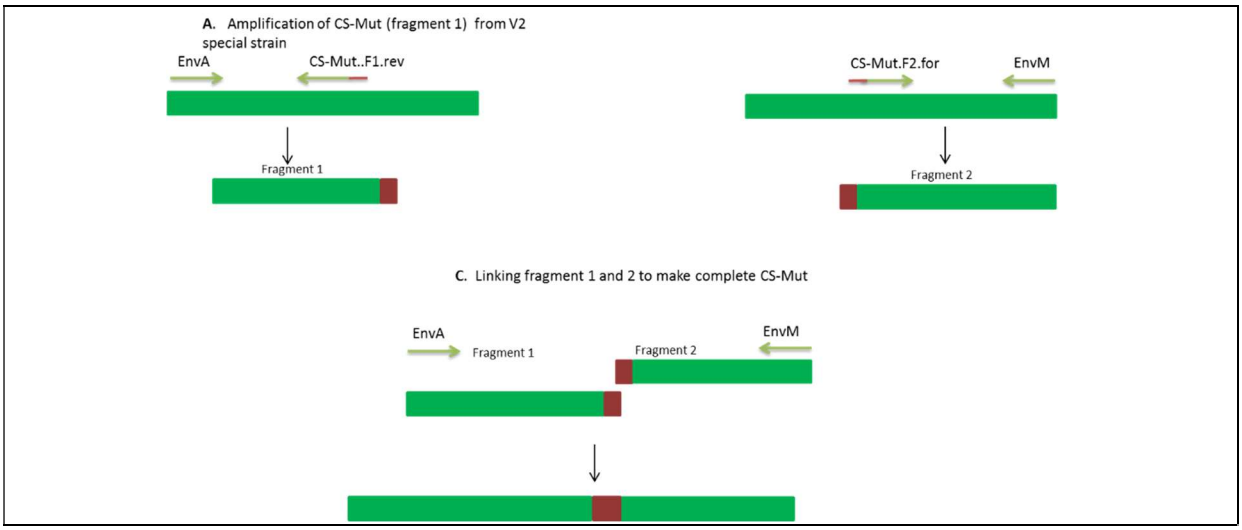

Figure 2.1: Overlapping PCR outline. A) Fragment one is the front portion of the envelope gene. This is amplified with the primer (CS-Mut.F1.rev) that contains half of the CS-Mut mutations (in brown) and Env A, the envelope specific primer. B) Fragment 2 is the gp41 end of the envelope gene and this is amplified using the primer (CS-Mut.F2.for) that contains the second half of the cleavage site mutations (In brown) and the envelope specific primer Env M. C) The products of PCR A and B are joined using primers Env A and Env M to form the full, mutated, envelope gene.

2.4 Gel electrophoresis and purification of DNA from gel

The correct DNA band sizes were determined by using gel electrophoresis to separate PCR products according to their size. The correct bands (1496 base pairs and 1096 base pairs) were identified using a suitable DNA molecular weight marker (Molecular weight marker IV from Roche Applied Sciences, Mannheim, Germany)). Each correct band was extracted from the agarose gel using the Qiagen gel extraction kit (Qiagen, Hilden, Germany). Each PCR reaction was run on a gel and each correct size band was sliced out of the gel. The gel slices were weighed and placed in clean 1.5 ml tubes. They were subsequently dissolved in buffer QG (supplied with the kit). Three volumes of buffer QG were used for one volume of gel. The tubes were incubated at 50°C for ten minutes to completely dissolve the gel. The kit uses a silica membrane to selectively bind DNA as described in section 2.8. Each dissolved gel was added to a spin column with the membrane at the base and spun down at full speed to bind the DNA. Contaminants were removed using 750 µL of wash buffer PE. DNA was eluted from the membrane using 50 µl of buffer EB, also provided with the kit.

Products of the first PCR reactions were quantified using a spectrophotometer and then used as templates for the second, joining PCR. The products of the joining PCR were sized (2,600 base pairs) and gel extracted the same way as those if the first round of PCR. The complete, mutated product for each virus was cloned as described below.

2.5 Cloning of Env genes into mammalian expression vector

Full length envelope genes derived from the overlapping PCR were cloned into a commercial vector, pcDNA3.1/V5-His-TOPO (Invitrogen/Thermo Scientific)) (**Figure 2.2**). The kit allows for quick cloning of *Taq* polymerase PCR products as it is supplied linearized with 3' deoxythymidine (T) overhangs. This enables easy TA cloning of the *Taq* polymerase PCR products, which have a deoxyadenosine (A) overhang. The vector comes bound to topoisomerase I that is obtained from *Vaccinia.* This topoisomerase binds to duplex DNA after the sequence CCCTT and cleaves the phosphodiester bond on one strand. The energy of the bond is used to covalently bind the topoisomerase 1 to the 3' end of the cleaved backbone. The reaction that binds

the PCR product uses the energy released from the covalent bond between the vector and the topoisomerase. This can be easily done as the covalent bond between the topoisomerase and vector DNA can be subsequently reversed by the 5' end of DNA backbone and the topoisomerase released as a result.

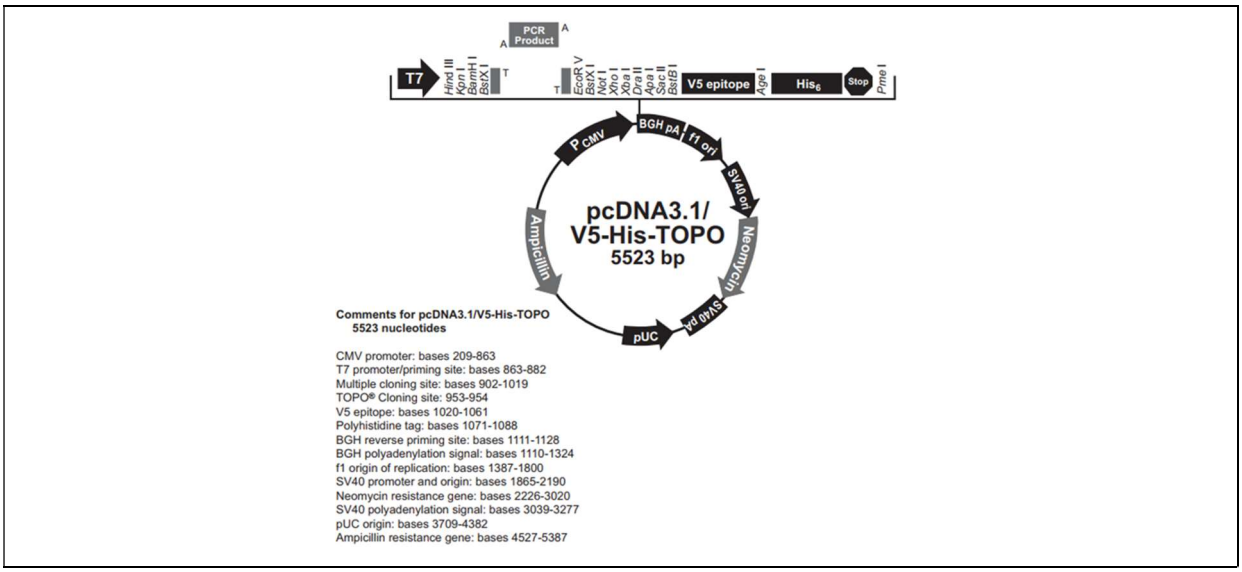

Figure 2.2: Properties of the pcDNA3.1/V5-His-TOPO vector into which HIV envelope genes had previously been cloned (Adapted from Invitrogen).

To clone our PCR product, we combined 2 µl of water, salt solution and 50 ng of the PCR product with the vector and incubated for five minutes at room temperature. The mixture was transformed into ultra-competent *E. coli* as described in section 2.6.

2.6 Transformation

For the purposes of DNA production, each sample was transformed into XL10 Gold Ultra-Competent *E. coli* cells (Agilent technologies, San Francisco, USA). The cells were thawed on ice and exposed to β-mercaptoethanol in order to destroy nucleases that may have reduced transformation efficiency. Pre-chilled tubes were aliquoted with 50 µl of the cells, and 50 ng of the cloned viral DNA was added to each aliquot.

Tubes were heat shocked at 42°C for 30 seconds to increase the fluidity of bacterial membranes and thus allow DNA into the cells, and incubated on ice for 2 minutes. Two hundred and fifty microliters of super optimization broth with catabolite repression (SOC) media was added to each isolate and they were incubated in a shaking incubator at 37° for an hour. For each envelope plasmid, 50 µl of transformed cells was plated on LB (Lysogeny Broth) agar containing ampicillin (100 µg/ml) for selection of transformed cells. These were incubated overnight at 37°C.

2.7 Colony Polymerase Chain Reaction

Colonies were screened for the insert using colony PCR and gel electrophoresis. This method makes use of the DNA inside the bacteria as a template with specific primers that amplify the correct insert.

We ensured that only the inserts that were cloned in the correct orientation were amplified by using the vector specific primer T7 (**Table 2.4**) as a forward primer. The insert specific primer EnvM was used as a reverse primer (**Table 2.4**). Each reaction was a total of 10 µl, containing 1 µl of 10× reaction buffer (supplied with the kit), 1 µl of Magnesium chloride, 0.5 µl 10 mM dNTP, 0.5 µl of each 20 mM primer, 0.2 µl of the Supertherm *Taq* polymerase (JMR Holdings, Commerce Township, USA) and PCR grade distilled water to bring the total volume of each reaction to 10 µl. A 96 well culture plate into which we added 200 µl LB growth media was also prepared so as to keep a stock of viable bacteria from each colony to grow up after screening.

Each colony was picked from the agar plate and dipped first into a PCR well, and then into a corresponding well on the culture plate. The thermal cycling conditions are shown in **Table 2.2**. The product of each colony PCR reaction was screened using gel electrophoresis as described in section 2.4.

Table 2.2: The colony PCR thermal cycling conditions used for screening cloned inserts

SEGMENT	CYCLES	TEMPERATURE	TIME
Initial denaturation	1	94°C	5 minutes
Denaturation	35	94°C	30 seconds
Annealing		55°C	30 seconds
Extension		68°C	1 min/kb (4 minutes)
Final extension	1	68°C	5-10 minutes

For large scale DNA preparations, 200 ml of LB Broth was inoculated using one colony of transformed cells and incubated overnight at 37ºC in a shaking incubator (150 rpm). Small scale preparations were used after mutagenesis and cloning in order to screen a number of colonies for the necessary mutations before large scale preparations of the mutated DNA were made. These were done using the Qiagen QIAprep® spin mini prep kit, and the bacterial colonies were grown in 15 ml of LB broth each.

2.8 Small-scale production of plasmids from cloned envelope DNA

Small-scale preparations of each of the cloned envelopes were produced using the Qiagen plasmid mini prep kit. Each positive colony PCR product was seeded into 15 ml of LB media and incubated in a shaking incubator overnight at 37°C. The bacterial culture was pelleted at 5000 rpm for fifteen minutes and the LB supernatant discarded. The bacterial pellet was re-suspended in 250 µl of re-suspension buffer P1 (provided with the kit). The kit uses a three-step method to purify plasmid DNA from bacterial culture:

Bacteria are lysed under alkaline conditions. A volume of 250 µl of lysis buffer P2 was added to the pelleted cells, and mixed well in order to lyse the cells.

The lysate is neutralized and adjusted to high salt binding conditions. High salt conditions are optimal for selective binding of DNA onto the silica gel membrane used by this kit. A volume of 350 µl neutralization buffer N3 was added, which neutralized the lysate as well as optimized conditions for DNA binding onto the silica membrane.

Upon addition of the neutralization buffer to the lysate, a precipitate (containing proteins and genomic DNA) forms. Plasmid DNA remains in the supernatant. The mix of the protein and genomic DNA precipitate and dissolved plasmid DNA was centrifuged at 13 000 rpm for ten minutes to pellet the precipitate, and the supernatant containing the dissolved plasmid DNA was added to a spin column, which was spun down at high speed to bind the DNA onto the membrane.

Bound DNA is washed and subsequently eluted from the silica membrane. Since the DNA was for subsequent use in mammalian cells, each bound isolate was washed with 700 µl of endotoxin removing buffer. The buffer removes any of the natural bacterial toxins that render the DNA less optimal for use in mammalian cells. The membrane bound DNA was then washed with 700 µl of buffer PE (10 ml provided with the kit and then combined with 40 ml of 99% ethanol) to remove any salts that may have been bound to the membrane. The DNA was eluted in 50 µl buffer EB and quantified on a NanoDrop® ND-1000 Spectrophotometer (Thermo Scientific). For quantification, the spectrophotometer was blanked using 2 µl of the elution buffer that was used to elute DNA from the column membrane. In order to measure DNA concentration, 2 µl of the DNA solution was mounted onto the spectrophotometer and measured.

Each DNA preparation was screened for the correct sequence using Sanger sequencing as described in section 2.9.

2.9 Sanger Sequencing

Mutations were verified using Sanger sequencing with the Applied Biosystems Big Dye sequencing kit (supplied by Bioline, London UK). Sequencing was performed using site specific primers along the envelope glycoprotein gene. For cleavage site specific sequencing, the primer E55 was used. For sequencing of the full envelope gene, a set of eight primers were used (**Table 2.4**). The eight primers spanned the full gene and generated overlapping sequence reads, generating a full-length envelope sequence. The reactions were set up as recommended by manufacturer (**Figure 2.3**). The BigDye® Terminator V3.1 Cycle Sequencing Ready Reaction reagent includes

four ddNTPs, each labeled with a different fluorescent dye, which enables their separation on a Genetic Analyser.

Component	Diluted reaction (0.5X)		
	Quantity per reaction	Example Forward	Example Reverse
BigDye™ Terminator 3.1 Ready Reaction Mix	4 µL	4 µL	4 µL
BigDye™ Terminator v1.1 & v3.1 5X Sequencing Buffer	2 µL	2 µL	2 µL
Forward primer (3.2 µM)	3.2 pmol	2 µL[1]	—
Reverse primer (3.2 µM)		—	2 µL[1]
Deionized water (RNase/DNase-free)	Varies based on template and primer volume	10 µL	10 µL
Template	300ng	2 µL[2],[3]	2 µL[2],[3]
Total volume	**20 µL**	**20 µL**	**20 µL**

Figure 2.3 Sanger sequencing: The sequencing reaction set up was done according to the manufacturer's specifications (Adapted from Applied Biosystems).

The sequencing thermal cycling conditions were set up as specified by the manufacturer (**Table 2.3**). After thermal cycling, the sequencing reactions were purified to remove any salts and other impurities prior to being read on the genetic analyser. For a 96 well plate, sequencing reaction clean-up was performed by mixing 300 µl of sodium acetate (3 molar) with 8 ml of 99% ethanol. Each well received 50 µl of the mixture, and the plate was centrifuged for 30 minutes at a speed of 2000 rpm. To remove residual supernatant, the plates were inverted and spun at 150 rpm for one minute. To each well, 100 µl of cold 70% ethanol was added and the plate spun at 2000 rpm for five minutes. The residual supernatant was removed as described and the reactions were dried at 65°C for three minutes. The cleaned pellets were each re-suspended in 10 µl HiDi formamide (Applied Biosystems, Foster City, USA) and analyzed on the ABI Prism® 3500xl Genetic Analyzer.

Table 2.3: Cycling conditions for sanger sequencing using the Big dye terminator kit

SEGMENT	CYCLES	TEMPERATURE	TIME
Initial denaturation	1	96°C	1 minutes
Denaturation	25	96°C	10 seconds
Annealing		50°C	5 seconds
Extension		60°C	4 minutes
Hold	1	4°C	Until use

2.10 Sequence analysis

After sequencing reactions were run on the Genetic Analyser, the resulting sequences were analyzed using Sequencher 5.4 software (Gene Codes Corporation, Ann Abor, USA). Sequences that showed double peaks on the software chromatograms were discarded, as this was an indication that more than colony had been picked. Sequences were compiled and aligned to the parental (wild type plasmid) using Sequencher 5.4 and Bioedit 7.0.9 (Ibis Biosciences, Carlsbad, USA).

2.11 Large-scale production of plasmids from cloned envelope DNA

Large-scale preparations of each of the cloned envelopes were produced using the Qiagen plasmid plus maxi prep kit. Each colony of transformed bacterial cells was seeded into 200 ml LB media and incubated overnight at 37°C in a shaking incubator. The bacterial culture was pelleted at 5000 rpm for fifteen minutes and the LB supernatant discarded. Each bacterial pellet was re-suspended in 8 ml of re-suspension buffer P1 (provided with the kit). The kit uses the same three-step method outlined in section to purify plasmid DNA from bacterial culture:

The bacterial pellet was re-suspended in 8 ml of re-suspension buffer P1 (provided with the kit). A volume of 8 ml of lysis buffer P2 was added to the pelleted cells, and mixed well in order to lyse the cells. A volume of 8 ml neutralization buffer S3 was added, which neutralized the lysate as well as optimized conditions for DNA binding onto the silica gel membrane. The DNA was eluted in 400 µl buffer EB and quantified

on a NanoDrop® ND-1000 Spectrophotometer (Thermo Scientific). For quantification, the spectrophotometer was blanked using 2 µl of the elution buffer that was used to elute DNA from the column membrane. In order to measure DNA concentration, 2 µl of the DNA solution was mounted onto the spectrophotometer and measured.

2.12 Site Directed Mutagenesis

In order to introduce individual cleavage site mutations into the viral envelope DNA, site directed mutagenesis was performed using the Quickchange Lightning site directed mutagenesis kit (Agilent technologies). The kit works by using a double stranded DNA vector with the insert of interest. In this case the vector used was pcDNA 3.1 (Invitrogen) (**Figure 2.2**), and the insert was an HIV-1 envelope glycoprotein gene. Two synthetic oligonucleotide primers were used, each complementary to one strand of the insert DNA, both containing the desired mutation(s) (**Table 2.4**).

Table 2.4: Sequences of primers used in the study

Table 2.4a*: Sequences of Primers used for sequencing.*

PRIMER NAME	SEQUENCE (5' – 3')
Sanger Sequencing Primers	
EnvB	AGAAAGAGCAGAAGACAGTGGCAATGA
A589	GTGTAAAGTTAACCCCACTCTG
E85	GTCCCTCATATCTCCTCCTCCAGGTCT
E55	GCCCCAGACTGTGAGTTGCAACAGATG
Mf	GGAGGAGATATGAGGGACAATTGG
CT1Re	GACTTCCCAGATACTTAAGAGCTTCCCACC
E210	TAACAAATTGGCTGTGGTATATAA
A589Re	CAGAGTGGGGTTAACTTTACAC
FCMVR	CTAGTTAACGGTGGAGGGCAGTGT

Table 2.4b*: Sequences of Primers used for overlapping CS-Mut PCR. F (forward) indicates the 3'-5' primer, and R (reverse) indicates the reverse complement.*

Overlapping CS-Mut PCR Primers	
Env A Stop	CACCGGCTTAGGCATCTCCTATAGCAGGAAGAA
Env M	TAGCCCTTCCAGTCCCCCCTTTTCTTTTA
ZM233 F	CCTACTAAGGCACAAAGGAGAATGGTGGGAAAAAAGAAAAGAGCAGTAGGAATAGGAGCTGTGTTCCTTG
ZM233 R	CCTACTAAGGCACAAAGGAGAATGGTGGGAAAAAAGAAAAGAGCAGTAGGAATAGGAGCTGTGTTCCTTG

CM244 F	CCACCAAAGCACAGAGAAGAATGGTGGGGAGAGAAAAAAGA GCAGTGGGAATAGGAGCTATGAT
CM244 R	ATCATAGCTCCTATTCCCACTGCTCTTTTTTCTCTCCCCACCATTCTTCTC TGTGCTTTGGTGG
CAP256 SU F	GAAGTTAAGCCATTAGGAATAGCACCCACTAAAGCACAAAGGAGAATGG TGGGGAAAGGGAAAAG
CAP256 SU R	TAAAGCACAAAGGAGAATGGTGGGGAAAGGGAAAAGAGCAGTAGTGGG ATTAGGAGCTGTGTTC
T250-4 F	GTACAAATTGAACCACTAGGTGTGGCACCCACCAAAGCACAAAGAAGAA TGGTGGGGAAAGGAAAA
T250-4 R	CCACCAAAGCACAAAGAAGAATGGTGGGGAAAGGAAAAAGAGCAGTTG GACTGGGAGCTGTC
WITO.33 F	GTAGTAAAAATTGAACCATTAGGAATAGCACCCACCAAGGCACAGAGAAG AATGGTGGGGAAAAAAAAAAGAG
WITO.33 R	CCAAGGCACAGAGAAGAATGGTGGGGAAAAAAAAAAGAGCAGTGACGC TGGGAGCTGTGTTC

Table 2.4c*: Sequences of Primers used for site directed mutagenesis. F (forward) indicates the 3'-5' primer, and R (reverse) indicates the reverse complement.*

Site Directed Mutagenesis Primers	
CAP45.G3 E500K F	GCACCCACTAAGGCAAGAAG
CAP45.G3 E500K R	CTTCTTGCCTTAGTGGGTGC
CAP45.G3 R502Q F	GCACCCACTGAGGCACAAAGG
CAP45.G3 R502Q R	CCTTTGTGCCTCAGTGGGTGC
CAP45.G3 V505M F	CAAGAAGGAGAATGGTGGAGAG
CAP45.G3 V505M R	CTCTCCACCATTCTCCTTCTTG
CAP45.G3 E507G F	GAGTGGTGGGGAGAGAAAAAAGAG
CAP45.G3 E507G R	CTCTTTTTTCTCTCCCCACCACTC
CAP45.G3 R508K F	GTGGTGGAGAAAGAAAAAAGAGC
CAP45.G3 R508K R	GCTCTTTTTTCTTTCTCCACCAC
CAP45.G3 E509G F	GGAGAGAGGAAAAAGAGCAGTG
CAP45.G3 E509G R	CACTGCTCTTTTTCCTCTCTCC
CAP45.G3 R502Q/V505M/E507 G F	GGCACAAAGGAGAATGGTGGGGAGAGAAAAAAG
CAP45.G3 R502Q/V505M/E507 G R	CTTTTTTCTCTCCCCACCATTCTCCTTTGTGCC
CAP256 SU E500K/R502Q F	CACTAAAGCACAAAGGAGAGTGGTGCAGAAAGAGAAAAG
CAP256 SU E500K/R502Q R	CTTTTCTCTTTCTGCACCACTCTCCTTTGTGCTTTAGTG
CAP256 SU V505M/E507G F	CACTAAAGCACAAAGGAGAATGGTGGGGAAAGAGAAAAG
CAP256 SU V505M/E507G R	CTTTTCTCTTTCCCCACCATTCTCCTTTGTGCTTTAGTG
CAP256 SU R508K/E509G F	ACTAAAGCACAAAGGAGAATGGTGGGGAAAGAGAAAAG
CAP256 SU R508K/E509G R	CTTTTCTCTTTCCCCACCATTCTCCTTTGTGCTTTAGT
T250-4 E500K/R502Q F	CCACCAAAGCACAAAGAAGAGTGGTGGAGAGAGAAAAAAG

T250-4 E500K/R502Q R	CTTTTTTCTCTCTCCACCACTCTTCTTTGTGCTTTGGTGG
T250-4 V505M/E507G F	CCACCAAAGCACAAAGAAGAATGGTGGGGAGAGAAAAAAG
T250-4 V505M/E507G R	CTTTTTTCTCTCCCCACCATTCTTCTTTGTGCTTTGGTGG
T250-4 R508K/E509G F	CCACCAAAGCACAAAGAAGAATGGTGGGGAGAGAAAAAAG
T250-4 R508K/E509G R	CTTTTTTCTCTCCCCACCATTCTTCTTTGTGCTTTGGTGG
WITO.33 CS-Mut F	CACCAAGGCACAGAGAAGAATGGTGGGGAAAGGAAAAAGAG
WITO.33 CS-Mut R	CTCTTTTTCCTTTCCCCACCATTCTTCTCTGTGCCTTGGTG
CM244 E500K/R502Q F	CCACCAAAGCACAGAGAAGAGTGGTGGAGAGAGAAAAAAG
CM244 E500K/R502Q R	CTTTTTTCTCTCTCCACCACTCTTCTCTGTGCTTTGGTGG
CM244 V505M/E507G F	CCACCAAAGCACAGAGAAGAATGGTGGGGAGAGAAAAAAG
CM244 V505M/E507G R	CTTTTTTCTCTCCCCACCATTCTTCTCTGTGCTTTGGTGG
CM244 R508K/E509G F	CCACCAAAGCACAGAGAAGAATGGTGGGGAAAGGAAAAAG
CM244 R508K/E509G R	CTTTTTCCTTTCCCCACCATTCTTCTCTGTGCTTTGGTGG
ZM233 E500K/R502Q F	CCTACTAAGGCACAAAGGAGAGTGGTGGAGAGAGAGAAAAG
ZM233 E500K/R502Q R	CTTTTCTCTCTCTCCACCACTCTCCTTTGTGCCTTAGTAGG
ZM233 V505M/E507G F	CCTACTAAGGCACAAAGGAGAATGGTGGGAAGAGAGAAAAG
ZM233 V505M/E507G R	CTTTTCTCTCTTCCCACCATTCTCCTTTGTGCCTTAGTAGG
ZM233 508K/E509G F	CCTACTAAGGCACAAAGGAGAATGGTGGGAAGAGAGAAAAG
ZM233 508K/E509G R	CTTTTCTCTCTTCCCACCATTCTCCTTTGTGCCTTAGTAGG

Table 2.4d*: Sequence of the vector specific colony PCR primer.*

Vector Specific colony PCR Primer	
T7	TAATACGACTCACTATAGGG

Stages of the thermo-cycler reaction included denaturation of the dsDNA, annealing of the synthetic primers and elongation to produce the mutant plasmid in accordance to the manufacturer's instructions (**Figure 2.2 and Table 2.2**). To ensure that only mutated plasmid remained in the mutagenesis reaction prior to its retransformation, the wild type plasmid was digested using the *Dpn*I endonuclease enzyme (target sequence 5'-Gm^{6}ATC-3'), at 37°C for an hour.

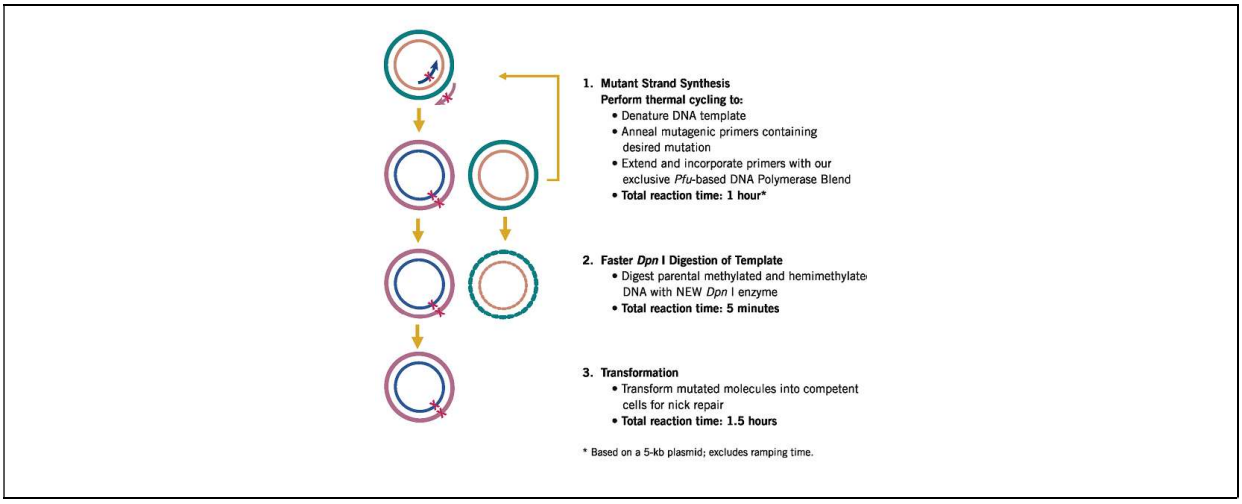

Figure 2.4: Overview of the Quickchange Lightning site directed mutagenesis system (Adapted from Agilent Technologies).

The enzyme specifically selects for methylated or hemi-methylated DNA. Most *E. coli* strains from which dsDNA vectors are obtained are dam$^+$, meaning their DNA is methylated. The *Dpn*I enzyme in this reaction therefore targeted the wild type DNA and did not digest the synthetic, non-methylated mutated DNA.

Table 2.5: The Quickchange Site Directed Mutagenesis thermal cycling conditions used for mutating HIV-1 envelope plasmids.

SEGMENT	**CYCLES**	**TEMPERATURE**	**TIME**
Initial denaturation	1	95°C	2 minutes
Denaturation	18	95°C	20 seconds
Annealing		60°C	10 seconds
Extension		68°C	30 seconds
Final extension	1	68°C	5 minutes

Each mutagenesis reaction was transformed as described in section 2.3. To screen for successful mutations, four bacterial colonies were used to inoculate 15 ml cultures of LB broth which were incubated in a shaking incubators (150 rpm) overnight at 37°C. Thereafter DNA was extracted from these as described in section 2.5. Each mini-prep was screened for the presence of mutations using Sanger sequencing as described in section 2.7. The wild type envelope gene sequence was compared to that of the

Sanger sequences obtained along with the mutant primer sequences. If the Sanger sequences matched the primer sequence rather than that of the wild type gene, then mutagenesis was considered a success. Subsequent sequencing of each full mutant envelope gene was done to ensure no off-site mutations were inserted.

2.13 Cell lines

Three different cell lines were used in this study. Human embryonic kidney cells (HEK293T) were obtained from Dr. George Shaw (then at University of Alabama, Birmingham, AL) and used for the transfection of pseudoviruses (section 2.17). The 293 Freestyle cells were used to express antibodies (section 2.14), and were obtained from the Vaccine Research Center, USA. TZM-bl cells, also known as JC53BL-13 cells were provided by the NIH AIDS Research and Reference Reagent Program (Catalogue number 8129) and used for antibody neutralization assays as mentioned in section 2.18.

The TZM-bl and HEK293T cells were grown in Dulbecco's Modified Eagle's Medium (DMEM) containing 10% fetal bovine serum, 2.5% HEPES ((4-(2-hydroxyethyl)-1-piperazineethanesulfonic acid) buffer and 50 µg/ml gentamycin. The cells were maintained by re-suspension and re-seeding at confluence. To do this, the media was carefully removed from the cells, and 6 ml of phosphate buffered saline (PBS) was used to wash the cells. In order to detach the cells from the flask, a volume of 2.5 ml of 0.25% trypsin in 1 mM ethylenediaminetetraacetic acid was added, and cells incubated at 37°C for four minutes. The cells were washed off using 10 ml of complete DMEM and transferred to a sterile tube. After each re-suspension, the cells were counted and reseeded as needed. The 293Freestyle cells were cultured in 293Freestyle media and diluted every 72 hours in order to stay below the concentration of 5×10^6 cells per milliliter.

2.14 Antibody Expression

Several antibodies used in this study had previously been expressed in the laboratory. Antibodies specifically required for this study were cloned and expressed as detailed below. Mature and germline reverted antibodies were expressed from plasmids

available in the laboratory. The cloned heavy and light chain plasmids for each antibody were transformed into JM109 competent cells and grown overnight at 37°C. The DNA was extracted from the bacterial cells using the Qiagen maxi-prep kit and sequence confirmed as described above (sections 2.4 and 2.7). The vector specific primer FCMVR was used to sequence the antibody genes (**Table 2.1**). A combination of 200 µg of heavy chain DNA and 200 µg of light chain DNA was transfected into 293Freestyle suspension cells using Polyethyleneimine (PEI) Max. Each culture was a total volume of 400 ml at a cell count of $2x10^6$ cells/ml. For each antibody, 1.2 ml of PEI (at a concentration of 1 mg/ml) was added to 10 ml of Optimem medium. The mixture was mixed gently and incubated at room temperature for five minutes. The heavy and light chain plasmids were added to a further 10 ml of Optimem and the plasmids were filter sterilized and added to the PEI mixture. The total mixture was incubated at room temperature for twenty minutes prior to being added drop-wise to 293Freestyle cells. The cells were then incubated at 37°C and 10% CO_2 for seven days.

2.15 Antibody purification

The antibody rich supernatant was collected by spinning down the cells at 4500 rpm and then IgG purification was performed using affinity column chromatography on a Protein A column. For each 400 ml supernatant, 5 ml of a protein A bead solution was added to a plastic column, and liquid was allowed to run through until there was about 2 ml of beads left in the plastic column. The beads were washed with 1x PBS, and then antibody supernatant was slowly passed through the column, which captured the IgG. For elution of the bound IgG, the column environment was rendered acidic using 12.6 ml of a 0.1 molar glycine buffer that was pH adjusted to 2.5 using 1 molar hydrochloric acid. The IgG was eluted into an alkaline 1 molar Trizma neutralization buffer that was pH adjusted to 8 using 1 molar hydrochloric acid.

The eluted IgG was concentrated down to about 1 ml in volume by centrifugation in a Vivaspin® protein concentrator (Sartorius stedim, France). The concentrators use a membrane with a molecular weight cut off (in this case we used the 10 000 MWCO PES).

Approximately 20 ml of protein eluent was added onto the concentrator tube, and the solution passed through the membrane by centrifugation at 4500 rpm for ten minutes. The protein was mixed after each spin and the process was repeated until there was only 1 ml or less left in the concentrator. The IgG concentrations were measured on a Nanodrop® spectrophotometer (Thermo Scientific).

2.16 SDS-Polyacrylamide gel electrophoresis analysis of purified mAbs

In order to ensure that the antibodies expressed as desired and that no unexpected impurities or aggregations were present in the antibody preparations, a protein SDS-PAGE was performed. This method uses sodium dodecyl sulfate (SDS), a negatively charged detergent, to denature proteins and give them a uniform charge. SDS breaks down the proteins' secondary, tertiary and quaternary structures by binding to amino acids and resulting in uniformly charged molecules. SDS-PAGE separates the negatively charged protein molecules according to their molecular weight as they migrate through an acrylamide gel towards a positively charged electrode. We performed this for the expressed MPER bNAbs in several steps. Firstly, a 12% acrylamide resolving gel was prepared by combining the reagents as instructed by the manufacturer (Invitrogen NuPAGE® and Sigma Aldrich, St Louis, USA) (**Table 2.6**).

Table 2.6: Reagents used to prepare a 12% resolving gel.

Reagent	**Volume**
H2O	6.5 ml
40% acrylamide	4.5 ml
1.5M Tris (pH 8.8)	3.8 ml
10% SDS	0.15 ml
10% APS	0.15 ml
TEMED	0.015 ml

A gel mold was prepared using two glass sheets that were cleaned, dried, and held upright together in a gel cast. During preparation of the resolving gel, the TEMED (tetramethylethylenediamine), which along with the APS (ammonium persulfate)

catalyzes the polymerization of acrylamide gels, was added last when the gel mold had been assembled. Approximately 5 ml of the gel solution (or as much as was needed to fill the mold and leave approximately 1.5 cm at the top for the stacking gel) was carefully poured into the glass mold using a 5 ml serological pipette. The top of the gel was covered with absolute isopropanol in order to exclude air (air would prevent the setting of the gel) and ensure that the top of the gel was straight. The gel was allowed to set for 30 minutes. We next prepared the stacking gel according to the manufacturer's instructions (**Table 2.7**). The stacking gel typically contains a lower concentration of acrylamide and is used to arrange proteins together into one band before they enter into the resolving gel for separation.

Table 2.7: Reagents used to prepare a protein stacking gel.

Reagent	**Volume**
H_2O	6.2 ml
40% acrylamide	1.2 ml
0.5M Tris (pH 6.8)	2.4 ml
10% SDS	0.1 ml
10% APS	0.1 ml
TEMED	0.01 ml

Once the resolving gel had fully set, the isopropanol layer was carefully removed from the top as it would interfere with the continuous layer of the two gels if not sufficiently evaporated. The stacking gel solution was poured on top of the resolving gel, all the way to the very top of the glass mold. A suitable comb was inserted into the stacking gel in order to form the necessary wells for loading the protein (twelve 1 mm wells). The stacking gel was allowed to set for thirty minutes.

While the gel was setting, the antibody samples were prepared for running on the gel. A reducing agent (Invitrogen 10×) was used to break the disulphide bonds that hold the heavy and light chains of each antibody together. This would allow the two to run separately on the gel for separate sizing. Approximately 12 mg of each antibody was combined with 1 µl of the reducing agent, 1 µl of 1M DTT (to ensure complete reduction) and 4 µl of loading dye (NuPAGE® LDS sample buffer) and incubated at 95ºC for 5 minutes to break the disulphide bonds. The sample tubes were spun down

at 1 500 rpm to bring down any evaporated droplets from the tube lids. A 10× running buffer was prepared next using manufacturer's (Sigma Aldrich) instructions (**Table 2.8**), and subsequently diluted to a 1× buffer for the running of the gel (100 ml of the buffer was combined with 900 ml of distilled water to do this).

Table 2.8: Reagents used to prepare a 10× protein running buffer

Reagent	**Mass/Volume**
SDS	10 g
Tris	30.3 g
Glycine	144.1 g
H2O	800 ml

The gel and buffer were loaded onto vertical electrophoresis apparatus (Bio-Rad, Hercules, USA), and the proteins were loaded onto the gel and run at a constant voltage of 100 for fifteen minutes to allow the proteins to stack before entering the resolving gel. Thereafter, the proteins were allowed to run at a constant voltage of 200 for a further 45 minutes. A Novex® (Invitrogen) molecular weight marker was used to size the protein bands, with sizes ranging from 260 kDa 3.5 kDa.

The gel was washed in distilled water and subsequently stained by incubation with coomassie brilliant blue protein safe stain for one hour. The protein was gently shaken in the stain during incubation to allow for constant mixing of the stain. Distilled water was used to wash off any residual stain that was not bound to protein. The gel was incubated in water and gently shaken overnight for effective destaining. The gel was photographed and band sizes recorded.

2.17 Production of Env-pseudoviruses

Two million HEK293T cells were seeded in 10 ml of DMEM in a 10 mm culture dish and incubated for 24 hours at 37°C and 5% CO_2. Cell monolayers were thus 50-80% confluent 24 hours later. The cloned virus plasmids (mutants and wild type Envs) were transfected into the cells along with pSG3ΔEnv, which encodes the whole HIV genome

but contains two stop codons in the *env* gene. The transfected cells therefore only transcribe the envelope deficient genome into viral mRNA, and pseudovirus particles are therefore infectious but unable to generate progeny virions. An amount of 4 µg of envelope plasmid and 4 µg of the pSG3ΔEnv vector was combined with 500 µl DMEM and 25 µl of the transfection reagent PEI max (1 mg/ml). The mixture was incubated at room temperature for thirty minutes before being transferred to the cells that were seeded 24 hours prior to the transfection and incubated at 37ºC/ 5% CO_2. The supernatant containing the pseudoviruses was harvested after 48 hours, filter sterilized and stored at -80°C. The viruses were used in the TZM-bl neutralization assay as described in section 2.18 below. In order to determine entry potential differences between mutant and wild type viruses, head to head transfections were conducted as described in six well plates. Volumes were adjusted according to differences in surface area.

2.18 Titration of Env-pseudoviruses

The amount of virus in the supernatant was determined by titration of the virus out on a 96 well plate using TZM-bl cells (described in section 2.13). This assay measures levels of HIV as a function of the expression of the Tat-regulated Luciferase reporter gene after one cycle of infection in the TZM-bl cell line (130). The gene encodes firefly luciferase, which uses ATP as a cofactor to mono-oxygenate luciferin. The reaction results in luminescence, one of the highest quantum yields to result from such a reaction.

The TZM-bl cells were also modified to express high surface levels of the CD4, CCR5 and CXCR4 receptors which are used by different strains of HIV-1 to infect host cells (130, 131). The cells can therefore be infected by viral isolates that exhibit both R5 and X4 tropism (130-132). An HIV based vector was used to stably introduce firefly luciferase and β-galactosidase gene coding sequences into the cell line (131). The genes make it possible to accurately quantify the level of HIV infection in the cell line by quantifying the reduction in luminescence, or lack thereof (133).

A volume of 150 µl of complete DMEM was added to every well of a flat-bottomed 96 well plate. 50 µl of relevant pseudovirus was added to row A, except for columns 1 and 2 which served as background controls. 50 µl was transferred down the plate from row A to H, therefore diluting the virus. 100 ml of TZM-bl cells and diethylaminoethyl (DEAE) dextran were added to each well and the plates incubated at 37°C for 48 hours. Levels of luminescence were measured on an illuminometer to determine viral infection of the cells.

The luminescence was analyzed using the Bright Glo™ Luciferase assay, which contains the luciferase substrate (luciferin) necessary for luminescence. From each plate, 150 µl of media was removed from each well and replaced with 100 µl of the luciferase Bright Glo reagent (Fitchburg, USA). The plate was incubated for two minutes at room temperature to allow for cell lysis and for the reaction between enzyme and substrate to take place. The activity of luciferase was quantified as RLUs, which are directly proportional to the number of infectious virus particles present in the culture (130). Luminescence levels were detected or read on a Perkin Elmer Victor X (Perkin Elmer, Watham, USA) illuminometer and saved on a Microsoft Excel spreadsheet. The antibody titer was calculated as the dilution of plasma that inhibited half the viruses from infecting the reporter cell (IC_{50}).

2.19 The TZM-bl Neutralization assay

To measure the effects of different mutations on virus neutralization by MPER and other antibodies, we used the TZM-bl neutralization assay. This assay measures the neutralization of HIV as a function of the reduction in expression of the Tat-regulated Luciferase reporter gene after one cycle of infection in the TZM-bl cell line (described in section 2.18). The assay was carried out in 96-well plates using the TZM-bl cells and media described in section 2.13. Each plate tested five samples or antibodies at eight dilutions and in duplicate (131). A volume of 100 µl of complete DMEM was added into each well on the plates, except for row H **(Figure 2.5).**

			Titers									
			Sample 1		*Sample 2*		*Sample 3*		*Sample 4*		*Sample 5*	
	1	**2**	**3**	**4**	**5**	**6**	**7**	**8**	**9**	**10**	**11**	**12**
A	CC	VC	Dil 8		Dil 8		Dil 8		Dil 8		Dil 8	
B	CC	VC	Dil 7		Dil 7		Dil 7		Dil 7		Dil 7	
C	CC	VC	Dil 6		Dil 6		Dil 6		Dil 6		Dil 6	
D	CC	VC	Dil 5		Dil 5		Dil 5		Dil 5		Dil 5	
E	CC	VC	Dil 4		Dil 4		Dil 4		Dil 4		Dil 4	
F	CC	VC	Dil 3		Dil 3		Dil 3		Dil 3		Dil 3	
G	CC	VC	Dil 2		Dil 2		Dil 2		Dil 2		Dil 2	
H	CC	VC	Dil 1		Dil 1		Dil 1		Dil 1		Dil 1	

Figure 2.5: The layout of a 96 well plate during the TZM-bl neutralization assay: CC is cell control and VC is virus control. Dil 1 is the least diluted sample or antibody and Dil 8 is most dilute (Adapted from Montefiori *et* al, 2009).

Row H is where the antibodies or samples were added at the lowest antibody dilution (10 µg/mL or 25 µg/ml represented as Dil 1 on figure 2.5). The total volume therein was 150 µl of media and antibodies. Column 1 on each plate was the cell control column, that is, cells and media were added to the wells but not virus or antibody. Column 2 was the virus control column, that is, it had cells, media and virus and no antibody or sample. The two were useful in calculating background and were factored in on the final calculation described below (131).

50 µl of media and antibody was transferred from row H up the plate to row A, therefore titrating the antibody up to the most diluted at row A. 50 µl of each relevant virus was added to each plate, except for the cell control column. The viruses were each diluted to give approximately 40 000 relative light units (RLUs) according to the titration described in section 2.17. The plates were then incubated at 37°C for one hour before TZM-bl cells were added. Each plate received one million cells at a dilution of $5x10^5$ and 40 µl of DEAE dextran at 1 mg/ml. The dextran was added to the cell and media mixture to enhance infection of the cells, and each well received 100 µl of cells (131). The plates were incubated at 37°C for 48 hours to allow for pseudovirus infection. The amount of virus neutralized by the antibodies was measured using the Bright Glo™ Luciferase assay described above. Neutralization assays were repeated a minimum of three times.

2.20 Statistical analysis

The one sample t-test was used to compare viral fitness among mutants and wild type virus. GraphPad® Prism (Graphpad Software, La Jolla, USA) software was used for the analysis.

CHAPTER 3: RESULTS

Everybody infected with HIV mounts a neutralizing response which targets the envelope glycoprotein, Env, though only a subset go on to develop breadth (132). Regardless of the breadth of their response, HIV-1 viral isolates have been extensively shown to escape neutralization by the host immune system (81, 93, 133). Viral escape from neutralizing antibodies occurs in the form of mutations, insertions and deletions that alter the properties of Env such that the neutralizing antibodies cannot recognize and consequently neutralize the virus (93).

Within the CAPRISA cohort, we have defined escape from both strain-specific antibodies and bNAbs in several cases (67, 81). One of these donors was CAPRISA donor CAP248 whose autologous virus developed a set of six mutations in the furin cleavage site of gp160 (sites 500, 502, 505, 507, 508 and 509), a highly conserved region of Env (94). The mutations arose sequentially over time to escape host antibodies which targeted the gp120-gp41 interface of Env (94). Mutations were first noted at site 500 at one year post infection, and by three and a half years post infection, culminated in a set of six mutations (94). These mutations, when introduced simultaneously into both autologous and heterologous viruses neutralized by the CAP248 plasma, mediated complete escape from the autologous antibody, CAP248-2B (94).

However, we have also previously shown that in heterologous viruses, these escape mutations resulted in exposure of the MPER, which was evident from increased neutralization sensitivity to bNAbs targeting that region (94). That study did not, however, test whether the enhancement of the MPER was the combined effect of all six mutations, or if only one of the mutations was responsible for the MPER exposure.

Furthermore, the location of these mutations in otherwise conserved sites raised the question of whether introduction of these mutations had a fitness cost for the virus. Several previous studies of viral escape from bNAbs have shown this is associated with viral fitness costs (134-136). The simultaneous presence of multiple mutations makes it difficult to assess whether individual mutations are either resistance mutations or compensatory mutations required for restored viral fitness, as is frequently observed, for example during the evolution of drug resistance (136). Although previous studies had confirmed that the introduction of six mutations together

did not render viruses non-functional, the role of individual mutations had not been assessed (94).

The first aim of this study therefore sought to assess i) the individual effect of each mutation on viral fitness compared to the simultaneous presence of all six mutations, and ii) the effect of individual cleavage site mutations on neutralization by MPER bNAbs.

3.1 Assessing the effect of individual cleavage site mutations on viral fitness

3.1.1 Generation of single mutations within the gp120-gp41 cleavage site

Site directed mutagenesis was performed using the CAP45.G3 viral strain, which was the same strain that was used in the previously published CAP248 study to test the effect of the combined mutations simultaneously (94). Primers were designed to add each mutation individually into CAP45.G3 as described in section 2.6. DNA extracted from transformed *E. coli* cells was sequenced with primers flanking the cleavage site to identify individual mutations (**Table 2.1**, **Figure 3.1**). After identification of plasmids containing desired mutations the full envelope gene was sequenced using 8 primers as described in section 2.7 to ensure that the rest of the envelope was unchanged.

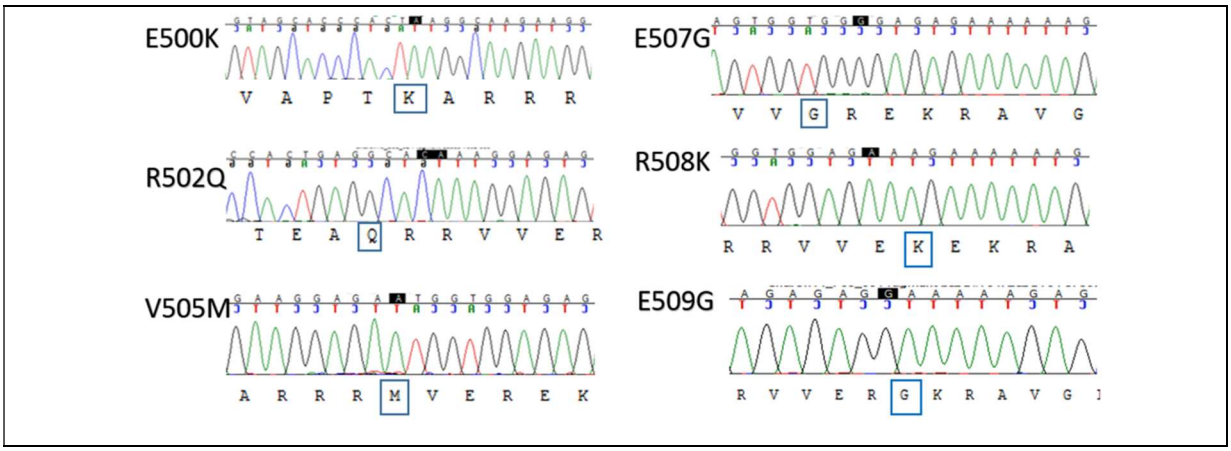

Figure 3.1: Sanger sequencing chromatograms for CAP45.G3 single mutants. The mutated residue is highlighted in each sequence. The peaks are color coded for each DNA base; red is for thymine (T), blue is for cytosine (C), green is for adenine (A) and black is for guanine (G). Amino acid sequences are shown below each chromatogram, and each mutated residue is highlighted in a blue box.

3.1.2 Confirmation of the functionality of mutant viruses

Env-pseudotyped viruses were produced by co-transfection of the HIV-1 envelope wild type and mutant envelope genes with a backbone containing the rest of the viral genome (pSG3$^{\Delta Env}$). The envelope gene in this plasmid contains two stop codons and is therefore not capable of generating replication competent virus. Co-transfection with an envelope encoded on a separate plasmid therefore generates pseudoviruses capable only of a single entry event, which simplifies measurements of entry fitness and future neutralization assays. The Env-pseudotyped viruses were tested for entry capacity using TZM-bl cells, which express the luciferase gene under a Tat responsive promoter, to confirm the functionality of each of the individually mutated viruses (**Table 3.1**). This confirmed that the individual cleavage site mutants were functional and capable of mediating viral entry into TZM-bl cells.

Table 3.1: Confirmation of the functional nature of CAP45.G3 viruses with single mutations in the gp120-gp41 cleavage site. The relative light values obtained for each mutant is a measure of maximum infectivity.

CAP45.G3 Mutation	**Maximum Infectivity (Relative Light Units)**
E500K	588,945
R502Q	259,909
V505M	469,387
E507G	602,193
R508K	483,122
E509G	611,618

3.1.3 Assessing the effect of individual gp120-gp41 cleavage site mutations on viral fitness

In the donor CAP248, depending on what time point was assessed, various combinations of mutations emerged in response to the development of bNAbs to the gp120-gp41 interface (94). Although individual escape mutations may confer a fitness cost, viral isolates *in vivo* are able to introduce additional mutations at various sites to

compensate for the loss of infectivity, and therefore they may continue to thrive (136). Interestingly, the viral load of donor CAP248 showed a dramatic decline at 958 days post infection, from 16,200 copies/ml to 4,260 copies/ml at 867 days post infection. This 74% decline in viral load indicates that the cleavage site mutations may have impacted viral fitness. The viral load however rebounded to 16,900 by 1,238 days post infection, suggesting that in the presence of bNAbs, fitness costs were off-set by compensatory mutations. Here, we aimed to assess the viral infectivity of the CAP45.G3 wild type envelope, envelopes containing each individual mutant, and the previously described CAP45.G3 CS-Mut (containing all six mutations) to establish whether the mutations affected viral fitness.

To test the effect of the cleavage site mutations on viral fitness, “head to head” transfections were performed in six well plates so as to eliminate batch to batch differences in transfection efficiency and cell viability. Comparison of the wild type and CAP45.G3 CS-Mut showed that the introduction of all six mutations simultaneously lead to a remarkable ten-fold reduction in viral fitness with a maximum infectivity of 87,325 RLUs compared to the wild type value of 810,356 RLUs (**Figure 3.2**).

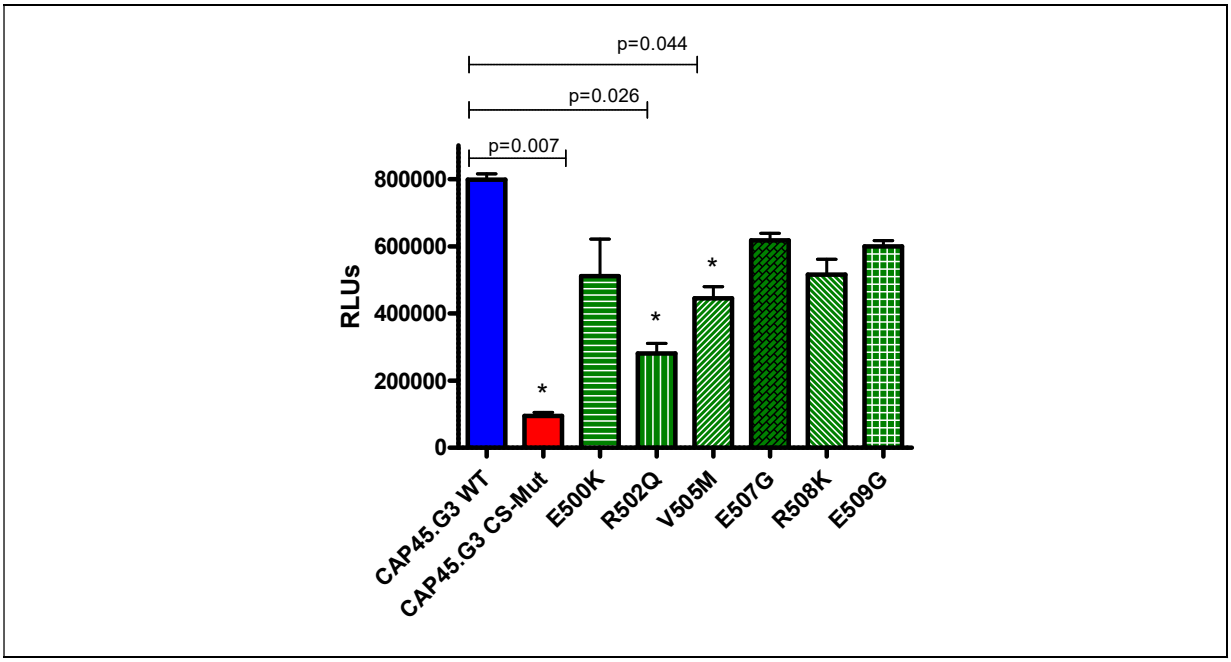

Figure 3.2: Comparison of viral entry efficiency between the CAP45.G3 wild type (shown in blue), the CAP45 CS-Mut (in red) and the single cleavage site mutants (each shown in varied green colors) Asterisks mark values that are statistically significant from the wild type value. P values are indicated for significant values.

The six mutations combined therefore lead to a significant 90% reduction in viral fitness (p = 0.007). In contrast, all other mutations, when introduced individually showed much less reduction in infectivity ranging from 611,618 RLUs for E509G, a 25% reduction in viral entry efficiency compared to the wild type, to 259,909 RLUs for R502Q, a 68% reduction in viral entry efficiency compared to the wild type. A statistically significant reduction in viral fitness was observed only for the R502Q and V505M mutants (**Figure 3.2**). Thus it was concluded that although viral fitness was reduced for each mutant, the single mutations have less of an effect on entry efficiency compared to the complete set of six mutations.

We next assessed whether the reduction in entry efficiency was directly proportional to how conserved the mutated site is, or how rare a residue is at that particular site. We had previously assessed the per site variability within this region by compiling three sequence logograms of the cleavage site, the first comprising of all known global HIV-1 viral sequences, the second comprising of subtype C sequences and the last made up of the CAP248 sequences at 3.5 years post infection. Each logogram shows which residues are common at each site for the analyzed group (**Figure 3.3**).

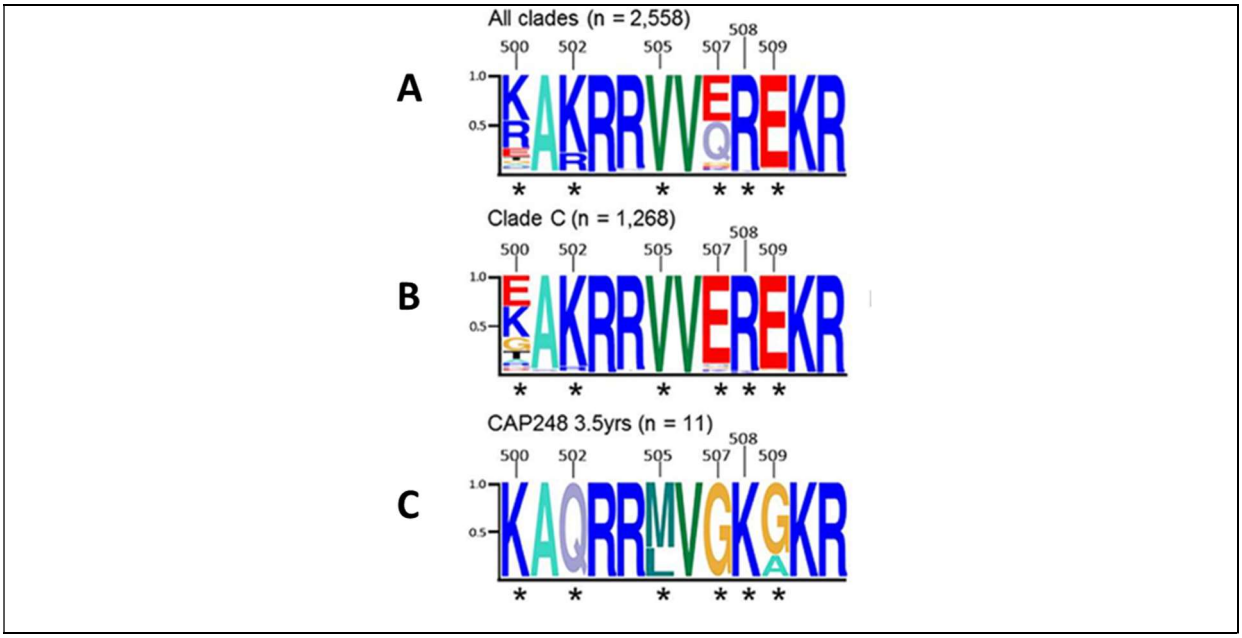

Figure 3.3: Logogram showing cleavage site residues in **A**) All global clades, **B**) Clade C strains and **C**) CAP248 viral variants at 3.5 years post infection. The residues shown in each logogram are from positions 500 to 511 of the HIV-1 envelope gene Env. The height of each bar represents the frequency of a residue at the site, with the larger letters indicating higher frequency. Positions showing the CAP248 mutations are marked with an asterisk. Numbering is according to the HXB2 strain of HIV-1. Colors of residues represent charge and pH (Wibmer *et al*, 2016).

Figure 3.3 shows that the CAP248 viruses accumulated unusual amino acids in normally conserved sites, an indication of the considerable immunogenic pressure the virus must have experienced at that epitope (94). We compared the entry efficiency cost of individual mutations with the level of conservation at each site.

Position 500 exhibits substantial variability within the globally circulating viruses as well as among the subtype C viral isolates. The CAP248 viruses mutated a glutamic acid residue at that position (present in 9% of global viruses), to a lysine residue (present in 47% of global viruses), both fairly common in globally circulating viral strains. Comparison of viral infectivity between the E500K mutant and the CAP45.G3 wild type showed a 32% reduction in the mutant, suggesting that mutation at this highly variable site does not have a major impact on viral fitness, as expected. Similarly, position 507 exhibits substantial variation, and the E507G mutation had a minimal effect on viral fitness, reducing infectivity by only 26%, despite the fact that a glutamic acid residue is relatively rare among circulating viruses.

In contrast to these more variable sites, residue 502 is highly conserved in global and clade C viruses, being occupied by positively charged residues (lysine or arginine) in 98% of these. In CAP248, this positively charged site is mutated to a distinctly unusual glutamine (present only in 1.4% of global viruses). When assessing the viral fitness of the CAP45.G3 R502Q mutant (**Table 3.1**), the reduction in entry efficiency was a significant 68% compared to that of the wild type ($p=0.026$), indicating that the unusual R502Q substitution resulted in a significant loss of infectivity for the virus. Similarly, when residue 505, also highly conserved as a valine in global viruses, was mutated to a methionine residue, only seen at this position in 0.08% of globally circulating virus strains, the reduction in entry potential was significant ($p=0.044$).

However, this was not true for position 509, also highly conserved. The CAP248 viruses mutated a negatively charged glutamic acid, which is present in 95% of the global viruses, to a glycine, which is only present in 2% of global viruses. However, when the viral infectivity of the CAP45 E509G mutant was compared to that of the wild type, the reduction was just 25%, only slightly less than that of the change at variable position 500.

Overall, while all individual single cleavage site mutants were viable, R502Q and V505M were significantly negatively affected in terms of viral entry potential. However,

the reduced fitness of each mutation was distinctly less than that of all the mutations combined (as in the CS-Mut). Overall these data suggest the likelihood that the CAP248.2B lineage exerted significant immune pressure on CAP248, with fitness deficits offset by the need for viral escape from a broadly neutralizing response in the donor plasma. However, for vaccine design, the increased entry capacity of each of the individual mutants compared to the CS-Mut suggests that these constructs have the capacity to be better vaccine candidates when incorporated into virus-like particles, if they are also able to mediate MPER exposure.

3.2 Assessing the effect of single cleavage site mutations on MPER exposure

Since the combined cleavage site mutations in CAP248 conferred an increase in sensitivity to neutralization by MPER bNAbs, this study sought to assess whether any individual mutation within the cleavage site resulted in similar exposure of the MPER. BNAbs to the MPER were therefore expressed and tested against the CAP45.G3 single mutants as well as the wild type and CAP45.G3 CS-Mut. Neutralization curves and antibody concentrations necessary to neutralize 50% of each mutant (IC_{50}) were compiled and compared to those of the wild type CAP45.G3. A difference of more than threefold the IC_{50} of the wild type was considered to be MPER enhancement, whereas anything less than threefold was regarded as being in the same range of neutralization as the wild type. This is in line with international norms for the TZM-bl neutralization assay, which has an approximately three fold error (131).

3.2.1 Neutralization sensitivity of CAP45.G3 cleavage site mutants to MPER antibodies

For this study, we expressed six MPER directed antibodies with varying breadth and potency for use in the neutralization assays. The details of the published breadth and potency for each are shown below in **Table 3.2**.

Table 3.2: Reported neutralization breadth and potency of the MPER bNAbs used in this study (101, 106, 137, 138). Percentage breadth is reported for various published viral panels, with the size of the panels indicated in parentheses. The final column indicates the yield of purified plasmids (in 400 µl) after purification. H (blue) is for heavy chain plasmid and L (red) is for light chain plasmid

bNAb	% Breadth	Geometric mean IC_{50} (µg/ml)	Reference	Plasmid Total Yield (µg)
DH511	99 (n=208)	0.39	(106)	H: 520 L: 784
10E8	97 (n=208)	0.22	(101)	H: 378 L: 497
4E10	98 (n=181)	1.3	(106)	H: 594 L: 800
M66.6	93 (n=41)	8.46	(139)	H: 321 L: 924
2F5	57 (n=181)	1.92	(137)	H: 350 L: 923
Z13e1	Limited neutralization data available		(138)	H: 285 L: 658

Antibodies consist of a two heavy and two light chains arranged in a Y structure. Antibody expression requires co-transfection of heavy and light chain plasmids to generate the full antibody protein. The heavy and light chain DNA for all the bNAbs (**Table 3.2**) had previously been cloned into the CMVR vector, which was resistant to the antibiotic kanamycin. The CMVR expression vector that was used encodes a signal peptide sequence, variable and constant regions of IgG1 heavy and light chain expressed under control of the HCMV (human cytomegalovirus immediate-early) promoter. Plasmids were transformed into ultra-competent *E. coli* cells as described in section 3.1.1, and used to prepare maxi preps of plasmid DNA. The yields of each plasmid preparation ranged from 285 µg to 924 µg (**Table 3.2**). Sanger sequencing with the vector specific primer FCMVR (**Table 2.1**) was used to confirm the sequences of each heavy and light chain plasmid as described in section 3.1.1.

The heavy and light chain plasmids for each antibody were transfected into 293Freestyle cells and expressed antibody was harvested after seven days. Affinity column chromatography using a protein A resin was used to purify each antibody as described in section 2.15. Spectrophotometry was used to quantify the amount of antibody obtained, which ranged from 0,7 to 3.3 mg per 100 ml of starting culture (**Table 3.3**). Each antibody was subsequently concentrated or diluted to 1 mg/ml

(depending on initial concentration), aliquoted for use in the neutralization assay and stored at -80ºC.

Table 3.3: The yield of each expressed MPER antibody in milligrams per 100 ml of starting culture.

bNAb	**Yield (mg/100 ml of starting culture)**
DH511	1.6
10E8	3.3
4E10	1.9
M66.6	1.8
2F5	0.7
Z13e1	0.9

In order to confirm that the antibodies expressed as expected, a reducing SDS-PAGE gel was run to confirm the size of the heavy and light chains of each bNAb. Reducing agents enable more accurate estimation of the size of expressed proteins. The expected sizes for the heavy and light chains were approximately 50 kDa and 25 kDa respectively. The bands on the gel confirmed that the heavy and light chains for each antibody were of the expected size, with minimal impurities (**Figure 3.4**). The light chain sizes, although similar in size, showed some variation due to differences in glycosylation patterns as well as different properties for lambda and kappa light chains.

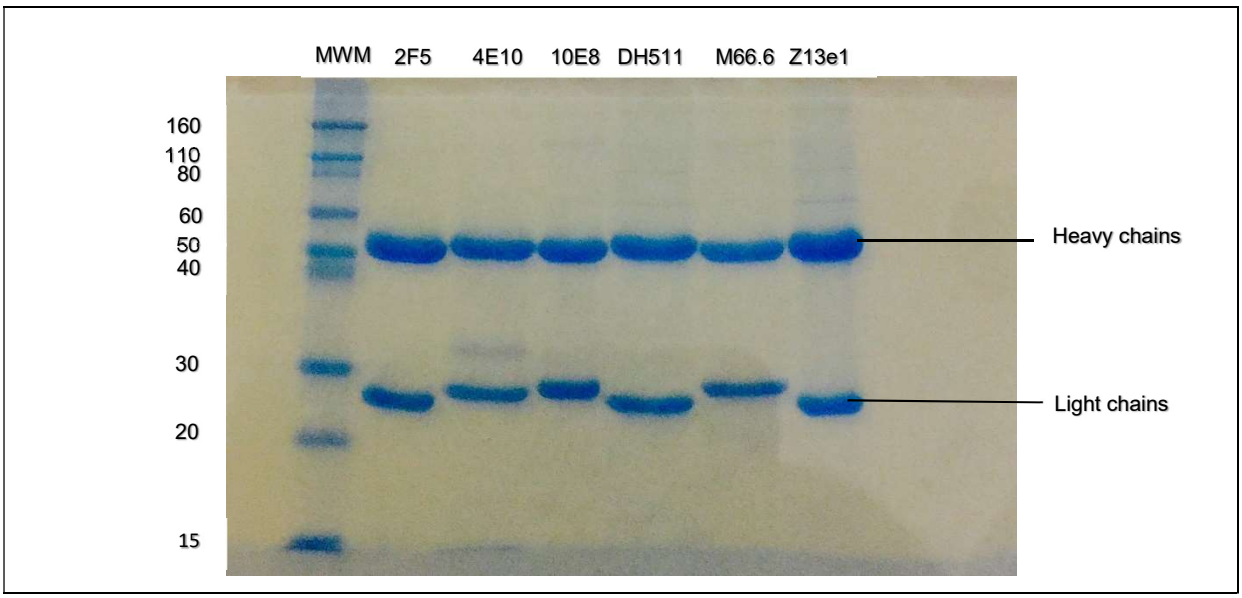

Figure 3.4: SDS PAGE gel showing the antibody heavy and light chains of the expressed MPER bNAbs. Molecular weight marker sizes are in kDa. MWM refers to the molecular weight marker.

Neutralization experiments were performed to confirm that the expressed antibodies showed neutralization profiles comparable to previous studies. All expressed bNAbs were tested for neutralization using one sensitive virus and one resistant virus for each bNAb to confirm epitope specificity. Neutralization titers were compared to those that had been obtained previously in the lab (**Table 3.4**).

Table 3.4: IC_{50} values obtained during the antibody quality control test. The table shows neutralization data for sensitive and resistant viruses tailored to all six antibodies. For the broadest antibodies, 10E8 and 4E10, resistant viruses contained mutations at bNAb contact sites. The warmer the color of the cell, the more potent the neutralization. Red denotes IC_{50} values between 0.01 µg/ml and 1 µg/ml, orange for values between 1 µg/ml and 5 µg/ml, yellow for values between 5 µg/ml and 10 µg/ml, and blue for 10 µg/ml (which represents neutralization resistance). A tick indicates neutralization data for newly expressed antibodies was concordant with historical neutralization data.

bNAb	Virus	Historical IC_{50} (µg/ml)	Actual IC_{50} (µg/ml)	Result
DH511	DU151	0,34	0,52	√
	X2088	>10	>10	√
10E8	6471	3,02	2,94	√
	6471 W672L/T673I	>10	>10	√
4E10	COT6	0,3	0,32	√
	COT6 W672A	>10	>10	√
2F5	C1	3,4	3,81	√
	C1C	>10	>10	√
Z13e1	C1	0,1	0,3	√
	RHPA	>10	>10	√
M66.6	MN.3	1,4	0,98	√
	DU172	>10	>10	√

All the antibodies neutralized the sensitive viruses as expected, with IC_{50} values that were highly concordant with historic data, and failed to neutralize the viruses that were known to be resistant to them. This confirmed the specificity and neutralization capacity of the MPER bNAbs that were required for additional studies below.

We next tested the sensitivity of CAP45.G3 viruses with individual mutations within the cleavage site to MPER antibodies to assess whether these mutations conferred enhanced neutralization, as with the combination of multiple cleavage site mutations.

All the MPER bNAbs were initially tested against the CAP45.G3 wild type virus and the CAP45.G3 CS-Mut virus in order to determine which of the bNAbs would neutralize the wild type virus, and confirm previously reported enhancement for CAP45 CS-Mut. Starting concentrations were determined by the previously determined potency of

each antibody against the CAP45.G3 virus. MAbs DH511, 10E8 and 4E10 neutralized the CAP45.G3 CS-Mut virus, though 4E10 failed to neutralize the wild type virus, in line with previous data. In contrast, mAbs 2F5, Z13e1 and M66.6, which are known to have little breadth (**Table 3.2**) showed no neutralization of either the CAP45.G3 wild type or CAP45.G3 CS-Mut at a maximum concentration of 25 µg/ml (**Table 3.5**). This lack of neutralization was not surprising since they are among the less broad bNAbs targeting the MPER region. We therefore proceeded to test DH511, 10E8 and 4E10 against the single mutants to assess MPER exposure. Antibodies M66.6, 2F5 and Z13e1 were not tested further as they did not neutralize the wild type or the CS-Mut.

Table 3.5: Neutralization of CAP45.G3 wild type and CAP45.G3 CS-Mut viruses by six MPER bNAbs. The warmer the color, the more potent the neutralization. Maroon denotes IC_{50} values below 0.01 µg/ml, red is for 0.01 µg/ml to 0.1 µg/ml, orange for values between 0.1 µg/ml and 1 µg/ml, yellow for values between 5 µg/ml and 10 µg/ml, and blue for more than 25 µg/ml (which represents neutralization resistance). Fold differences that exceed three are highlighted in purple.

bNAb	CAP45.G3 WT (µg/ml)	CAP45.G3 CS-Mut (µg/ml)	Fold difference
10E8	0.6	0.008	75
DH511	0.54	0.01	54
4E10	>25	0.12	<25
M66.6	>25	>25	1
2F5	>25	>25	1
Z13e1	>25	>25	1

Figure 3.5 shows the comparison of CAP45.G3, CAP45.G3 CS-Mut and each single mutant when tested against mAb 4E10. For CAP45.G3 WT, an IC_{50} was not obtained at the maximum starting concentration, though the curve indicated sub-IC_{50} neutralization (**Figure 3.5**). The CAP45.G3 CS-Mut, however, showed a notable increase in sensitivity and was 100% neutralized with an IC_{50} of 0.12 µg/ml, confirming previous data (94). Comparison of the single mutants with CAP45.G3 CS-Mut showed that although most of them exhibited an increase in sensitivity to 4E10 (**Figure 3.5**), none of them were as sensitive as the CS-Mut. E500K was similar to the wild type in that an IC_{50} was not reached. CAP45.G3 R502Q, E507G, R508K and E509G all showed increased neutralization sensitivity to 4E10 compared to the wild type with IC_{50} values of 0.5 µg/ml, 0.8 µg/ml, 1.3 µg/ml and 1.8 µg/ml respectively (with titers shown in Table 3.6).

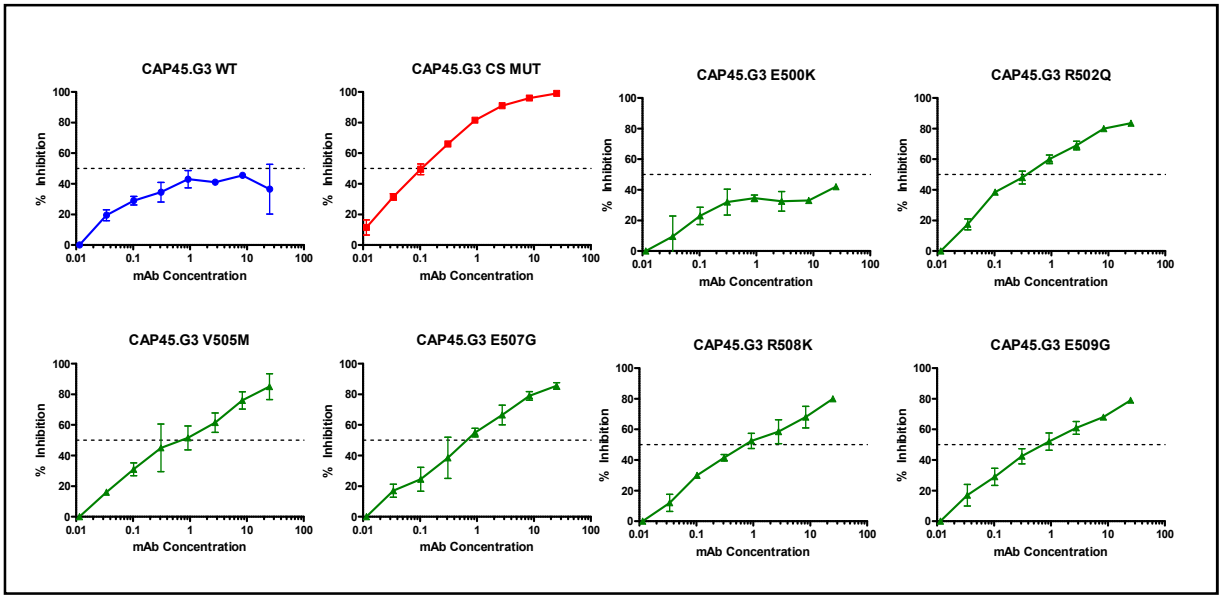

Figure 3.5: **Neutralization of CAP45.G3 wild type and mutants by 4E10.** Graphs showing the neutralization of the CAP45.G3 wild type and mutants by the bNAb 4E10. The wild type is shown in blue, the CAP45.G3 CS-Mut in red and the single mutants (in numerical order) in green. Vertical axis shows percentage inhibition and horizontal axis shows antibody concentration in µg/ml. Experiments were conducted three times.

In contrast to 4E10, where most individual mutants showed enhanced neutralization, for 10E8, most mutants that showed similar sensitivity to the bNAb as the wild type virus. In this case, the wild type CAP45.G3 was neutralized with an IC_{50} of 0.6 µg/ml. The CAP45.G3 CS-Mut showed the highest increase in neutralization sensitivity to 10E8, with a steep neutralization curve compared to the gentle sigmoidal curves that were obtained for the wild type and single mutants, and an IC_{50} of 0.008 µg/ml (**Figure 3.5**). The fold difference between the CAP45.G3 wild type and CAP45.G3 CS-Mut titers was 75, much higher than those of the other mutants (**Table 3.6**).

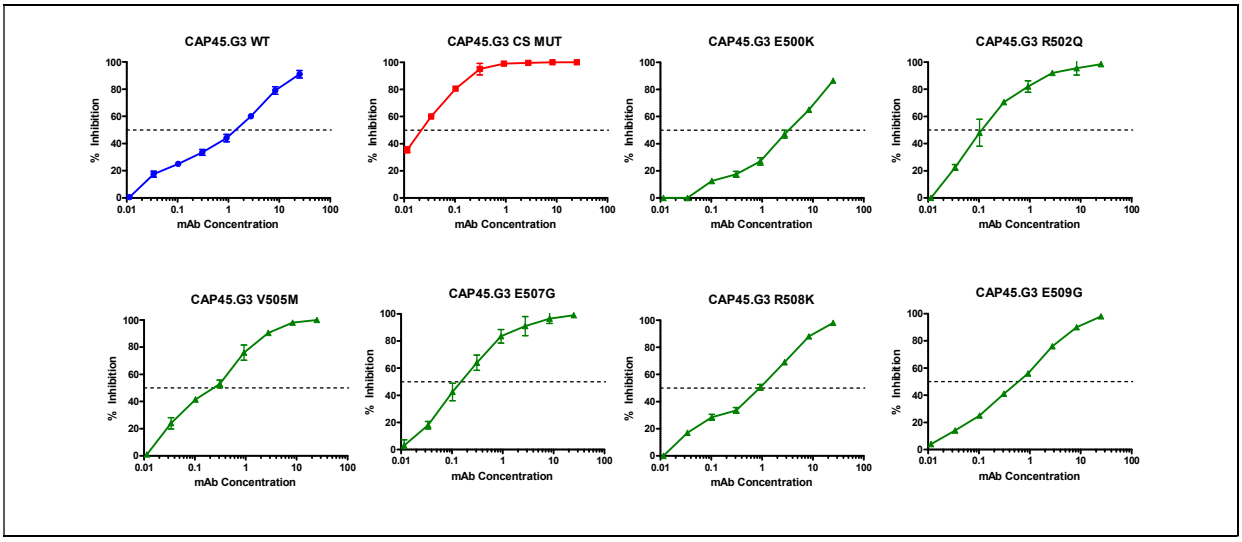

Figure 3.6: Neutralization of CAP45.G3 mutants and wild type by 10E8: Graphs showing the neutralization of the CAP45.G3 wild type and mutants by the MPER bNAb 10E8. The CAP45.G3 wild type is shown in blue, the CAP45.G3 CS-Mut in red and the single mutants in green. Vertical axis shows percentage inhibition and horizontal axis shows antibody concentration in µg/ml. Experiments were conducted three times.

Among the single mutants, only CAP45.G3 R502Q and CAP45.G3 V505M showed greater than threefold increased sensitivity compared to the wild type, indicating enhanced neutralization sensitivity to 10E8. Since E500K, E507G, R508K and E509G all had IC_{50} values less than threefold that of the wild type, it can be concluded that they did not show enhanced neutralization sensitivity to 10E8 (**Figure 3.6**).

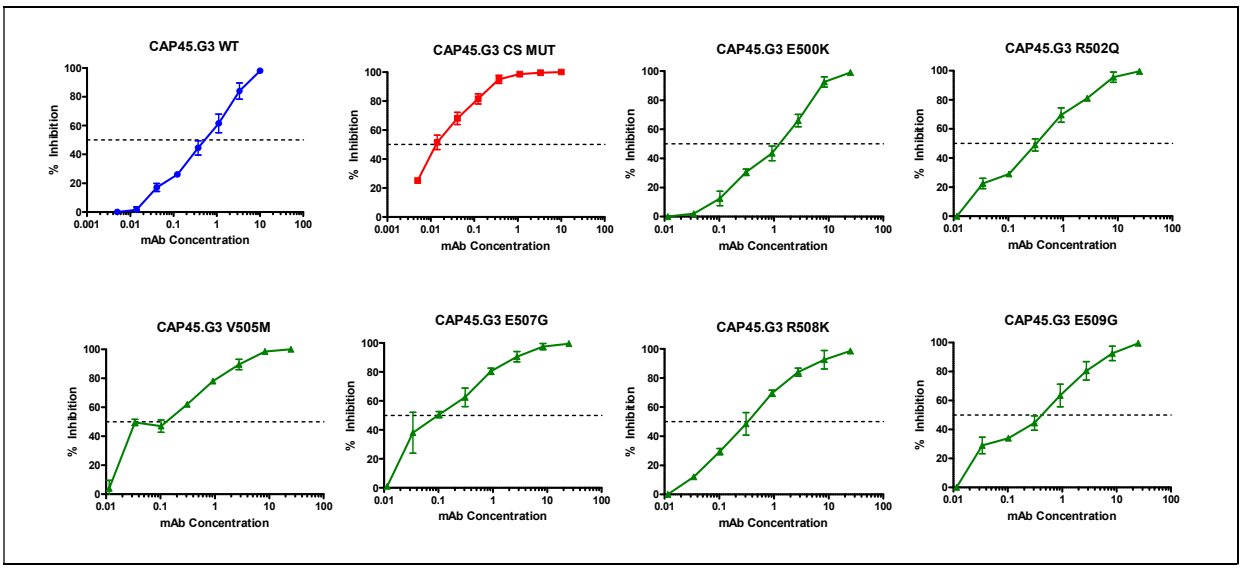

Figure 3.7: Graphs showing the neutralization of the CAP45.G3 wild type and mutants by the MPER bNAb DH511. The wild type is shown in blue, the complete CS-Mut in red and the single mutants in green. Vertical axis shows percentage inhibition and horizontal axis shows antibody concentration in µg/ml. Experiments were conducted three times.

DH511 is very similar to 10E8 in its neutralization properties, but it has been found to be more potent than 10E8 and 4E10 for some viruses (107). In this study DH511 neutralized the CAP45.G3 wild type with an IC_{50} of 0.54 µg/ml (**Table 3.6**). There was a fold difference of 54 between the CAP45.G3 wild type and CAP45.G3 CS-Mut IC_{50}, showing enhanced sensitivity to DH511 (**Figure 3.7**). Only CAP45.G3 E500K and R508K showed little to no enhancement in sensitivity to DH511. CAP45.G3 E507G showed the highest increase in sensitivity among the single mutants, with an IC_{50} of 0.02 µg/ml, and R502Q, V505M and R508K showed fold differences of 4, 8 and 4 respectively compared to that of the wild type.

Table 3.6: Summary of IC_{50} values showing neutralization of CAP45.G3 single mutants by MPER bNAbs. The warmer the color, the more potent the neutralization of the virus by the bNAb. Maroon shows IC_{50} values below 0.1 µg/ml, red denotes values between 0.01 µg/ml and 1 µg/ml, orange for values between 1 µg/ml and 5 µg/ml, yellow for values between 5 µg/ml and 10 µg/ml, and blue for more than 25 µg/ml (which represents neutralization resistance). Fold changes that exceed three are in purple.

bNAb	***Virus***							
	WT	CS-Mut	E500K	R502Q	V505M	E507G	R508K	E509G
10E8	0.6	0.008	1.46	0.12	0.08	1.19	0.3	0.2
Fold diff.	-	**75**	2	**5**	**7.5**	2	2	3
DH511	0.54	0.01	0.42	0.15	0.07	0.02	0.16	0.14
Fold diff.	-	**54**	1	**4**	**8**	**27**	3	**4**
4E10	>25	0.12	>25	0.5	0.2	0.8	1.3	1.1
Fold diff.	-	**208**	1	**55**	**125**	**31**	**20**	**23**

Thus, the single CAP45.G3 mutants, while showing varying degrees of enhancement compared to the CAP45.G3 wild type, did not expose the MPER epitope as well as the complete set of mutations combined. The E500K mutation did not differ from the wild type in its exposure of the MPER, while the R502Q, V505M and E507G mutations showed the best MPER exposure among the single mutants. 4E10 was the most enhanced among the MPER bNAbs. These data suggest that for an MPER-directed immunogen, while the full CAP45.G3 CS-Mut has superior MPER enhancement

compared to the single CAP45.G3 mutants, a combination of the three single mutants that showed the best MPER exposure may result in a better balance between neutralization enhancement and fitness.

3.2.2 Neutralization sensitivity of CAP45.G3 cleavage site mutants to gp120-gp41 Interface antibodies

Wibmer et al (2017) previously showed that the cleavage site mutations enhanced neutralization of the CAP45.G3 virus by the gp120-gp41 interface bNAb 35O22 (94). In contrast, a bNAb that was isolated from CAP248, termed CAP248-2B, failed to neutralize the CAP45.G3 CS-Mut despite potent neutralization of the CAP45.G3 wild type as mutations in this region directly affected its epitope (94). It was thus necessary to test the neutralization profiles of bNAbs that target the gp120-gp41 interface against the single CAP45.G3 cleavage site mutants in order to establish their effect on that epitope. When we tested the single mutants against the CAP248-2B antibody, there was no change in neutralization sensitivity except for CAP45.G3 V505M, which had increased resistance to the antibody. This data supported the findings of the previous study conducted in the lab (94).

Table 3.7: Neutralization of CAP45.G3 wild type, CAP45.G3 CS-Mut and single mutants by gp120-gp41 interface antibody CAP248-2B. *An IC_{50} was not obtained for this mutant, although the neutralization curve shows that the antibody neutralizes 45% of the virus.

CAP45.G3 mutant	**CAP248.28 IC_{50} (µg/ml)**
Wild Type	0.0255
CS-Mut	>10
E500K	0.0256
R502Q	0.0474
V505M	>10*
E507G	0.0158
R508K	0.0200
E509G	0.0154

Several interface bNAbs, namely 35O22, 3BC315, VRC34, PGT151 and 8ANC195 were tested using the neutralization assay against the CAP45.G3 wild type, single mutants, and CS-Mut. IC_{50} values and fold differences from the wild type values were shown for each gp120-gp41 interface directed bNAb (**Table 3.8**). There was some increase in sensitivity of the CS-Mut and E500K mutants to 35O22, which is in line with data shown in a previous study where 35O22 neutralization of CAP45.G3 was enhanced by the cleavage site mutations (94).

Table 3.8: Neutralization of CAP45.G3 wild type and single mutants by gp120-gp41 interface-directed bNAbs. The warmer the color of the cell, the more potent the neutralization of the virus by the bNAb in question. Maroon is for values below 0.01 µg/ml, red denotes values between 0.01 µg/ml and 1 µg/ml, orange for values between 1 µg/ml and 5 µg/ml, yellow for values between 5 µg/ml and 10 µg/ml, and blue for more than10 µg/ml (which represents neutralization resistance).

bNAb	**Virus**							
	WT	**CS-Mut**	**E500K**	**R502Q**	**V505M**	**E507G**	**R508K**	**E509G**
35022	0.02	0.006	0.007	0.01	0.03	0.03	0.03	0.02
3BC315	>10	>10	>10	7.1	2.4	9.9	>10	>10
VRC34	0.03	0.08	0.02	0.02	0.04	0.04	0.03	0.04
PGT151	0.02	0.48	0.01	0.01	0.01	0.02	0.01	0.01
8ANC195	>10	>10	>10	>10	>10	>10	>10	>10

The R502Q, V505M and E507G mutants were sensitive to neutralization by 3BC315 and IC_{50}s were obtained in spite of the fact that the wild type was resistant to the gp120-gp41 interface bNAb. The mutations at positions 502, 505 and 507 therefore exposed the 3BC315 epitope such that neutralization of the virus was enhanced, with V505M showing the greatest increase in sensitivity to this bNAb. There was no enhancement of neutralization by VRC34 for any of the mutants, indicating that this bNAb epitope was not affected by the mutations. CAP45.G3 CS-Mut showed a remarkable 24-fold decrease in neutralization sensitivity to PGT151 however the single mutants showed no decrease or enhancement in sensitivity to PGT151. 8ANC195 failed to neutralize the wild type or any of the mutants.

In summary, the CAP45.G3 CS-Mut thus shows a range of effects on the bNAbs targeting the gp120-gp41 interface, with increased sensitivity to 35O22 and 3BC315 while showing a decrease in sensitivity to PGT151. However, the single mutants showed that little enhancement in neutralization sensitivity to a few of these bNAbs.

3.2.3 Neutralization sensitivity of CAP45.G3 cleavage site mutants to bNAbs targeting other epitopes

Conformation of the viral envelope spike may have been altered by the cleavage site mutations such that the MPER and interface epitopes were not the only ones that were exposed. It was therefore necessary to establish whether any of the mutations exposed other bNAb epitopes. We thus assessed sensitivity of individual mutants to V2, V3 and CD4bs targeting bNAbs. For the two V2 targeting bNAbs, PG9 and PGT145, IC50 values for the CS-Mut and for individual viruses were similar to that of the wild type viruses. No differences above threefold that of the wild type IC_{50} were observed, and the mean fold difference from the wild type was one (**Table 3.9**).

Table 3.9: Neutralization of CAP45.G3 wild type and mutant pseudoviruses by bNAbs targeting the V2, CD4bs and V3 epitopes of Env. The warmer the color of the cell, the more potent the neutralization of the virus by the bNAb in question. Maroon is for values below 0.01 µg/ml, Red denotes values between 0.01 µg/ml and 1 µg/ml, orange for values between 1 µg/ml and 5 µg/ml, yellow for values between 5 µg/ml and 10 µg/ml, and blue for more than10 µg/ml (which represents neutralization resistance)

bNAb	**Virus**							
	WT	**CS-MUT**	**E500K**	**R502Q**	**V505M**	**E507G**	**R508K**	**E509G**
PG9	0.01	0.01	0.01	0.01	0.01	0.008	0.01	0.009
PGT145	0.006	0.006	0.007	0.005	0.006	0.005	0.004	0.005
VRC01	1.22	2.02	1.19	0.36	1.64	1.22	1.52	1.55
3BNC117	1.24	1.21	0.55	0.31	1.29	0.42	0.62	0.44
PGT121	0.79	1.05	0.22	0.28	0.27	0.15	0.21	0.27
PGT130	>10	>10	>10	>10	>10	>10	>10	>10

For the CD4 binding site bNAbs, VRC01 and 3BNC117, all the mutant IC_{50}s were within the wild type value range except for the R502Q mutant, which was four fold

more sensitive to both VRC01 and 3BNC117, indicating slightly enhanced sensitivity. This mutation therefore exposed the CD4bs epitope and increased sensitivity of the virus to the CD4bs bNAbs. The V3 bNAbs PGT121 and PGT130 were not enhanced by any of the mutations, and all the CAP45.G3 viruses including the wild type were resistant to neutralization by PGT130. In conclusion, with a few exceptions, the IC_{50} values for the mutants did not differ substantially from those of the wild type strain for any of the bNAbs targeting epitopes other than the MPER. It can therefore be concluded that the increase in sensitivity was largely limited to the MPER region, and that these mutations did not result in gross changes in Env conformation.

3.3 Design and testing of a CAP45.G3 triple mutant for viral fitness and MPER exposure

As the single mutations did not enhance MPER neutralization to the same extent as the CS-Mut, it was clear that a combination of mutations was necessary for optimal MPER exposure. We hypothesized that a combination with fewer mutations was more likely to have better entry potential compared to the CS-Mut, rendering it more favorable for use in future vaccine studies using virus-like particles. In order to establish if a smaller subset of the cleavage site mutations could accomplish the same MPER exposure as the CS-Mut while exhibiting improved entry potential, the three CAP45.G3 single mutants that resulted in the highest increase in sensitivity to MPER bNAbs (CAP45.G3 R502Q, V505M, and E507G) were combined into a triple mutant, termed CAP45.G3 R502Q/V505M/E507G.

3.3.1 Generation of a CAP45.G3 triple mutant plasmid and pseudovirus production

Mutagenesis primers were designed to insert all three mutations into CAP45.G3 at the same time using site directed mutagenesis as described in section 2.6. Mutagenesis products were transformed into ultra-competent cells as described in section 2.3, and DNA was extracted using miniprep kits as described in section 2.5. DNA was screened for mutations using Sanger sequencing. The resulting triple mutant plasmid was subsequently used to produce pseudovirus as described in section 2.17.

As noted in section 3.1, mutating conserved regions of the envelope can have a negative effect on viral entry potential. A second “head to head” transfection and pseudovirus quantification was performed so as to compare the entry potential of the triple mutant and the CAP45.G3 CS-Mut. The triple mutant showed a 23% reduction in entry potential (from 810,356 RLUs to 621,873 RLUs) compared to the wild type ($p = 0.063$), less than that of the CS-Mut, which exhibited a significant 90% reduction ($p = 0.007$). The three mutations together thus did not reduce fitness much more than the individual mutations, as might have been expected. The triple mutant may therefore be favorable for use as an immunogen in that it has improved entry potential compared to the CS-Mut.

3.3.2 Neutralization of the CAP45.G3 triple mutant by MPER bNAbs

To determine the level at which the MPER sensitivity increased with the three mutations combined, we tested the neutralization sensitivity of the triple mutant to the same MPER bNAbs that were tested for the single mutants. A comparison in MPER neutralization between the CAP45.G3 CS-Mut and the CAP45.G3 triple mutant was made (**Figure 3.8** and **Table 3.10**).

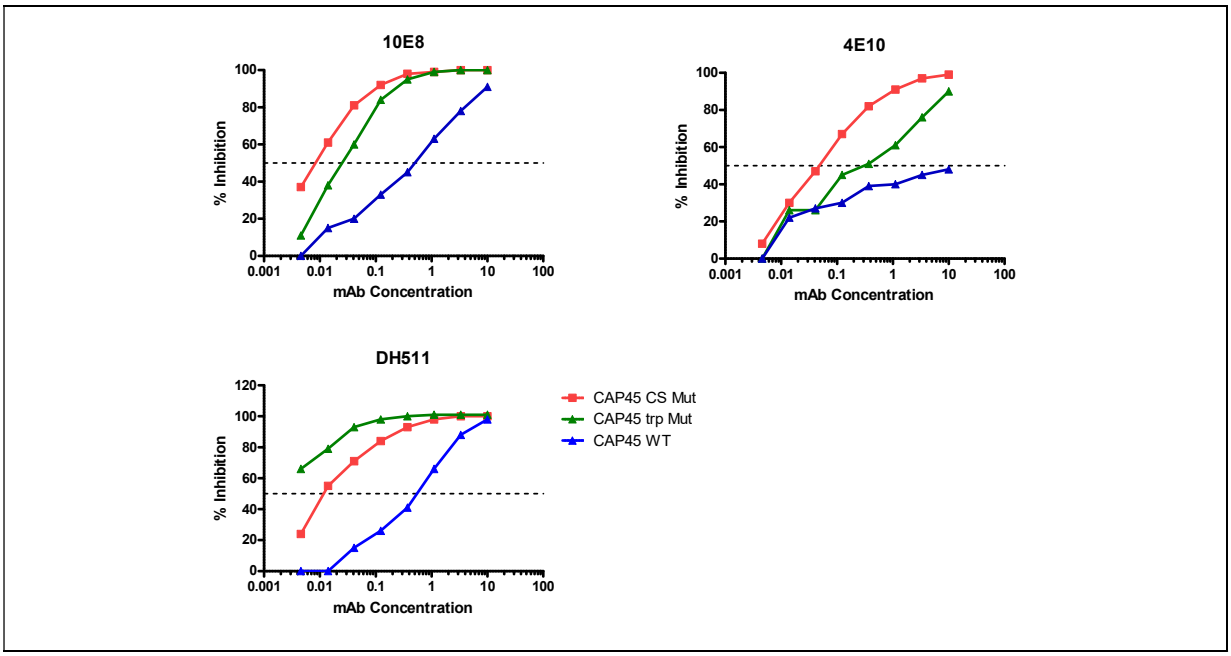

Figure 3.8: Neutralization of the CAP45.G3 triple mutant (R502Q/V505M/E507G) by MPER bNAbs The x axis represents bNAb concentration in µg/ml, and the y axis represents percentage inhibition. Experiments were conducted three times.

Similar to the CAP45.G3 wild type and single mutants, the CAP45.G3 triple mutant was not sensitive to neutralization by the MPER bNAbs 2F5, Z13e1 and M66.6. However, the rest of the MPER bNAbs, 4E10, 10E8 and DH511 showed potent neutralization of the triple mutant (**Figure 3.8**). For 4E10 and 10E8, we observed a significant increase in neutralization sensitivity of the triple mutant to these bNAbs compared to the wild type CAP45.G3, with fold differences of 33 and 24 respectively. These effect was even more pronounced, at 27 fold, for DH511, where the triple mutant was more potently neutralized than the CAP45.G3 CS-Mut.

In conclusion, the three mutations alone were able to significantly increase MPER neutralization, though not to the same level as that of the complete CS-Mut for 10E8 and 4E10. Unlike the other MPER bNAbs, neutralization by DH511 is optimal in the presence of the three mutations as opposed to all six. This indicates, the triple mutant is sufficient for epitope exposure and enhancement of viral sensitivity to these bNAbs, and a viable vaccine candidate for future studies.

3.3.3 Neutralization of the CAP45.G3 triple mutant by gp120-gp41 Interface bNAbs

We further tested bNAbs targeting the gp120-gp41 interface, the V2, V3 and CD4bs epitopes to establish if the three mutations exposed any other epitopes, thus increasing the virus sensitivity to bNAbs targeting those epitopes (**Table 3.10**).

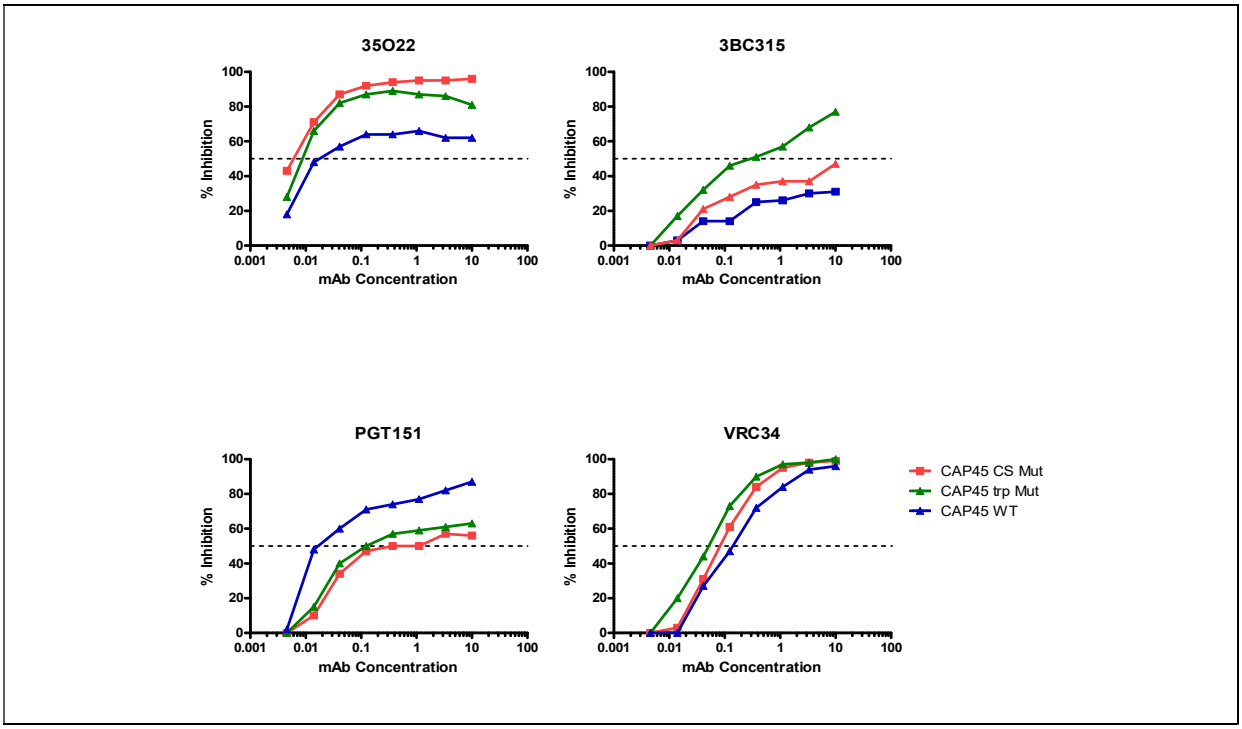

Figure 3.9: Neutralization of the CAP45.G3 wild type, CS-Mut and triple mutant viruses by gp120-gp41 interface bNAbs. The x axis represents bNAb concentration and the y axis represents percentage inhibition. The dotted line indicates the IC_{50} point.

The triple mutant resulted in improved neutralization by 35O22 and 3BC315. For 35O22, neutralization titers using the triple mutant were comparable with the CS-Mut, however for 3BC315 the triple mutant showed higher antibody titers compared to the CS-Mut. (**Figure 3.9**). This is consistent with our previous data showing that each of the single mutations included in the triple mutant, R502Q, V505M and E507G, also enhanced neutralization by 3BC315 (**Table 3.8**). In contrast, for PGT151, the triple mutant, like the CS-Mut, exhibited a six-fold decrease in sensitivity to PGT151 compared to the CAP45.G3 wild type virus (**Figure 3.9**). No change in sensitivity was observed for VRC34.

3.3.4 Neutralization of the CAP45 triple mutant by bNAbs targeting the V2, V3 and CD4bs epitopes

The CAP45.G3 triple mutant neutralization profile for bNAbs targeting other epitopes showed values within range of both the wild type (**Table 3.10**). This suggests that the V2, V3, and CD4bs epitopes were not exposed by the cleavage site mutations, and

this effect was limited to the MPER and the gp120-gp41 interface epitopes only. Moreover, this is an indication that the envelope trimer structure was still intact despite the addition of the three mutations to it.

Table 3.10: Neutralization of the CAP45.G3 triple mutant by bNAbs targeting the MPER, gp120-gp41 interface, CD4bs, V2 and V3 epitopes. The neutralization profile of the CAP45.G3 wild type and CS-Mut are also shown. Fold differences between the wild type and triple mutant are recorded in the fifth column and values above threefold that of the wild type are highlighted in purple. Values indicating decrease in sensitivity are highlighted in green. KO (Knock out) indicates neutralization resistance where there was previously sensitivity. The warmer the color of the cell, the more potent the neutralization of the virus by the bNAb in question. Maroon is for values below 0.01 µg/ml, Red denotes values between 0.01 µg/ml and 1 µg/ml, orange for values between 1 µg/ml and 5 µg/ml, yellow for values between 5 µg/ml and 10 µg/ml, and blue for more than 10 µg/ml.

bNAb	Epitope	CAP45 WT	CAP45 CS Mut	fold difference from WT	CAP45 triple mutant	fold difference from WT
2F5	MPER	>10	>10	1	>10	1
M66.6		>10	>10	1	>10	1
Z13e1		>10	>10	1	>10	1
4E10		>10	0,12	208	0,3	33
10E8		0,6	0,008	75	0,025	24
DH511		0,54	0,01	54	0,02	27
35O22	Interface	0,02	0,006	3	0,008	3
3BC315		>10	>10	1	0,31	32
CAP248-2B		0,03	>10	KO	>10	KO
PGT151		0,02	0,48	24	0,12	6
VRC34		0,03	0,08	3	0,05	2
8ANC195		>10	>10	1	>10	1
PG9	V2	0,01	0,01	1	0,007	1
PGT145		0,02	0,02	1	0,02	1
VRC01	CD4bs	1,22	2,02	2	3,5	3
3BNC117		1,24	1,21	1	2,7	2
PGT121	V3	0,79	1,05	1	0,56	1
PGT130		>10	>10	1	>10	1

3.4 Designing dual germline targeting envelopes as HIV-1 vaccine immunogens

Active vaccination is based on using antigens derived or engineered from the infecting agent to stimulate the immune system to mount a response to the antigen (140). As part of this process, precursor B-cells are activated, mature through successive rounds of affinity maturation and give rise to memory B-cells expressing antibodies to

neutralize future threats to the host (141). In order to give rise to breadth, the antigen used in an HIV vaccine would have to specifically select for B-cells that have the capacity to eventually develop into bNAbs. For HIV vaccine design, this is especially challenging as bNAb precursors often possess unique features that differentiate them from most antibodies. These features include long CDRH3s, a feature commonly seen in MPER bNAbs, or short CDRL3s. In many cases, it is not clear how the bNAb precursors were selected. The fact that only a subset of people make bNAbs may suggest the possibility that they were infected with unique viruses that have the capacity to stimulate the precursors of bNAbs. This is the basis of several published studies that have sought to identify unique subsets of viral isolates that can be used as immunogens to stimulate a broadly neutralizing response (81, 126, 127). One such example is the identification of 5 viruses (in two separate studies) that bind to the precursors of V2 directed antibodies, and are the basis of this aim.

A second challenge in the design of germline targeting immunogens is the lack of data on precursor B-cells that eventually give rise to bNAbs, or the UCAs of bNAb lineages. It is not always possible to identify an actual UCA from an infected person without detailed and expensive longitudinal studies of bNAb ontogeny. Importantly, no such studies have yet been conducted for MPER-directed antibodies. For this reason, germline-like antibodies (or germline reverted antibodies) are inferred from mature bNAbs for research purposes. The process of germline reversion involves back mutating regions of the antibodies to match their germline genes, however the CDRH3 which cannot be accurately reverted is left in its mature, mutated form in the germline reverted bNAbs. Thus although the inferred germline-reverted bNAbs are not an entirely accurate representation of the UCA, they are the best available option for testing the potential of immunogens to elicit MPER antibodies.

The second aim of this study was based on the hypothesis that enhancement of neutralization by mature MPER bNAbs would also translate to enhanced neutralization by their germline reverted counterparts. The study therefore aimed to design dual germline targeting viral envelopes by adding the CAP248 cleavage site mutations into several viruses previously shown to have a high probability of binding to germline reverted forms of bNAbs that target the V2 epitope of HIV-1 (126, 127). If binding by germline MPER antibodies was enhanced, this would result in a dual germline targeting group of viruses able to elicit both MPER and V2-directed antibodies. Such

a dual targeting immunogen would be more likely to elicit a broad response compared to immunogens with a single target epitope.

The full set of six cleavage site mutations was therefore added to each of five viruses previously shown to be reactive with V2 bNAb precursors using site directed mutagenesis. Thereafter env-pseudotyped viruses were grown, and the effect of the cleavage site mutations on infectivity of each virus was assessed, given that we have previously shown that these mutations reduce viral fitness. Each parental wild type virus and its matched CS-Mut virus was tested for neutralization sensitivity to mature MPER bNAbs first, to confirm that in this viral context there was increased exposure of the MPER. Sensitivity of mutants to bNAbs targeting other epitopes were also tested to determine if any other epitope was aberrantly exposed by the cleavage site mutations. Finally, germline reverted MPER bNAbs were tested to establish if the cleavage site mutations exposed the MPER such that the inferred germline MPER-directed bNAbs could neutralize the viruses.

3.4.1 Site directed Mutagenesis of viral plasmids

The six MPER enhancing mutations were introduced into five previously described viral isolates, namely, ZM233, CAP256 SU, CM244, T250-4 and WITO.33. Each of these viruses has enhanced reactivity with V2-directed precursors, and are hereafter referred to as the “special strains” (126, 127). An alignment of the viral sequences at the region of interest is shown in **Figure 3.10**.

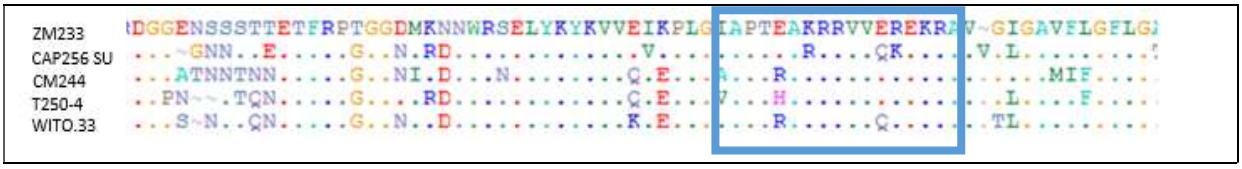

Figure 3.10: Alignment of V2 “special strain” viral envelopes into which CS-Mut was added to engineer dual germline targeting strains. The location of the cleavage site to be mutated is highlighted in the blue box.

Due to the large number of mutations that needed to be added to the viruses, an effort was made to introduce them simultaneously to each envelope by way of overlapping

PCR, described in section 2.9. However, the PCR proved challenging and the desired product was not obtained this way after several attempts. We therefore opted to add the mutations sequentially (two at a time) to each envelope using site directed mutagenesis. Site specific primers were designed to introduce the cleavage site mutations into each virus two at a time. The first set of primers introduced the E500K/R502Q, then to that double mutant, the second pair of primers introduced the V505M/E507G pair and to that mutant, the third and last set of primers introduced the R508K/E509G pair of mutations.

The set of sequential mutagenesis reactions resulted in the complete CS-Mut for each "special strain" virus. Once each round of mutagenesis was performed, mutants were screened using Sanger sequencing as described in section 2.7. When the mutations were confirmed for each virus, each full envelope DNA was sequenced using eight forward and reverse primers to sequence the full gene (**Table 2.1**). One correctly sequenced clone was selected for each wild type and CS-Mut virus and subsequently used to produce pseudotyped viruses.

3.4.2 Production of pseudoviruses and determining the effect of CS-Mut on viral fitness

Each special strain wild type and CS-Mut pair was transfected as described in section 2.17. In addition to the transfection of large viral stocks for future neutralization assays, a small-scale "head to head" transfection in a six well plate was performed for all the "special strains" and their mutants so as to eliminate batch to batch variation and accurately assess the infectivity of each virus. The maximum infectivity for each viral strain was quantified using the TZM-bl assay as described in section 2.18.

The effect on viral fitness was determined by comparing the maximum infectivity values of the wild type viruses to those of their CS-Mut counterparts. This comparison showed that there was a substantial reduction in viral fitness for all five "special strains" (**Table 3.11**).

Table 3.11: Comparison on the infectivity of wild type "special strains" and their CS-Mut counterparts. Fold differences show a reduction in viral fitness with each mutant. The red text indicates abrogation of infectivity in the CS-Mut virus.

Virus	Wild Type Infectivity	CS-Mut Infectivity	Fold Difference
CAP256 SU	4,272,521	1,613,920	5
WITO.33	279,744	47,234	6
T250-4	164,768	38,922	4
ZM233	49,320	864	57
CM244	143,038	1,272	112

In the cases of ZM233 and CM244, no functional pseudoviruses were obtained for the CS-Mut, as the mutants exhibited 98% and 99% reduction in viral fitness respectively. These two viruses were therefore not included further in the study (**Figure 3.11**).

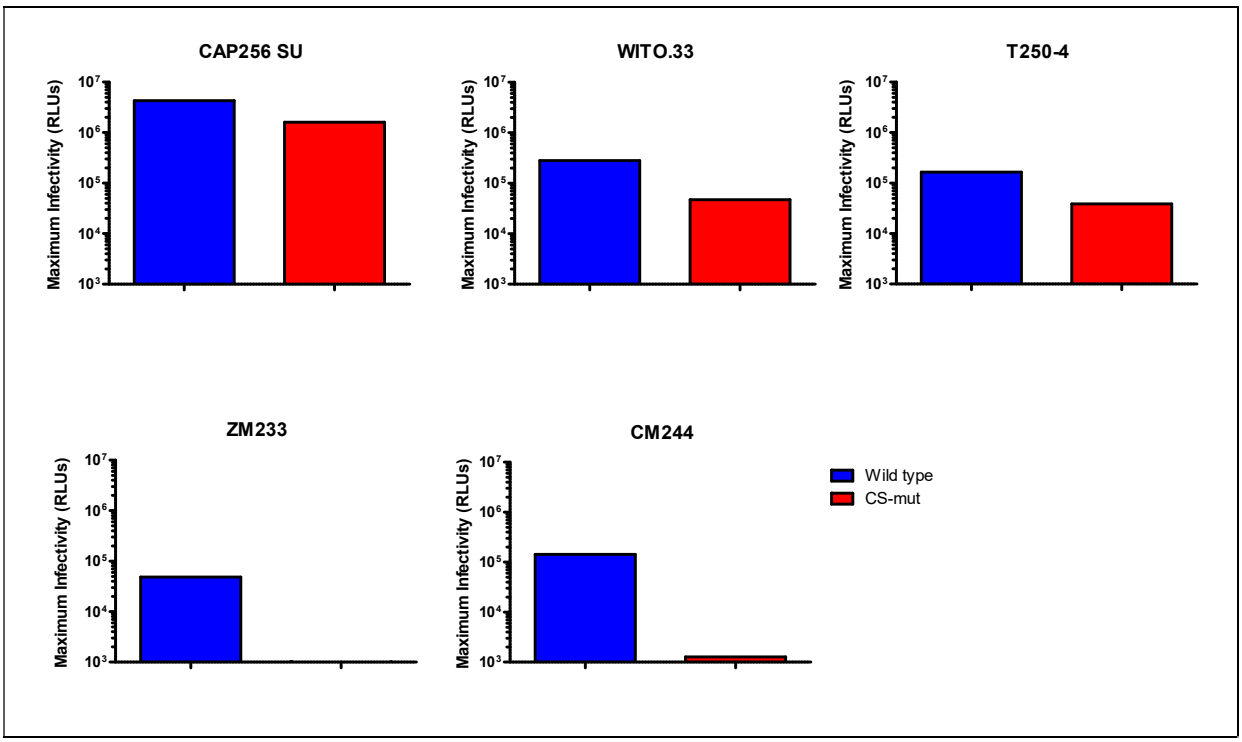

Figure 3.11: Graphs showing the difference between the infectivity of the wild type V2 "special strains" and their cleavage site mutants. The y axis indicates maximum infectivity (measured in relative light units). Blue bars represent the wild type virus in each graph and red bars represent the CS-Mut virus in each graph. Experiments were conducted three times.

Substantial reductions in viral infectivity were also observed for CAP256 SU CS-Mut, WITO.33 CS-Mut and T250-4 CS-Mut, with reduction of 62%, 83% and 76%

respectively in comparison to their wild type viruses. Despite this reduction in entry capacity, functional viruses were obtained. Interestingly, in the two viruses where the mutant viruses failed to produce viable virus, the infectivity for the corresponding wild type viruses was lowest.

The opposite was true for CAP256 SU in that the wild type strain was highly infectious, with over four million RLUs, and its CS-Mut also retained high entry efficiency, with over a million RLUs when undiluted. Future selection of strains for immunogen design including these cleavage site mutants should therefore focus on viral isolates that are highly efficient at mediating cell entry.

3.4.3 Neutralization sensitivity of V2 "special strains" and their CS-Mut mutants to mature MPER bNAbs

The next objective was to assess the neutralization profiles of the wild type "special strain" viruses and compare those to the matched CS-Mut viruses for different classes of bNAbs. The sensitivity of each special strain virus and its mutated equivalent were first assessed using mature MPER bNAbs (10E8, 4E10, DH511, 2F5, Z13e1 and M66.6). The neutralization curves were plotted and compared, along with the actual IC_{50} values.

We first assessed T250 and T250-4 CS-Mut, which showed an increase in neutralization susceptibility to all the mature MPER bNAbs compared to the wild type (**Figure 3.12**). DH511, 10E8, 4E10 and 2F5 were especially potent in their neutralization of the mutant T250-4 virus, with IC_{50} values below 1 µg/ml.

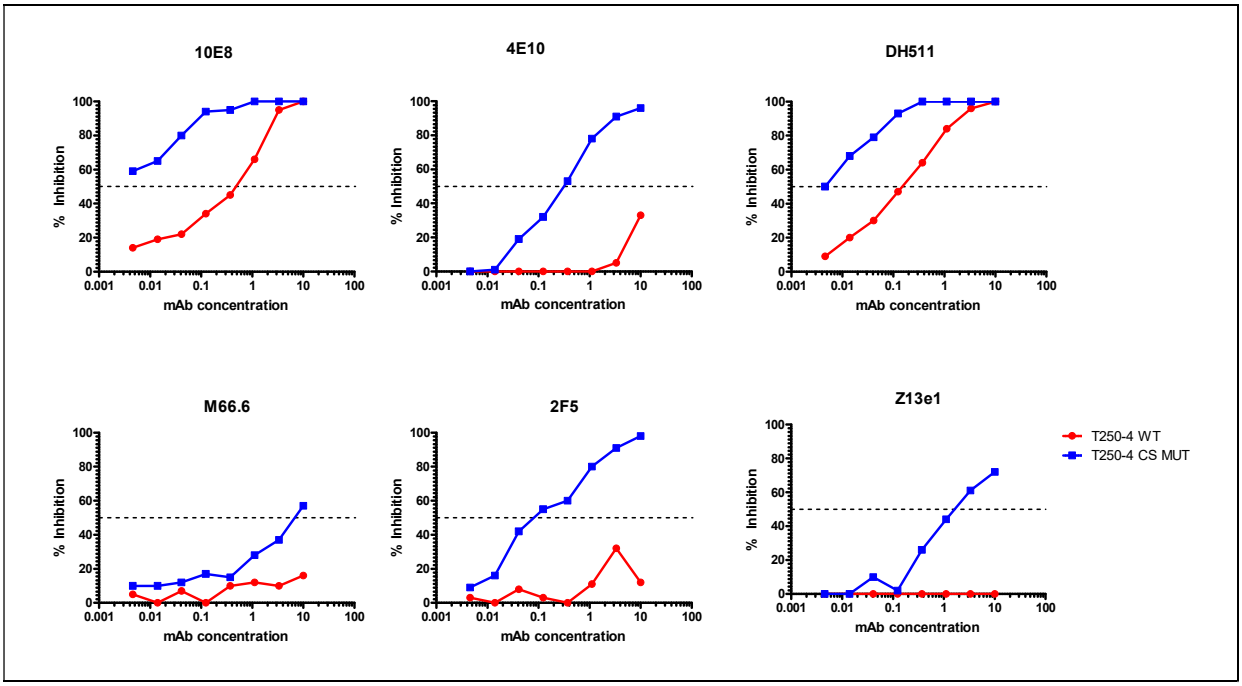

Figure 3.12: Neutralization of T250-4 and T250-4 CS-Mut by mature MPER bNAbs. The x axis shows mAb concentration in µg/ml and the y axis shows percentage inhibition. A dotted line marks the IC_{50} point on each graph. Experiments were conducted three times.

Strikingly, in the cases of 2F5, 4E10 and M66.6, neutralization of the wild type T250-4 virus failed to reach IC_{50} values, with only 12%, 33% and 16% neutralization respectively. However, the T250-4 CS-Mut was potently neutralized by these bNAbs at 98%, 96% and 76% respectively. Similarly, the wild type was altogether resistant to Z13e1, whereas the T250-4 CS-Mut was neutralized by this bNAb at 72%. The enhancement was remarkable in the case of 2F5, which had a 121-fold difference between mutant and wild type but less striking for Z13e1 with only a 6-fold difference compared to the wild type (**Table 3.12**). It can thus be concluded that in the viral context of T250-4, that neutralization of all mature MPER-directed antibodies was enhanced by inclusion of the cleavage site mutations.

Table 3.12: IC_{50} values showing the fold difference in neutralization of T250-4 wild type virus and the T250-4 CS-Mut by mature MPER bNAbs. Fold differences between the wild type and CS-Mut are recorded in the last column and values above threefold that of the wild type are highlighted in purple. The warmer the color of the cell, the more potent the neutralization of the virus by the bNAb in question. Maroon is for values below 0.01 µg/ml, Red denotes values between 0.01 µg/ml and 1 µg/ml, orange for values between 1 µg/ml and 5 µg/ml, yellow for values between 5 µg/ml and 10 µg/ml, and blue for more than 10 µg/ml (which represents neutralization resistance).

bNAb	IC_{50}		FOLD DIFFERENCE
	T250	**T250 CS-Mut**	
DH511	0.15	0.02	8
10E8	0,5	0,02	25
2F5	>10	0,08	121
Z13e1	>10	1,72	6
4E10	>10	0,34	33
M66.6	>10	6.91	1

Similar observations were made for the CAP256 SU virus strain, with an increase in sensitivity to the mature MPER bNAbs observed for DH511, 10E8, 4E10 and Z13e1 (**Figure 3.13**).

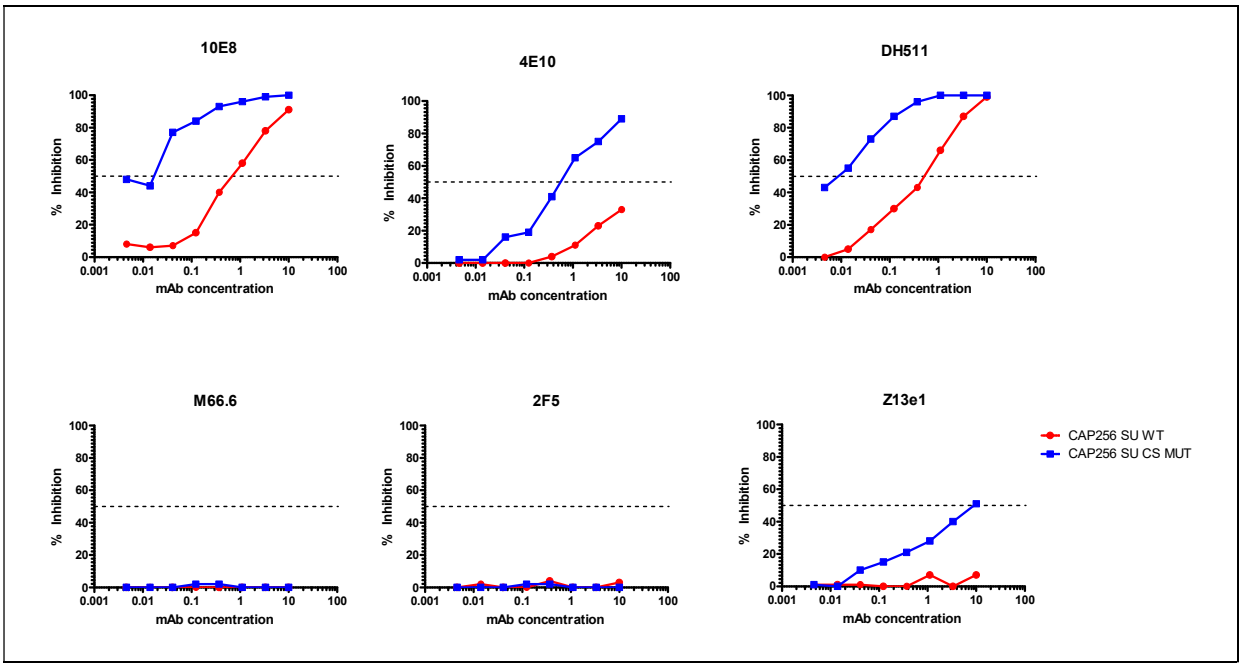

Figure 3.13: Neutralization of CAP256 SU CS-Mut and wild type by mature MPER bNAbs**.** The x axis shows mAb concentration in µg/ml and the y axis shows percentage inhibition. A dotted line marks the IC_{50} point on each graph. Experiments were conducted three times.

Neutralization of the wild type by 4E10 peaked at 33% and an IC_{50} was thus not reached. The CS-Mut exhibited increased sensitivity to 4E10 and neutralization peaked at 89%, with an IC_{50} value of 0.6 (**Table 3.13**). This was indicative of improved exposure of the 4E10 epitope on the CS-Mut envelope. For Z13e1, the cleavage site mutations introduced neutralization to an otherwise completely resistant wild type, with neutralization peaking at 50% for the CS-Mut compared to less than 10% for the wild type.

Table 3.13: IC_{50} values showing the neutralization profiles of mature MPER bNAbs against the CAP256 SU wild type and CAP256 SU CS-Mut. Fold differences between the wild type and CS-Mut are recorded in the last column and values above threefold that of the wild type are highlighted in purple. The warmer the color of the cell, the more potent the neutralization of the virus by the bNAb in question. Maroon is for values below 0.01 µg/ml, Red denotes values between 0.01 µg/ml and 1 µg/ml, orange for values between 1 µg/ml and 5 µg/ml, yellow for values between 5 µg/ml and 10 µg/ml, and blue for more than 10 µg/ml (which represents neutralization resistance).

bNAb	IC_{50}		FOLD DIFFERENCE
	CAP256 SU	CAP256 SU CS-Mut	
10E8	0,7	0.07	10
2F5	>10	>10	1
Z13e1	>10	8,9	<10
4E10	>10	0,6	18
M66.6	>10	>10	1
DH511	0,5	0.09	5

The neutralization data is suggestive of increased exposure of the MPER region by the cleavage site mutations. However, there was little or no neutralization of either the wild type or mutant viruses by Z13e1 and M66.6. Failure of 2F5 and M66.6 to neutralize both the CAP256 SU wild type and CS-Mut viruses indicates the absence of their shared epitope on this envelope. Similarly, DH511 and 10E8 share an epitope and have similar neutralization profiles in terms of CAP256 SU, although the fold difference between the mutant and wild type is slightly higher for 10E8. This data suggests that although the MPER was exposed by the cleavage site mutations in CAP256 SU, the absence of the M66.6 and 2F5 epitope on this virus renders it less ideal as an immunogen for the elicitation of several MPER antibodies.

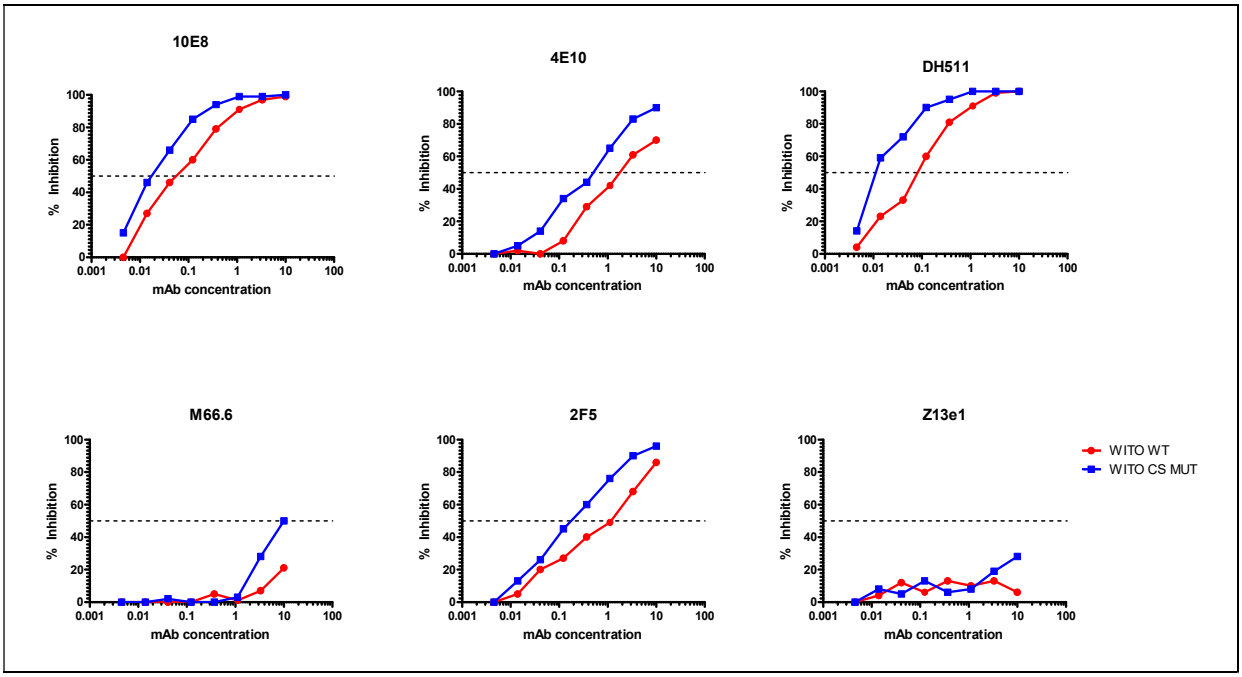

Figure 3.14: Neutralization of WITO.33 CS-Mut and wild type by mature MPER bNAbs. The x axis shows mAb concentration in µg/ml and the y axis shows percentage inhibition. A dotted line marks the IC_{50} point on each graph. Experiments were conducted three times.

The least enhancement of viral sensitivity to MPER bNAbs was seen with WITO.33 CS-Mut (**Figure 3.14**). A comparison of the IC_{50} values between the WITO.33 wild type and CS-Mut showed that only 2F5, 4E10 and DH511 had notable fold differences (seven, four and eight respectively) between the wild type and mutant viruses (**Table 3.14**). Although some enhancement in the neutralization of the WITO.33 CS-Mut by 10E8, Z13e1 and M66.6 was observed, it was not as remarkable as that observed for CAP256 SU and T250-4. DH511 showed the most enhancement in neutralization between wild type and CS-Mut (**Table 3.14**) with an eight-fold difference.

The fact that for WITO.33, introduction of cleavage site mutations resulted in limited enhancement of MPER neutralization may suggest that the MPER region of this virus is naturally in an exposed confirmation, such that cleavage site mutations provide no additional benefit. It is thus possible that the epitopes were already better exposed in the WITO.33 wild type virus compared to the other V2 “special strain” viruses.

Table 3.14: IC_{50} values showing the fold difference in neutralization of WITO.33 wild type and WITO.33 CS-Mut by mature MPER bNAbs. Fold differences between the wild type and CS-Mut are recorded in the third column and values above threefold that of the wild type are highlighted in purple. The warmer the color of the cell, the more potent the neutralization of the virus by the bNAb in question. Maroon is for values below 0.01 µg/ml, Red denotes values between 0.01 µg/ml and 1 µg/ml, orange for values between 1 µg/ml and 5 µg/ml, yellow for values between 5 µg/ml and 10 µg/ml, and blue for more than 10 µg/ml (which represents neutralization resistance)

bNAb	IC_{50}		Fold Difference
	WITO.33 WT	**WITO.33 CS-Mut**	
10E8	0,1	<0,02	3
2F5	1,2	0,2	7
Z13e1	>10	>10	1
4E10	1,8	0,5	4
M66.6	>10	>10	1
DH511	0,08	0,01	8

3.4.4 Neutralization of cleavage site mutants by germline reverted MPER bNAbs

Our next aim was to assess whether the cleavage site mutations that enhanced exposure of the MPER allowed for the binding of inferred germline bNAbs which are known not to engage well with viruses. To assess this, we used germline reverted MPER antibodies to test neutralization of wild type and CS-Mut "special strain" viruses (**Table 3.15**).

Table 3.15: Neutralization of V2 "special strain" wild type and CS-Mut viruses by germline reverted MPER-directed bNAbs. The warmer the color of the cell, the more potent the neutralization of the virus by the bNAb in question. Red denotes values between 0.01 µg/ml and 1 µg/ml, blue for more than 200 µg/ml (which represents neutralization resistance).

Virus	bNAb						
	g10E8	gDH511	g4E10	g2F5	gZ13e1	gM66.6	(Pos. control)
CAP256 SU WT	>200	>200	>200	>200	>200	>200	0,7
CAP256 SU CS-Mut	>200	>200	>200	>200	>200	>200	0,07
T250 WT	>200	>200	>200	>200	>200	>200	0,15
T250 CS-Mut	>200	>200	>200	>200	>200	>200	0,02
WITO WT	>200	>200	>200	>200	>200	>200	0,1
WITO CS-Mut	>200	>200	>200	>200	>200	>200	0,02

Since the germline reverted antibodies are unmutated and have not matured towards breadth, they were very unlikely to neutralize the viruses. We therefore used relatively high concentrations of the antibodies, starting at 200 µg/ml. Neutralization assays showed that none of the germline reverted MPER bNAbs neutralized the wild type or the CS-Mut viruses. We thus concluded that although the cleavage site mutations enhanced neutralization by mature MPER bNAbs, this did not confer sensitivity to their germline reverted counterparts (142).

3.4.5 Neutralization sensitivity of V2 special strains and their CS-Mut to bNAbs targeting other epitopes

In order to assess if the cleavage site mutations enhanced neutralization by bNAbs targeting epitopes other than the MPER, we tested neutralization of the wild type and CS-Mut "special strains" by bNAbs targeting the gp120-gp41 interface, V2, V3 and CD4bs epitopes. An example curve was plotted for the V3 targeting bNAb PGT130 to show the neutralization curve of the wild type viruses and the CS-Mut of each special strain virus (**Figure 3.15**). The figure shows that the IC_{50}s for the wild type and CS-Mut are identical.

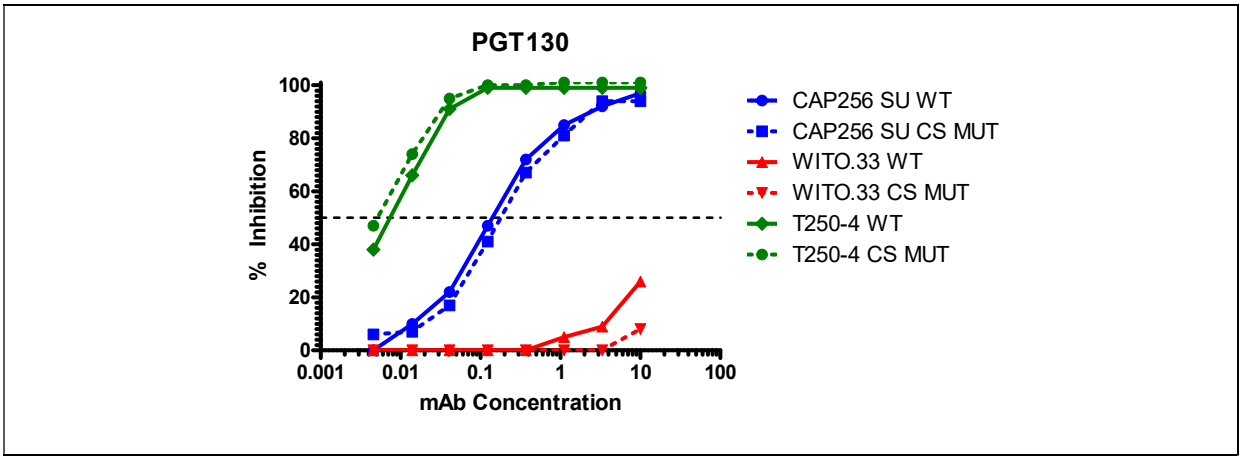

Figure 3.15: Comparison of neutralization between CS-Mut and WT V2 special strains by PGT130, targeting the V3 epitope of the HIV-1 envelope. Vertical axis shows percentage inhibition and horizontal axis shows antibody concentration in µg/ml. Experiments were conducted three times.

Similar experiments were conducted for eight other bNAbs targeting diverse epitopes. None of the bNAbs neutralized the CS-Mut viruses better than the wild type "special strains" (**Table 3.16)**, and it can therefore be concluded that these epitopes were not further exposed by the cleavage site mutations.

Table 3.16: Neutralization of wild type and CS-Mut V2 special strains by bNAbs targeting the V2, V3, gp120-gp41 interface and CD4bs epitopes of HIV-1. The warmer the color of the cell, the more potent the neutralization. Maroon is for values below 0.01 µg/ml, red denotes values between 0.01 µg/ml and 1 µg/ml, orange for values between 1 µg/ml and 5 µg/ml, yellow for values between 5 µg/ml and 10 µg/ml, and blue for more than 10 µg/ml (which represents neutralization resistance).

CAP256 SU

	mAb	WT (µg/ml)	CS-Mut (µg/ml)	Fold Difference
V2	PG9	0,06	0,03	2
	PGT145	1,6	1,2	1
CD4bs	VRC01	1,13	1,14	1
	3BNC117	0,4	0,4	1
INTERFACE	VRC34	<10	<10	1
	35O22	0.03	0.02	1
	8ANC195	<10	<10	1
V3	PGT121	0,04	0,04	1
	PGT130	0,14	0,18	1

WITO.33

	mAb	WT	CS-Mut	Fold Difference
V2	PG9	0,01	0,01	1
	PGT145	0,002	0,002	1
CD4bs	VRC01	0,2	0,2	1
	3BNC117	0,03	0,05	1
INTERFACE	VRC34	0,2	0,14	1
	35O22	>10	>10	
	8ANC195	>10	>10	1
V3	PGT121	1,9	2,9	2
	PGT130	>10	>10	1

T250-4

	mAb	WT	CS-Mut	Fold Difference
V2	PG9	0,002	0,002	1
	PGT145	0,002	0,002	1
CD4bs	VRC01	>10	>10	1
	3BNC117	>10	>10	1
	VRC34	0,07	0,04	1
	35O22	>10	>10	
INTERFACE	8ANC195	>10	>10	1
V3	PGT121	0,002	0,002	1
	PGT130	0,007	0,005	1

3.5 Assessing the effects of the cleavage site mutations on Envelope structure using polyclonal plasma

Making changes to particular regions of the envelope have previously been shown not only to reduce viral infectivity, but to alter the structure of the spike such that epitopes that were previously concealed become exposed and the envelope exhibits a highly sensitive phenotype (143). Changes in the MPER, for example, have been associated with increased resistance to gp120 antibodies while increasing sensitivity to MPER antibodies (144-146).

To check that the cleavage site mutations in the three V2 “special strain” viruses did not reduce envelope integrity such that sensitivity was increased to most antibodies, we tested the neutralization of the wild type and mutant viruses by plasma that was known to have limited breadth. Changes in neutralization patterns between the wild type and CS-Mut viruses (**Table 3.17**) provided an indication of whether or not the mutated envelopes were unstable or intact.

In the case of T250-4, most of the plasma samples failed to neutralize the wild type while neutralizing the CS-Mut virus. This indicates that in the case of this virus, the envelope integrity may have been compromised by the introduction of the cleavage site mutants. In terms of viral immunogens for a vaccine, it would thus not be ideal to use T250-4 for this reason. For CAP256 SU CS-Mut, there was introduction of low level neutralization for four out of ten samples (**Table 3.17**) which indicate is indicative of some alteration to envelope conformation, although not to the same extent as T250-4. The third virus, WITO.33 CS-Mut exhibited no notable increases in neutralization sensitivity to any of the tested plasma samples compared to the wild type.

Table 3.17: Comparison of neutralization ID_{50} of wild type and CS-Mut special strain viruses by non-broadly neutralizing plasma. The warmer the color of the cell, the more potent the neutralization. Orange is for dilution factor values between 101 and 500, yellow for values between 41and 100, and blue for less than 40 (which represents neutralization resistance).

T250-4

SAMPLE	WT	CS-Mut	FOLD DIFFERENCE
CAP88	<40	166	4
CAP188	<40	<40	1
CAP200	<40	54	1
CAP225	<40	114	3
CAP228	<40	80	2
CAP229	<40	360	9
CAP237	<40	150	4
CAP244	<40	120	3
CAP268	<40	93	2
CAP281	<40	60	1

CAP256 SU

SAMPLE	WT	CS-Mut	FOLD DIFFERENCE
CAP88	<40	<40	1
CAP188	<40	<40	1
CAP200	<40	<40	1
CAP225	<40	<40	1
CAP228	<40	53	1
CAP229	<40	52	1
CAP237	<40	77	1
CAP244	<40	55	1
CAP268	<40	<40	1
CAP292	<40	<40	1

WITO.33

SAMPLE	WT	CS-Mut	FOLD DIFFERENCE
CAP88	<40	<40	1
CAP188	<40	<40	1
CAP200	<40	<40	1
CAP225	<40	<40	1
CAP228	<40	<40	1
CAP229	<40	<40	1
CAP237	<40	<40	1
CAP244	<40	<40	1
CAP268	<40	<40	1
CAP281	<40	<40	1

CHAPTER 4: DISCUSSION AND CONCLUSIONS

HIV vaccine development continues to be a major focus of public health research in South Africa, which bears the brunt of the epidemic (1). A variety of strategies are being pursued to develop this vaccine, one of which is the engineering of immunogens that are aimed at eliciting bNAbs, which have widely been shown to be able to prevent infection in animal studies (116, 147). Here we utilized previously published data in a novel approach to design, engineer and test natural viral variants as immunogens to stimulate bNAbs.

The first of these published studies described six uncommon viral escape mutations in the cleavage site of the envelope in CAPRISA donor CAP248 (94). When they were simultaneously introduced to various viruses, the mutations, while resulting in escape from the autologous response, also resulted in the enhancement of neutralization sensitivity to MPER bNAbs 4E10 and 10E8 (94). The second and third studies identified a subset of viruses that were shown to have a high probability of engaging the inferred germline versions or unmutated common ancestors of bNAbs directed to the V2 epitope of the envelope (126, 127). One of the studies used computational modelling to determine which viral isolates were most likely to bind bNAb precursors targeting the V2 epitope. The second study tested the neutralization profiles of a number of V2 germline antibodies against global viral isolates and identified several that were neutralized by these inferred germline bNAbs (126, 127). Despite these different approaches, three viruses were identified in both of these studies highlighting the likelihood that these strains have unique characteristics that are highly amenable to HIV vaccine design. Our hypothesis in this study was that these separate studies, when combined, had the potential to result in the development of dual bNAb germline targeting immunogens

While the earlier study of cleavage site mutations had assessed a combination of six mutations, in this study the effect of the individual CAP248 mutations within the cleavage site was assessed both for impact on entry efficiency and on MPER exposure. Introduction of the single mutations was shown to have a reduced fitness cost, as measured here by entry efficiency, compared to the combined mutations. However, these reduced fitness costs, which would be beneficial in immunogen design (see below), were off-set by the fact the no single mutation was individually able to

recapitulate the full MPER exposure previously shown for the combined mutations. In an attempt to improve the balance between entry efficiency and MPER exposure, we next combined three of the mutations that exhibited the best exposure of the MPER region into a triple mutant (R502Q/V505M/E507G). This engineered virus exhibited improved entry potential compared to the complete set of six mutations, along with good MPER exposure suggesting that this may be a better construct for immunogen design. Future studies should therefore further assess this construct for dual immunogen design by testing the triple mutant in additional viral isolates, including those shown to bind germline versions of V2 bNAbs, described above.

The ability of bNAbs to recognize diverse global viruses is a reflection of the fact that they target conserved regions of the viral envelope glycoprotein. This would suggest that viral escape from bNAbs should be challenging, though many studies have shown that viral escape does indeed occur (81, 93, 148). In donor CAP248, the negative impact of these mutations, individually or combined, on entry efficiency suggests that the pressure exerted on the virus by bNAbs dramatically impacted fitness (136). These cleavage site mutations arose as a consequence of viral escape from a bNAb targeting the gp120-gp41 interface and accumulated gradually over time (94). Viral escape within variable regions of the viral envelope has been shown to occur very rapidly, compared to the much slower viral escape from bNAbs, even within an individual donor (81, 135). This is similar to the slow accumulation of cleavage site mutations in CAP248, and has been associated with prolonged exposure of the viral epitopes which may contribute to the induction of bNAbs (81, 135). Our data further suggests that this prolonged and gradual escape may be associated with deficits in viral entry efficiency. It is possible that this is fitness cost specific to CAP248, in that cleavage site mutations may impact on the efficiency with which the gp160 envelope is cleaved by the host furin into gp120 and gp41. Our future studies will assess the effect of these mutations on envelope processing and incorporation into viral particles which may provide a mechanism for the reduced entry efficiency.

In vivo, in CAP248 this fitness cost was imperative for the virus to survive in the presence of the bNAbs and similar observations have been made for other bNAbs (136). However, if fitness costs prove to be a general feature of escape imposed by bNAbs, this is a feature that can potentially be used for HIV prevention and treatment strategies. In antibody-mediated prevention strategies, many of which are currently

underway in humans, fitness costs may result in the preferential transmission of crippled viruses, which contain resistance mutations enabling them to get across the stringent mucosal defenses despite the presence of bNAbs. Transmission of attenuated viruses might result in lower viral loads, similar to the cytotoxic T-lymphocyte (CTL) and ART escape mutants which have been associated with lower set point viral loads (149-152). In the context of treatment, published studies suggest viral escape is inevitable (75, 153-155), but this may drive the weakening of the virus while the antibody is present. This also highlights the need to use combinations for both prevention and therapy (113), as this is likely to impose even greater fitness costs which may be beneficial for patient outcomes.

Although fitness is multifactorial, we measured only entry efficiency because this project is ultimately aimed at vaccine design utilizing virus-like particles (VLPs) incorporating expressed mutated envelope. This platform has previously been tested and shown to have promise in small animal studies, eliciting robust neutralizing responses (156). VLPs are a favorable platform because they present the trimer (which is the only target of neutralizing antibodies) in a completely native form (157). Specifically, VLPs include the viral membrane which is a crucial part of the epitope of MPER antibodies. Also, in VLP models, the base of the trimer is not exposed. This is in contrast to the use of soluble SOSIP trimers. Immunogenicity studies with SOSIP trimers have shown considerable promise, eliciting robust neutralizing responses in rabbits and macaques (36, 48, 90). However, a drawback of SOSIP trimers is the absence of the viral membrane, and the fact that the base of the trimer, normally occluded within the membrane, is exposed. Recent studies suggest that the trimer base is highly immunodominant, eliciting antibodies that recognize a region of envelope that is occluded on transmitter/founder viruses and of little value therefore for immunogen design (158). The use of a VLP platform may therefore be optimal in avoiding such non-neutralizing responses, and is amenable to the inclusion of the engineered envelopes described in this study.

One of the advantages of both the VLP and soluble trimer models is that they aim to elicit many different bNAbs that target various epitopes on the viral envelope spike. The use of immunogens that target multiple bNAb epitopes is favorable as it increases the potential coverage that such a vaccine might have, as has been shown using combinations of bNAbs (113). To design an immunogen able to elicit at least two bNAb

specificities (MPER and V2), we therefore introduced the cleavage site mutants into viral isolates previously shown to engage V2 targeted germline bNAbs. The V2 epitope is considered a favorable vaccine target because these specificities are very commonly elicited during infection, and have been shown to acquire breadth rapidly by relatively little affinity maturation (73, 76, 83, 84).

Introduction of cleavage site mutations into these V2 “special strains” showed reduced entry efficiency, similar to the effect previously described in a single heterologous virus, CAP45.G3 (94). Moreover, the effect of MPER exposure was variable among the five viruses suggesting that other features of the viral envelope contribute to this enhancement. For example, the WITO.33 CS-Mut did not exhibit much improvement in MPER exposure compared to the wild type, whereas the T250-4 and CAP256 SU CS-Mut viruses exhibited a remarkable improvement for MPER exposure compared to their wild type counterparts. A notable difference between the two was that the T250-4 CS-Mut showed increased sensitivity to five out of the six MPER antibodies that were tested, suggesting that not only was the MPER exposed by the cleavage site mutations, but the sequence of the MPER region was representative of global viruses, and therefore the epitopes of all the tested bNAbs were intact. In contrast, despite showing MPER exposure, CAP256 SU possessed fewer of the MPER epitopes, as indicated by the failure of M66.6 and 2F5 to neutralize either the wild type or the CS-Mut viruses. CAP256 SU, however, exhibited better entry efficiency in both the wild type and CS-Mut viruses compared to T250-4, which may make this a better candidate for VLP vaccines. This once again highlights the trade-off between fitness and immunogenicity that is described above. Future studies should therefore perform comparisons of entry efficiency and immunogenicity studies in the V2 special strains engineered to contain the triple mutant, to assess the likelihood that these may be superior vaccine candidates than those described in this study.

As well as testing the exposure of the MPER using bNAbs, we also assessed the ability of these potential dual germline targeting immunogens to react with inferred precursors of MPER-directed antibodies, a crucial aspect of immunogen design (159). These antibodies are the best available test of whether these engineered dual germline targeting immunogens may be useful in activating MPER B cell precursors. Unfortunately, the cleavage site mutations did not introduce neutralization to the inferred germline MPER antibodies. The failure of the CS-Mut viruses to engage the

inferred MPER germline bNAbs does not dismiss these viruses entirely in terms of their use as immunogens to elicit MPER precursors *in vivo*. Neutralization may be too high a bar for immunogen evaluations as it is possible that lower level binding to B cell precursors will be enough to activate them (160). Future experiments should use cell surface binding assays and calcium based B cell activation assays to assess if the MPER germline antibodies bind the immunogens, despite the lack of neutralization seen here. The use of trimers expressed on the surface of cell membranes will provide an accurate indication of what can be expected should these immunogens be engineered into VLPs. Another potential caveat in the use of germline reverted antibodies is the fact that little is known about true MPER precursors (or unmutated common ancestors) that develop in infected individuals, as longitudinal studies of their ontogeny have not been conducted to define them. The inferred germline reverted antibodies which are generally used for these studies, still contain the CDRH3 of the mature antibodies from which they were derived, as this cannot be inferred using bioinformatic approaches. Thus, while useful, germline reverted MPER antibodies are not an accurate representation of the actual unmutated common ancestors. Future studies should aim to identify true MPER unmutated common ancestors which could be tested *in vitro* against the immunogens designed in this study.

Overall, this study has contributed to our understanding of the consequences of viral escape from bNAbs, which will be of value in the era of passive immunization studies. Furthermore, this study has enabled the design of a novel set of engineered viruses that can be used as a tool in future studies to assess their ability to elicit MPER B cells. The triple mutation, with good MPER exposure and entry capacity has potential for further studies *in vitro* and *in vivo*, using small animal immunizations. Similarly, the CAP256 SU which exhibited good MPER exposure and limited “off-target” effects is also a promising future immunogen.

CHAPTER 5: REFERENCES

1. UNAIDS. AIDS by the numbers. 2015.
2. Haynes BF, Moody MA, Alam M, Bonsignori M, Verkoczy L, Ferrari G, et al. Progress in HIV-1 vaccine development. The Journal of allergy and clinical immunology. 2014;134(1):3-10.
3. Haynes BF, Shaw GM, Korber B, Kelsoe G, Sodroski J, Hahn BH, et al. HIV-Host interactions: Implications for vaccine design. Cell Host and Microbe. 2016;19(3):292-303.
4. Liao H, Bonsignori M, Alam S, McLellan JS, Tomaras GD, Moody MA, et al. Vaccine Induction of Antibodies against a Structurally Heterogeneous Site of Immune Pressure within HIV-1 Envelope Protein Variable Regions 1 and 2. Immunity. 2013;88(1):176-86.
5. Thongcharoen P, Suriyanon V, Paris R, et al. . A phase 1/2 comparative vaccine trial of the safet y and immunogenicity of a CRF01_AE (subtype E) candidate vaccine: ALVAC-HIV (vCP1521) prime with oligomeric gp160 (92TH023/LAI-DID) or bivalent gp120 (CM235/SF2) boost. Journal of Acquired Immune Deficiency Syndrome 2007(46):48-55.
6. Rerks-Ngarm S, Pitisuttithum P, Nitayaphan S, Kaewkungwal J, Chiu J, Paris R, et al. Vaccination with ALVAC and AIDSVAX to prevent HIV-1 infection in Thailand. New England Journal of Medicine. 2009;361(23):2209-20.
7. Haynes BF, Gilbert PB, McElrath MJ, Zolla-Pazner S, Tomaras GD, Alam SM, et al. Immune-correlates analysis of an HIV-1 vaccine efficacy trial. New England Journal of Medicine. 2012;366(14):1275-86.
8. Tomaras GD, Plotkin SA. Complex Immune Correlates of Protection in HIV-1 Vaccine Efficacy Trials. Immunological Reviews. 2017;275 (1):245–61.
9. Junqueira D, SE A. HIV-1 subtype B: Traces of a pandemic. Virology. 2016(495):173-84.
10. Shaw GM, Hunter E. HIV Transmission. Cold Springs Harbor Perspectives in Medicine. 2012;a006965(2):1101.
11. Taylor B, Sobieszczyk M, McCutchan F, Hammer S. The challenge of HIV-1 Subtype Diversity. New England Journal of Medicine. 2008(358):1590-602.
12. Derdeyn CA, Decker JM, Bibollet-Ruche F, Mokili JL, Muldoon M, Denham SA, et al. Envelope-constrained neutralization-sensitive HIV-1 after heterosexual transmission. Science. 2004;303(5666):2019-22.

13. Fiebig E, Wright D, Rawal B, Garrett P, Schumacher R, Peddada L, et al. Dynamics of HIV Viremia And Antibody Seroconversion in Plasma Donors: Implications for Diagnosis and Staging Primary HIV Infections. AIDS 2003(17):1871-9.
14. Cohen M, Chen Y, McCauley M, Gamble T, Hosseinipour M, Kumarasamy N, et al. Prevention of HIV-1 Infection With Antiretroviral Therapy. New England Journal of Medicine. 2011(365):493-505.
15. El-Sadr W, Mayer K, Hodder S. AIDS in America, Forgotten But Not Gone. New England Journal of Medicine. 2010(362):967-70.
16. Boily M, Baggaley R, Wang L, Masse B, White R, Hayes R, et al. Heterosexual Risk of HIV-1 Infection per Sexual Act: Systematic Review and Meta-analysis of Observational Studies. Lancet of Infectious Diseases. 2009(9):118-29.
17. McKinnon L, Liebenberg L, Yende-Zuma N, Archary D, Ngcapu S, Sivro A, et al. Genital inflammation undermines the effectiveness of tenofovir gel in preventing HIV acquisition in women. Nature Medicine 2018.
18. Pope M, Haase AT. Transmission, acute HIV-1 infection and the quest for strategies to prevent infection. Nature Medicine. 2003;9(7):847-52.
19. Haase A. Targeting Early Infection to Prevent HIV-1 Mucosal Transmission. Nature Medicine 2010(464):217-23.
20. Ribeiro R, Qin L, Chavez L, Li D, Self S, Perelson A. Estimation of the initial Viral Growth Rate and Basic Reproductive Number During Acute HIV Infection. Journal of Virology. 2010(84):6096-102.
21. Palmer S, Wiegand A, Maldarelli F, Bazmi H, Mican J, Polis M, et al. New Real-time Reverse Transcriptase-Initiated PCR Assay With Single-Copy Sensitivity For Human Immunodeficiency Virus Type 1 RNA in Plasma. Journal of Clinical Microbiology. 2003(41):4531-6.
22. Wolinsky SM, Wike CM, Korber BT, Hutto C, Parks WP, Rosenblum LL, et al. Selective transmission of human immunodeficiency virus type-1 variants from mothers to infants. Science. 1992;255(5048):1134-7.
23. Iyer SS, Bibollet-Ruche F, Sherrill-Mix S, Learn GH, Plenderleith L, Smith AG, et al. Resistance to type 1 interferons is a major determinant of HIV-1 transmission fitness. PNAS. 2016:590-9.
24. Abrahams MR, Anderson JA, Giorgi EE, Seoighe C, Mlisana K, Ping LH, et al. Quantitating the multiplicity of infection with HIV-1 subtype C reveals a non-

Poisson distribution of transmitted variants. Journal of Virology. 2009;83(8):3556-67.

25. Keele BF, Giorgi EE, Salazar-Gonzalez JF, Decker JM, Pham KT, Salazar MG, et al. Identification and characterization of transmitted and early founder virus envelopes in primary HIV-1 infection. Proceedings of the National Academy of Sciences of the U S A. 2008;105(21):7552-7.
26. Li M, Gao F, Mascola J, Stamatatos L, Polonis VR, Koutsoukos M, et al. Human immunodeficiency virus type 1 env clones from acute and early subtype B infections for standardized assessments of vaccine-elicited neutralizing antibodies. Journal of Virology. 2005;79(16):10200-9.
27. Wilen CB, Parrish NF, Pfaff JM, Decker JM, Henning EA, Haim H, et al. Phenotypic and immunologic comparison of clade B transmitted/founder and chronic HIV-1 envelope glycoproteins. Journal of Virology. 2011;85(17):8514-27.
28. Carlson JM, Schaefer M, Monaco DC, Batorsky R, Claiborne DT, Prince J, et al. Selection bias at the heterosexual HIV-1 transmission bottleneck. Science. 2014(345).
29. Gnanakaran S, Bhattacharya T, Daniels M, Keele BF, Hraber PT, Lapedes AS, et al. Recurrent Signature Patterns in HIV-1 B Clade Envelope Glycoproteins Associated with either Early or Chronic Infections. PLoS Pathogens. 2011;7(9):e1002209.
30. Klimas N, Koneru AOB, Fletcher MA. Overview of HIV. Psychosomatic Medicine. 2008;70:523–30.
31. Chiu I, Yaniv A, Dahlberg, JE Gazit, ASkuntz S, Tronick S, et al. Nucleotide sequence evidence for relationship of AIDS retrovirus to lentiviruses. Nature Communications. 1985(317):366–8.
32. Turner BG, Summers MF. Structural Biology of HIV. Journal of Molecular Biology. 1999;8(285):1-32.
33. Bernacchi M, Paillart M, Vivet-Boudou, RP S. The Life-Cycle of the HIV-1 Gag-RNA Complex. Viruses. 2016;10(8).
34. Gelderblom HR, Pauli MÖ. Morphogenesis and morphology of HIV structure-function relations. Archives of virology. 1989;106(1-2):1-13.
35. Kirchhoff F. HIV Life Cycle: Overview. Encyclopedia of AIDS. 2016(4614):9610-6.

36. Sanders RW, Moore JP. Native-like Env trimers as a platform for HIV-1 vaccine design. Immunological Reviews. 2017;275:161-82.
37. Briggs JAG, Riches JD, Glass B, Bartonova V, Zanetti G, Kräusslich H-G. Structure and assembly of immature HIV. Proceedings of the National Academy of Sciences of the U S A. 2009;106(27):11090-5.
38. Herrera-Carrillo E, Berkhout B, Freed EO. Bone Marrow Gene Therapy for HIV/AIDS. Viruses. 2015;7(7):3910–36.
39. Smith J, Daniel R. Following the path of the virus: the exploitation of host DNA repair mechanisms by retroviruses. ACS Chemical Biology. 2006(1):217–26.
40. Potter S, Lacabaratz C, Lambotte O, Perez-Patrigeon S, Vingert B, Sinet M, et al. Preserved central memory and activated effector memory CD4 T-cell subsets in human immunodeficiency virus controllers: an ANRS EP36 study. Journal of Virology 2007;81:13904-5.
41. Adnan Bashir Bhatti, Muhammad Usman, Venkataramana Kandi. Current Scenario of HIV/AIDS, Treatment Options, and Major Challenges with Compliance to Antiretroviral Therapy. Cureus. 2016;8(3).
42. Checkley MA, Luttge BG, Freed EO. HIV-1 Envelope Glycoprotein Biosynthesis, Trafficking, and Incorporation. Journal of Molecular Biology. 2011;410(4):582-608.
43. Ward AB, Wilson IA. Insights Into the Trimeric HIV-1 Envelope Glycoprotein Structure. Trends Biochem Sci. 2015;40(2):101-7.
44. Mao Y, Wang L, Gu C, Herschhorn A, Désormeaux A, Finzi A, et al. Molecular architecture of the uncleaved HIV-1 envelope glycoprotein trimer. PNAS. 2013;110(30):12438-43.
45. Munro JB, Mothes W. Structure and Dynamics of the Native HIV-1 Env Trimer. Journal of Virology. 2015;89(11):5752-5.
46. Chan DC, Fass D, Berger JM, Kim PS. Core Structure of gp41 from the HIV Envelope Glycoprotein. Cell Host and Microbe. 1997;89(2):263–73.
47. www.nih.gov.
48. Sanders RW, Vesanen M, Schuelke N, Master A, Schiffner L, Kalyanaraman R, et al. Stabilization of the soluble, cleaved, trimeric form of the envelope glycoprotein complex of human immunodeficiency virus type 1. Journal of Virology. 2002;76(17):8875-89.

49. Binley JM, Sanders RW, Clas B, Schuelke N, Master A, Guo Y, et al. A recombinant human immunodeficiency virus type 1 envelope glycoprotein complex stabilized by an intermolecular disulfide bond between the gp120 and gp41 subunits is an antigenic mimic of the trimeric virion-associated structure. Journal of Virology. 2000;74(2):627-43.
50. Pancera M, Majeed S, Andrew Y-E, Chen B, Huang C-c, Kong L, et al. Structure of HIV-1 gp120 with gp41-interactive region reveals layered envelope architecture and basis of conformational mobility. PNAS. 2010;107(3):1166-71.
51. Kwong PD, Wyatt R, Majeed S, Robinson J, Sweet RW, Sodroski J, et al. Structures of HIV-1 gp120 envelope glycoproteins from laboratory-adapted and primary isolates. Structure Fold Des. 2000;8(12):1329-39.
52. Bartesaghi A, Merk A, Borgnia MJ, Milne JL, Subramaniam S. Prefusion structure of trimeric HIV-1 envelope glycoprotein determined by cryo-electron microscopy. Nature Structural and Molecular Biology. 2013;20(12):1352-7.
53. Stewart-Jones G, Soto C, Lemmin T, Chuang G, Druz A, Kong R, et al. Trimeric HIV-1-Env Structures Define Glycan Shields from Clades A, B, and G. Cell 2016;165(4):813-26.
54. Saunders CJ, McCaffrey RA, Zharkikh I, Kraft Z, Malenbaum SE, Burke B, et al. The V1, V2, and V3 regions of the human immunodeficiency virus type 1 envelope differentially affect the viral phenotype in an isolate-dependent manner. Journal of Virology. 2005;79(14):9069-80.
55. Kong L, Lee JH, Doores KJ, Murin CD, Julien JP, McBride R, et al. Supersite of immune vulnerability on the glycosylated face of HIV-1 envelope glycoprotein gp120. Nature Structural and Molecular Biology. 2013;20(7):796-803.
56. Behrens A, Crispin M. Structural principles controlling HIV envelope glycosylation. Current Opinion in AIDS. 2017(44):125-33.
57. Krumm S, Mohammed H, Le K, Crispin M, Wrin T, Poignard P, et al. Mechanisms of escape from the PGT128 family of anti-HIV broadly neutralizing antibodies. Retrovirology 2016;13(8):241-5.
58. Huang J, Kang BH, Pancera M, Lee JH, Tong T, Feng Y, et al. Broad and potent HIV-1 neutralization by a human antibody that binds the gp41-gp120 interface. Nature Medicine. 2014:138-42.
59. Falkowska E, Le KM, Ramos A, Doores KJ, Lee JH, Blattner C, et al. Broadly Neutralizing HIV Antibodies Define a Glycan-Dependent Epitope on the

Prefusion Conformation of gp41 on Cleaved Envelope Trimers. Immunity. 2014;40(5):657-68.

60. Buzon V, Natrajan G, David S, Felix C, Michael MK, Winfried W. Crystal Structure of HIV-1 gp41 Including Both Fusion Peptide and Membrane Proximal External Regions. PLoS Pathogens. May 6, 2010;10(1371).
61. Montero M, Houten NEV, Wang X, Scott JK. The Membrane Proximal External Region of the Human Immunodeficiency Virus type 1 Envelope: Dominant Site of Antibody Neutralization and Target for Vaccine Design. Microbiology and Molecular Biology Reviews. 2008;72(1):54-84.
62. Yuxian He, Jianwei Cheng, Jingjing Li, Zhi Qi, Hong Lu, Mingxin Dong, et al. Identification of a Critical Motif for the Human Immunodeficiency Virus Type 1 (HIV-1) gp41 Core Structure: Implications for Designing Novel Anti-HIV Fusion Inhibitors. Journal of Virology. 2008;82(13):6349-58.
63. W. Weissenhorn, A. Dessen, S. C. Harrison, Skehel JJ, Wiley DC. Atomic structure of the ectodomain from HIV-1 gp41. Nature Communications. 1997;387:426-30.
64. Beatriz Apellániz, Edurne Rujas, Soraya Serrano, Koldo Morante, Kouhei Tsumoto, Jose M. M. Caaveiro, et al. The Atomic Structure of the HIV-1 gp41 Transmembrane Domain and its Connection to the Inmmunogenic Membrane-proximal External Region

    Journal of Biological Medicine. 2015:644.
65. Kong R, Xu K, Zhou T, Acharya P, Lemmin T, Liu K, et al. Fusion peptide of HIV-1 as a site of vulnerability to neutralizing antibody. Science. 2016; 352(6287):828-33.
66. Moore PL, Gray ES, Choge IA, Ranchobe N, Mlisana K, Abdool Karim SS, et al. The C3-V4 region is a major target of autologous neutralizing antibodies in human immunodeficiency virus type 1 subtype C infection. Journal of Virology. 2008;82(4):1860-9.
67. Gray ES, Moore PL, Choge IA, Decker JM, Bibollet-Ruche F, Li H, et al. Neutralizing antibody responses in acute human immunodeficiency virus type 1 subtype C infection. Journal of Virology. 2007;81(12):6187-96.
68. Rong R, Bibollet-Ruche F, Mulenga J, Allen S, Blackwell JL, Derdeyn CA. Role of V1V2 and other human immunodeficiency virus type 1 envelope domains in

resistance to autologous neutralization during clade C infection. Journal of Virology. 2007;81(3):1350-9.

69. Moore PL, Gray ES, Morris L. Specificity of the autologous neutralizing antibody response. Current Opinion in AIDS. 2009;4(5):358-63.
70. Rong R, Li B, Lynch RM, Haaland RE, Murphy MK, Mulenga J, et al. Escape from autologous neutralizing antibodies in acute/early subtype C HIV-1 infection requires multiple pathways. PLoS Pathogens. 2009;5(9):e1000594.
71. Moore PL, WIlliamson C. Approaches to the induction of HIV broadly neutralizing antibodies. Current Opinion in AIDS. 2016;11.
72. Decker JM, Bibollet-Ruche F, Wei X, Wang S, Levy DN, Wang W, et al. Antigenic conservation and immunogenicity of the HIV coreceptor binding site. Journal of Experimental Medicine. 2005;201(9):1407-19.
73. Gray ES, Madiga MC, Hermanus T, Moore PL, Wibmer CK, Tumba NL, et al. HIV-1 neutralization breadth develops incrementally over 4 years and is associated with CD4+ T cell decline and high viral load during acute infection. Journal of Virology. 2011;85(10):4828-40.
74. Hraber P, Korber BT, Lapedes AS, Bailer RT, Seaman MS, Gao H, et al. Impact of Clade, Geography, and Age of the Epidemic on HIV-1 Neutralization by Antibodies. Journal of Virology. 2014;88(21):12623-43.
75. Klein F, Mouquet H, Dosenovic P, Scheid JF, Scharf L, Nussenzweig MC. Antibodies in HIV-1 vaccine development and therapy. Science. 2013;341(6151):1199-204.
76. Doria-Rose NA, Schramm CA, Gorman J, Moore PL, Bhiman JN, DeKosky BJ, et al. Developmental pathway for potent V1V2-directed HIV-neutralizing antibodies. Nature Medicine. 2014;509(7498):55-62.
77. Zhou T, Georgiev I, Wu X, Yang Z-Y, Dai K, Finzi A, et al. Structural Basis for Broad and Potent Neutralization of HIV-1 by Antibody VRC01. Science. 2010;329(5993):811-7.
78. Sather DN, Armann J, Ching LK, Mavrantoni A, Sellhorn G, Caldwell Z, et al. Factors associated with the development of cross-reactive neutralizing antibodies during human immunodeficiency virus type 1 infection. Journal of Virology. 2009;83(2):757-69.

79. Euler Z, van Gils MJ, Bunnik EM, Phung P, Schweighardt B, Wrin T, et al. Cross-reactive neutralizing humoral immunity does not protect from HIV type 1 disease progression. Journal of Infectious Diseases. 2010;201(7):1045-53.
80. Piantadosi A, Panteleeff D, Blish CA, Baeten JM, Jaoko W, McClelland RS, et al. Breadth of neutralizing antibody response to human immunodeficiency virus type 1 is affected by factors early in infection but does not influence disease progression. Journal of Virology. 2009;83(19):10269-74.
81. Bhiman JN, Anthony C, Doria-Rose NA, Karimanzira O, Schramm CA, Khoza T, et al. Viral variants that initiate and drive maturation of V1V2-directed HIV-1 broadly neutralizing antibodies. Nature Medicine. 2015;21(11):1332-6.
82. Walker LM, Huber M, Doores KJ, Falkowska E, Pejchal R, Julien JP, et al. Broad neutralization coverage of HIV by multiple highly potent antibodies. Nature Medicine. 2011;477(7365):466-70.
83. Rusert P, Kouyos R, Kadelka C, Ebner H, Schanz M, Huber M, et al. Determinants of HIV-1 broadly neutralizing antibody induction. Nature Medicine. 2016;22(11):1260-7.
84. Landais E, Huang X, Havenar-Daughton C, Murrell B, Price MA, Wickramasinghe L, et al. Broadly Neutralizing Andtibody Responses in a Large Longitudinal Sub-saharan HIV Primary Infection Cohort. PLOS Pathogens. 2016;12(1).
85. Zhang Z, Li S, Gu Y, Xia N. Antiviral Therapy by HIV-1 Broadly Neutralizing and Inhibitory Antibodies. International Journal of Molecular Sciences. 2016;17(1901).
86. Scheid J, Mouquet H, Feldhahn N, Walker B, Pereyra F, Cutrell E, et al. A method for identification of HIV gp140 binding memory B cells in human blood. Journal of Immunological Methods. 2009;343(2):65-7.
87. Walker LM, Phogat SK, Chan-Hui PY, Wagner D, Phung P, Goss JL, et al. Broad and potent neutralizing antibodies from an African donor reveal a new HIV-1 vaccine target. Science. 2009;326(5950):285-9.
88. Wu X, Yang ZY, Li Y, Hogerkorp CM, Schief WR, Seaman MS, et al. Rational design of envelope identifies broadly neutralizing human monoclonal antibodies to HIV-1. Science. 2010;329(5993):856-61.
89. Doria-Rose NA, Joyce MG. Strategies to guide the antibody affinity maturation process. Current Opinion in AIDS. 2015(11):137-47.

90. Sanders R, Derking R, Cupo A, Julien J, Yasmeen A, De Val N, et al. A next-generation cleaved, soluble HIV-1 Env Trimer, BG505 SOSIP.664 gp140, expresses multiple epitopes for broadly neutralizing but not non-neutralizing antibodies. PLoS Pathogens. 2013;9(9).
91. Ringe R, Sanders R, Yasmeen A, Kim H, Lee J, Cupo A, et al. Cleavage strongly influences whether soluble HIV-1 envelope glycoprotein trimers adopt a native-like conformation. Proceedings of the National Academy of Sciences of the U S A. 2013;110(45):18256–61.
92. Sok D, van Gils MJ, Pauthner M, Saye-Francisco KL, Hsueh J, Briney B, et al. A Recombinant HIV Envelope Trimer Selects for Quaternary Dependent Antibodies Targeting the Trimer Apex. Proceedings of the National Academy of Sciences of the U S A. 2014;30 Suppl 1:A7-8.
93. Wibmer CK, Bhiman JN, Gray ES, Tumba N, Abdool Karim SS, Williamson C, et al. Viral Escape from HIV-1 Neutralizing Antibodies Drives Increased Plasma Neutralization Breadth through Sequential Recognition of Multiple Epitopes and Immunotypes. PLoS Pathogens. 2013;9(10):e1003738.
94. Wibmer CK, Gorman J, Ozorowski G, Bhiman JN, Sheward DJ, Elliot DH, et al. Structure and recognition of a novel HIV-1 gp120-gp41 interface antibody that caused MPER exposure through viral escape. PLoS pathogens. 2016;13(1):e1006074.
95. Wibmer CK, Moore PL, Morris L. HIV broadly neutralizing antibody targets. Current Opinion in AIDS. 2015;10(3):135-43.
96. West AP, Jr., Scharf L, Scheid JF, Klein F, Bjorkman PJ, Nussenzweig MC. Structural Insights on the Role of Antibodies in HIV-1 Vaccine and Therapy. Cell. 2014;156(4):633-48.
97. Muster T, Steindl F, Purtscher M, Trkola A, Klima A, Himmler G, et al. A conserved neutralizing epitope on gp41 of human immunodeficiency virus type 1. Journal of Virology. 1993;67(11):6642-7.
98. Zwick MB, Labrijn AF, Wang M, Spenlehauer C, Saphire EO, Binley JM, et al. Broadly neutralizing antibodies targeted to the membrane-proximal external region of human immunodeficiency virus type 1 glycoprotein gp41. Journal of Virology. 2001;75(22):10892-905.
99. Munoz-Barroso I, K. Salzwedel, E. Hunter, Blumenthal R. Role of the membrane-proximal domain in the initial stages of human immunodeficiency

virus type 1 envelope glycoprotein-mediated membrane fusion. Journal of Virology. 1999(73):6089-92.

100. Liu M, Yang G, Wiehe K, Nicely N, Vandergrift N, Rountree W, et al. Polyreactivity and autoreactivity among HIV-1 antibodies. Journal of Virology. 2015;89(1):784-98.

101. Huang J, Ofek G, Laub L, Louder MK, Doria-Rose NA, Longo NS, et al. Broad and potent neutralization of HIV-1 by a gp41-specific human antibody. Nature Medicine. 2012;491(7424):406-12.

102. Broliden PA, Gegerfelt Av, P. Clapham, J. Rosen, Fenyo EM, B.Wahren, et al. Identification of human neutralization inducing regions of the human immunodeficiency virus type 1 envelope glycoproteins. Proceedings of the National Academy of Sciences of the U S A. 1992(89):461-5.

103. Gray ES, Madiga MC, Moore PL, Mlisana K, Abdool Karim SS, Binley JM, et al. Broad neutralization of human immunodeficiency virus type 1 mediated by plasma antibodies against the gp41 membrane proximal external region. Journal of Virology. 2009;83(21):11265-74.

104. Binley JM, Wrin T, Korber B, Zwick MB, Wang M, Chappey C, et al. Comprehensive cross-clade neutralization analysis of a panel of anti-human immunodeficiency virus type 1 monoclonal antibodies. Journal of Virology. 2004;78(23):13232-52.

105. Chen J, Frey G, Peng H, Rits-Volloch S, Garrity J, Seaman M, et al. Mechanism of HIV-1 neutralization by antibodies targeting a membrane-proximal region of gp41. Journal of Virology. 2013;88(2):1249-58.

106. LaTonya D. Williams, Gilad Ofek, Sebastian Schätzle, Jonathan R. McDaniel, Xiaozhi Lu, Nathan I. Nicely, et al. Potent and broad HIV-neutralizing antibodies in memory B cells and plasma

Science Immunology. 2017;2.

107. Williams L, Ofek G, Schätzle S, McDaniel J, X L, Nicely N, et al. Potent and broad HIV-neutralizing antibodies in memory B cells and plasma. Science Immunology. 2017;2(7).

108. Blattner C, Lee JH, Sliepen K, Derking R, Falkowska E, de la Pena AT, et al. Structural Delineation of a Quaternary, Cleavage-Dependent Epitope at the

gp41-gp120 Interface on Intact HIV-1 Env Trimers. Immunity. 2014;40(5):669-80.

109. Schoofs T, Klein F, Braunschweig M, Kreider E, Feldmann A, Nogueira L, et al. HIV-1 therapy with monoclonal antibody 3BNC117 elicits host immune responses against HIV-1. Science. 2016;352(6288):997-1001.

110. Julg B, Sok D, Schmidt S, Abbink P, Newman R, Broge T, et al. Protective Efficacy of Broadly Neutralizing Antibodies with Incomplete Neutralization Activity against Simian-Human Immunodeficiency Virus in Rhesus Monkeys. Journal of Virology. 2017;91(20):01187-17.

111. Nishimura Y, Gautam R, Chun T-W, Sadjadpour R, Foulds KE, Shingai M, et al. Early antibody therapy can induce long-lasting immunity to SHIV

Nature Medicine. 2017(543):559-63.

112. Kong R, Louder MK, Wagh K, Bailer R, de Camp A, Greene K, et al. Improving neutralization potency and breadth by combining broadly reactive HIV-1 antibodies targeting major neutralization epitopes. Journal of Virology. 2015(89):2659-71.

113. Wagh K, Bhattacharya T, Williamson C, Robles A, Bayne M, Garrity J, et al. Optimal combinations of broadly neutralizing antibodies for prevention and treatment of HIV-1 clade C infection. PLoS Pathogens. 2016(12).

114. www.hptn.org.

115. Pace C, Song R, Ochsenbauer C, Andrews C, Franco D, Yu J, et al. Bispecific antibodies directed to CD4 domain 2 and HIV envelope exhibit exceptional breadth and picomolar

potency against HIV-1. Proceedings of the National Academy of Sciences of t he U S A. 2013(110):13540–5.

116. Gautam R, Nishimura Y, Pegu A, Nason M, Klein F, Gazumyan A, et al. A single injection of anti-HIV-1 antibodies protects against repeated SHIV challenges. Nature Medicine. 2016;533:105–9.

117. Ko S, Pegu A, Rudicell R, Yang Z, Joyce M, Chen X, et al. Enhanced neonatal Fc receptor function improves protection against primate SHIV infection. Nature Medicine. 2014(514):642–5.

118. Moore PL, Williamson C, Morris L. Virological features associated with the development of broadly neutralizing antibodies to HIV-1. Trends in microbiology. 2015.
119. Gao F, Bonsignori M, Liao HX, Kumar A, Xia SM, Lu X, et al. Cooperation of B Cell Lineages in Induction of HIV-1-Broadly Neutralizing Antibodies. Cell. 2014;158(3):481-91.
120. MacLennan I. Germinal centers. Annual Review of Immunology. 1994(12):117–39.
121. Chan T, Brink R. Affinity-based selection and the germinal center response. Immunological Reviews. 2012;247(1):11-23.
122. Dosenovic P, von Boehmer L, Escolano A, Jardine J, Freund NT, Gitlin AD, et al. Immunization for HIV-1 Broadly Neutralizing Antibodies in Human Ig Knockin Mice. Cell. 2015;161(7):1505-15.
123. Georgiev IS, Rudicell RS, Saunders KO, Shi W, Kirys T, McKee K, et al. Antibodies VRC01 and 10E8 neutralize HIV-1 with high breadth and potency even with Ig-framework regions substantially reverted to germline. Journal of immunology. 2014;192(3):1100-6.
124. McGuire AT, Glenn JA, Lippy A, Stamatatos L. Diverse recombinant HIV-1 Envs fail to activate B cells expressing the germline B cell receptors of the broadly neutralizing anti-HIV-1 antibodies PG9 and 447-52D. Journal of Virology. 2014;88(5):2645-57.
125. Hoot S, McGuire AT, Cohen KW, Strong RK, Hangartner L, Klein F, et al. Recombinant HIV envelope proteins fail to engage germline versions of anti-CD4bs bNAbs. PLoS Pathogens. 2013;9(1):e1003106.
126. Gorman J. Structures of HIV-1 Env V1V2 with broadly neutralizing antibodies reveal commonalities that enable vaccine design. Nature Structural and Molecular Biology. 2015:1, 6-8.
127. Andrabi R, Voss JE, Liang C-H, Wong C-H, Poignard P, Burton DR. Identification of Common Features in Prototype Broadly Neutralizing Antibodies to HIV Envelope V2 Apex to Facilitate Vaccine Design. Immunity. 2015;43(5):959-73.
128. Van Loggerenberg F, Mlisana K, Williamson C, Auld SC, Morris L, Gray C, et al. Establishing a cohort at high risk of HIV infection in South Africa: challenges

and experiences of the CAPRISA 002 acute infection study. PLoS ONE. 2008;3(4):e1954.

129. Gray ES, Moody MA, Wibmer CK, Chen X, Marshall D, Amos J, et al. Isolation of a monoclonal antibody that targets the alpha-2 helix of gp120 and represents the initial autologous neutralizing-antibody response in an HIV-1 subtype C-infected individual. Journal of Virology. 2011;85(15):7719-29.
130. Wei X, Decker JM, Wang S, Hui H, Kappes JC, Wu X, et al. Antibody neutralization and escape by HIV-1. Nature Medicine. 2003;422(6929):307-12.
131. Montefiori DC. Measuring HIV neutralization in a luciferase reporter gene assay. Methods in Molecular Biology. 2009;485(26):395-405.
132. Moore PL, Ranchobe N, Lambson BE, Gray ES, Cave E, Abrahams MR, et al. Limited neutralizing antibody specificities drive neutralization escape in early HIV-1 subtype C infection. PLoS Pathogens. 2009;5(9):e1000598.
133. Moore P, Sheward D, Nonyane M, Ranchobe N, Hermanus T, Gray E, et al. Multiple pathways of escape from HIV broadly cross-neutralizing V2-dependent antibodies. Journal of Virology. 2013;87(9):4882-94.
134. Sather DN, Carbonetti S, Kehayia J, Kraft Z, Mikell I, Scheid JF, et al. Broadly neutralizing antibodies developed by an HIV-positive elite neutralizer exact a replication fitness cost on the contemporaneous virus. Journal of Virology. 2012;86(23):12676-85.
135. Anthony C, York T, Bekker V, Matten D, Selhorst P, Ferreria R-C, et al. Cooperation between Strain-Specific and Broadly Neutralizing Responses Limited Viral Escape and Prolonged the Exposure of the Broadly Neutralizing Epitope. Journal of Virology. 2017;91(18):e00828-17
136. Lynch RM, Wong P, Tran L, O'Dell S, Nason MC, Li Y, et al. HIV-1 Fitness Cost Associated with Escape from the VRC01 Class of CD4 Binding Site Neutralizing Antibodies. Journal of Virology. 2015;89(8):4201-13.
137. Ofek G, Tang M, Sambor A, Katinger H, Mascola JR, Wyatt R, et al. Structure and mechanistic analysis of the anti-human immunodeficiency virus type 1 antibody 2F5 in complex with its gp41 epitope. Journal of Virology. 2004;78(19):10724-37.
138. Nelson JD, Brunel FM, Jensen R, Crooks ET, Cardoso RM, Wang M, et al. An affinity-enhanced neutralizing antibody against the membrane-proximal external region of human immunodeficiency virus type 1 gp41 recognizes an

epitope between those of 2F5 and 4E10. Journal of Virology. 2007;81(8):4033-43.

139. Zhu Z, Qin HR, Chen W, Zhao Q, Shen X, Schutte R, et al. Cross-Reactive HIV-1-Neutralizing Human Monoclonal Antibodies Identified from a Patient with 2F5-Like Antibodies. Journal of Virology. 2011;85(21):11401–8.
140. Johnston MI, Fauci AS. An HIV vaccine--challenges and prospects. New England Journal of Medicine. 2008;359(9):888-90.
141. Johnston MI, Flores J. Progress in HIV vaccine development. Current Opinion in Pharmacology. 2001;1(5):504-10.
142. Moore PL, Gorman J, Doria-Rose NA, L. M. Ontogeny-based immunogens for the induction of V2-directed HIV broadly neutralizing antibodies. Immunological Reviews. 2017;275(1):217-29.
143. Bradley T, Trama A, Tumba N, Gray E, Lu X, Madani N, et al. Amino Acid Changes in the HIV-1 gp41 Membrane Proximal Region Control Virus Neutralization Sensitivity. EBioMedicine. 2016(12):196-207.
144. Blish CA, Nguyen MA, Overbaugh J. Enhancing exposure of HIV-1 neutralization epitopes through mutations in gp41. PLoS Medicine. 2008;5(1):e9.
145. Ringe R, Sharma D, Zolla-Pazner S, Phogat S, Risbud A, Thakar M, et al. A single amino acid substitution in the C4 region in gp120 confers enhanced neutralization of HIV-1 by modulating CD4 binding sites and V3 loop. Virology. 2011;418(2):123-32.
146. Ringe R, Bhattacharya J. Association of enhanced HIV-1 neutralization by a single Y681H substitution in gp41 with increased gp120-CD4 interaction and macrophage infectivity. PLoS One. 2012;7(5).
147. Burton D, Mascola J. Antibody responses to envelope glycoproteins in HIV-1 infection. Immunology. 2015;16(6):571-6.
148. Moore PL, Gray ES, Sheward D, Madiga M, Ranchobe N, Lai Z, et al. Potent and Broad Neutralization of HIV-1 Subtype C by Plasma Antibodies Targeting a Quaternary Epitope Including Residues in the V2 Loop. Journal of Virology. 2011;85(7):3128-41.
149. Murakoshi H, M. T. Control of HIV infection and selection/ accumulation of HIV escape mutants by HIV-specific cytotoxic T lymphocytes (CTLs). Uirusu. 2013;63(2):209-18.

150. Murakoshi H, Akahoshi T, Koyanagi M, Chikata T, Naruto T, Maruyama R, et al. Clinical Control of HIV-1 by Cytotoxic T Cells Specific for Multiple Conserved Epitopes. Journal of Virology. 2015;89(10):5330-9.
151. Chopera DR, Woodman Z, Mlisana K, Mlotshwa M, Martin DP, Seoighe C, et al. Transmission of HIV-1 CTL escape variants provides HLA-mismatched recipients with a survival advantage. PLoS Pathogens. 2008;4(3).
152. Liu D, Zuo T, Hora B, Song H, Kong W, Yu X, et al. Preexisting compensatory amino acids compromise fitness costs of a HIV-1 T cell escape mutation. Retrovirology. 2014;11(101):12977-014.
153. Caskey M, Schoofs T, Gruell H, Settler A, Karagounis T, Kreider E, et al. Antibody 10-1074 suppresses viremia in HIV-1-infected individuals. Nature Medicine. 2017;23(2):185-91.
154. Klein F, Halper-Stromberg A, Horwitz JA, Gruell H, Scheid JF, Bournazos S, et al. HIV therapy by a combination of broadly neutralizing antibodies in humanized mice. Nature Medicine. 2012;492(7427):118-22.
155. Lynch R, Boritz E, Coates E, DeZure A, Madden P, Costner P, et al. Virologic effects of broadly neutralizing antibody VRC01 administration during chronic HIV-1 infection. Sci Transl Med. 2015;7(319).
156. Tong T, Crooks ET, Osawa K, Robinson JE, Barnes M, Apetrei C, et al. Multi-Parameter Exploration of HIV-1 Virus-Like Particles as Neutralizing Antibody Immunogens in Guinea Pigs, Rabbits and Macaques. Virology. 2014(456-457):55–69.
157. Tong T, Crooks ET, Osawa K, Binley JM. HIV-1 virus-like particles bearing pure env trimers expose neutralizing epitopes but occlude nonneutralizing epitopes. Journal of Virology. 2012;86(7):3574-87.
158. Kulp DW, Steichen JM, Pauthner M, Hu X, Schiffner T, Liguori A, et al. Structure-based design of native-like HIV-1 envelope trimers to silence non-neutralizing epitopes and eliminate CD4 binding. Nature Communications. 2017;8(1655).
159. Schief W, Ban Y, Stamatatos L. Challenges for structure-based HIV vaccine design. Current Opinion in AIDS. 2009;4(5):431-40.
160. Stamatatos L, Pancera M, McGuire A. Germline-targeting immunogens. Immunological Reviews. 2017;275(1):203-16.

CHAPTER 6: APPENDICES

APPENDIX A: SEQUENCE ACCESSION NUMBERS (GENBANK)

VIRUS	ACCESSION NUMBER
CAP256 SU	KF996583
WITO.33	AY835451
T250-4	EU513189
CM244	JQ715397
ZM233	DQ388517
CAP45.G3	DQ435682.1

APPENDIX B: ETHICS CLEARANCE CERTIFICATE

R14/49 Ms Vimbai Sharon Madzorera

HUMAN RESEARCH ETHICS COMMITTEE (MEDICAL)

CLEARANCE CERTIFICATE NO. M170388

NAME: (Principal Investigator)	Ms Vimbai Sharon Madzorera
DEPARTMENT:	Virology National Institute of Communicable Diseases
PROJECT TITLE:	Engineering HIV Viral Variants as Immunogents to Stimulate Broadly Neutralizing Antibodies (bnAbs)
DATE CONSIDERED:	31/03/2017
DECISION:	Approved unconditionally
CONDITIONS:	
SUPERVISOR:	Prof Penelope Moore
APPROVED BY:	Professor P. Cleaton-Jones, Chairperson, HREC (Medical)
DATE OF APPROVAL:	29/11/2017

This clearance certificate is valid for 5 years from date of approval. Extension may be applied for.

DECLARATION OF INVESTIGATORS

To be completed in duplicate and **ONE COPY** returned to the Research Office Secretary on the 3rd floor, Phillip Tobias Building, Parktown, University of the Witwatersrand. I/We fully understand the conditions under which I am/we are authorised to carry out the above-mentioned research and I/we undertake to ensure compliance with these conditions. Should any departure be contemplated, from the research protocol as approved, I/we undertake to resubmit to the Committee. **I agree to submit a yearly progress report**. The date for annual re-certification will be one year after the date of convened meeting where the study was initially reviewed. in this case, the study was initially review January and will therefore be due in the month of January each year. Unreported changes to the application may invalidate the clearance given by the HREC (Medical).

Principal Investigator Signature

Date 17-01-2018

PLEASE QUOTE THE PROTOCOL NUMBER IN ALL ENQUIRIES

APPENDIX C: PLIAGIARISM DECLARATION

UNIVERSITY OF THE WITWATERSRAND, JOHANNESBURG

FACULTY OF HEALTH SCIENCES

PLAGIARISM DECLARATION TO BE SIGNED BY ALL HIGHER DEGREE STUDENTS

SENATE PLAGIARISM POLICY: APPENDIX ONE

I Vimbai S. Madzorera (Student number: 1762624) am a student registered for the degree of Master of Science in Medicine in the academic year 2017-18.

I hereby declare the following:

- I am aware that plagiarism (the use of someone else's work without their permission and/or without acknowledging the original source) is wrong.
- I confirm that the work submitted for assessment for the above degree is my own unaided work except where I have explicitly indicated otherwise.
- I have followed the required conventions in referencing the thoughts and ideas of others.
- I understand that the University of the Witwatersrand may take disciplinary action against me if there is a belief that this is not my own unaided work or that I have failed to acknowledge the source of the ideas or words in my writing.
- I have included as an appendix a report from "Turnitin" (or other approved plagiarism detection) software indicating the level of plagiarism in my research document.

Signature:  Date: 11-04-2018